

Synthesis, characteristic and application of mesocellular foam carbon (MCF-C) as
catalyst for dehydrogenation of ethanol



A Dissertation Submitted in Partial Fulfillment of the Requirements
for the Degree of Doctor of Engineering in Chemical Engineering

Department of Chemical Engineering

FACULTY OF ENGINEERING

Chulalongkorn University

Academic Year 2020

Copyright of Chulalongkorn University

การสังเคราะห์ การวิเคราะห์คุณลักษณะและการประยุกต์ใช้ของตัวเร่งปฏิกิริยาเมโซเซลลูลาร์โฟม
คาร์บอนสำหรับปฏิกิริยาเอทานอลดีไฮโดรจิเนชัน



วิทยานิพนธ์นี้เป็นส่วนหนึ่งของการศึกษาตามหลักสูตรปริญญาวิทยาศาสตรดุษฎีบัณฑิต
สาขาวิชาวิศวกรรมเคมี ภาควิชาวิศวกรรมเคมี
คณะวิศวกรรมศาสตร์ จุฬาลงกรณ์มหาวิทยาลัย
ปีการศึกษา 2563
ลิขสิทธิ์ของจุฬาลงกรณ์มหาวิทยาลัย

Thesis Title	Synthesis, characteristic and application of mesocellular foam carbon (MCF-C) as catalyst for dehydrogenation of ethanol
By	Mr. Yoottapong Klinthongchai
Field of Study	Chemical Engineering
Thesis Advisor	Professor Dr. BUNJERD JONGSOMJIT, Ph.D.
Thesis Co Advisor	Associate Professor Dr. SEEROONG PRICHANONT, Ph.D.

Accepted by the FACULTY OF ENGINEERING, Chulalongkorn University in
Partial Fulfillment of the Requirement for the Doctor of Engineering

..... Dean of the FACULTY OF
ENGINEERING
(Professor Dr. SUPOT TEACHAVORASINSKUN, D.Eng.)

DISSERTATION COMMITTEE

..... Chairman
(Assistant Professor Dr. Ekrachan Chaichana, Ph.D.)

..... Thesis Advisor
(Professor Dr. BUNJERD JONGSOMJIT, Ph.D.)

..... Thesis Co-Advisor
(Associate Professor Dr. SEEROONG PRICHANONT, Ph.D.)

..... Examiner
(Professor Dr. JOONGJAI PANPRANOT, Ph.D.)

..... Examiner
(Assistant Professor Dr. SUPHOT PHATANASRI, Ph.D.)

..... Examiner
(Dr. Supareak Prasertthdam)

ยุทธพงศ์ กลิ่นธงชัย : การสังเคราะห์ การวิเคราะห์คุณลักษณะและการประยุกต์ใช้ของ
 ตัวเร่งปฏิกิริยาเมโซเซลลูลาร์โฟมคาร์บอนสำหรับปฏิกิริยาเอทานอลดีไฮโดรจิเนชัน. (
 Synthesis, characteristic and application of mesocellular foam carbon
 (MCF-C) as catalyst for dehydrogenation of ethanol) อ.ที่ปรึกษาหลัก : ศ. ดร.
 บรรเจิด จงสมจิตร, อ.ที่ปรึกษาร่วม : รศ. ดร.สิริรุ่ง ปริษานนท์

งานวิจัยนี้มุ่งเน้นการศึกษาของตัวเร่งปฏิกิริยาเมโซเซลลูลาร์โฟมคาร์บอนสำหรับ
 ปฏิกิริยาเอทานอลดีไฮโดรจิเนชัน โดยงานวิจัยนี้แบ่งออกเป็น 3 ส่วน ได้แก่ การสังเคราะห์ตัวเร่ง
 ปฏิกิริยาเมโซเซลลูลาร์โฟมคาร์บอนจากการใช้ตัวรองรับเมโซเซลลูลาร์โฟมซิลิกาเป็นต้นแบบและ
 นำไปทดสอบการเร่งปฏิกิริยาเอทานอลดีไฮโดรจิเนชัน ซึ่งพบว่าสารลดแรงตึงผิวที่เป็นแหล่ง
 คาร์บอนสามารถถูกเปลี่ยนไปเป็นเมโซเซลลูลาร์โฟมคาร์บอนได้ อีกทั้งเมื่อนำไปทดสอบ
 ประสิทธิภาพการเร่งปฏิกิริยาเอทานอลดีไฮโดรจิเนชันพบว่าเมโซเซลลูลาร์โฟมคาร์บอนสามารถเร่ง
 ปฏิกิริยาดีไฮโดรจิเนชันจากเอทานอลไปเป็นอะเซทัลดีไฮด์ได้ดี โดยในส่วนของ 2 ของงานวิจัยนั้นได้
 ทดสอบการเสื่อมสภาพของตัวเร่งปฏิกิริยาเมโซเซลลูลาร์โฟมคาร์บอนที่อุณหภูมิแตกต่างกันเป็น
 เวลา 12 ชั่วโมง พบว่าอุณหภูมิที่ 400 องศาเซลเซียสให้ความเสถียรภาพของตัวเร่งปฏิกิริยาสูงที่สุด
 เนื่องด้วยเกิดโค้กที่ต่ำที่สุดซึ่งทำให้พื้นผิวของตัวเร่งปฏิกิริยามีความสามารถในการเร่งปฏิกิริยา
 อย่างต่อเนื่องเป็นระยะเวลา 12 ชั่วโมง และในงานวิจัยส่วนสุดท้ายนั้นได้ทำการศึกษาผลของการ
 เปลี่ยนแปลงปริมาณของ TMB/P123 เพื่อศึกษาผลของขนาดรูพรุนที่มีผลกระทบต่อ การเร่ง
 ปฏิกิริยาเอทานอลดีไฮโดรจิเนชัน การเปลี่ยนแปลงปริมาณของ TMB/P123 ให้ลักษณะโครงสร้าง
 ทางกายภาพที่แตกต่างกัน แต่อย่างไรก็ตามลักษณะทางเคมีไม่ต่างกันมากนัก และผลจากการเร่ง
 ปฏิกิริยาพบว่าปริมาณที่เหมาะสมของ TMB/P123 ที่ 3.5 มีผลต่อการเร่งปฏิกิริยาเอทานอลดี
 ไฮโดรจิเนชันไปเป็นอะเซทัลดีไฮด์ อันเนื่องมาจากผลของการถ่ายเทมวลสารของลักษณะรูพรุนและ
 พื้นที่ผิวที่แตกต่างกัน

สาขาวิชา วิศวกรรมเคมี
 ปีการศึกษา 2563

ลายมือชื่อนิสิต
 ลายมือชื่อ อ.ที่ปรึกษาหลัก
 ลายมือชื่อ อ.ที่ปรึกษาร่วม

6071434021 : MAJOR CHEMICAL ENGINEERING

KEYWORD: Mesocellular foam carbon, ethanol dehydrogenation, acetaldehyde, pore size, catalyst deactivation

Yoottapong Klinthongchai : Synthesis, characteristic and application of mesocellular foam carbon (MCF-C) as catalyst for dehydrogenation of ethanol . Advisor: Prof. Dr. BUNJERD JONGSOMJIT, Ph.D. Co-advisor: Assoc. Prof. Dr. SEEROONG PRICHANONT, Ph.D.

This research aims to investigate the synthesis of MCF-C as catalyst for dehydrogenation of ethanol. The study was classified into 3 parts. In the first part, the mesocellular foam silica (MCF-Si) was converted to mesocellular foam carbon using a surfactant residue as a carbon source, and followed by testing the dehydrogenation of ethanol to acetaldehyde. Surfactant residue in the inside of MCF-Si could be used as the carbon source for MCF-C synthesis. The obtained material could maintain the meso-structure, and exhibited higher activity for ethanol dehydrogenation in comparison to MCF-Si. For the second part, MCF-C was examined for 12 h for catalyst deactivation at various temperature. The low operating temperature at 300 °C exhibited the highest ethanol conversion changed, which was accorded to the higher coke formation to obstruct the catalysis process. Thus, the operating temperature of ethanol dehydrogenation using MCF-C as catalyst was significantly affected to the coke formation. The final part was examined for the effect of pore size of MCF-C to optimize the selectivity and yield of acetaldehyde. MCF-C was synthesized with the various ratios of TMB/P123 and tested in ethanol dehydrogenation reaction. The higher ratio of TMB/P123 significantly changed the physical properties as pore size and provided higher catalytic activity.

Field of Study: Chemical Engineering

Student's Signature

Academic Year: 2020

Advisor's Signature

Co-advisor's Signature

ACKNOWLEDGEMENTS

I would like to be thankful the deepest consultant to my dissertation advisor and co-advisor, Professor Dr. Bunjerd Jonsomjit and Associate Professor Dr. Seeroong Prichanont for greatly guiding and constructive recommendation during the first step in the member of Ethanol Reaction group and development research in total step. This doctoral dissertation cannot be accomplished without them. Moreover, I would like to be greatly sincere Professor Dr. Piyasan Prasertthdam for suggestion and teaching in catalysis laboratory.

I sincerely thank Assistant Professor Ekrachan Chaichana, as the chairman, Assistant Professor Suphot Phatanasri, Professor Dr. Joongjai Panpranot, and Dr. Supareak Prasertthdam, as the examiner of this dissertation for their precious guidance and revision of my dissertation.

I would like to special thanks to the Cat-React industrial project (Thailand) for the kind support in all chemicals in my laboratory.

I appreciate many thanks to many friends in the Center of Excellence on Catalysis and Catalytic Reaction Engineering, Department of Chemical Engineering, Faculty of Engineering, Chulalongkorn University

Finally, I do sincere thank my lovely family, my best friend, and my girlfriend for their grateful encouragement and perfect support during this dissertation and doctoral life.

Yoottapong Klinthongchai

TABLE OF CONTENTS

	Page
ABSTRACT (THAI).....	iii
ABSTRACT (ENGLISH).....	iv
ACKNOWLEDGEMENTS.....	v
TABLE OF CONTENTS.....	vi
Lists of Tables.....	0
Lists of Figures.....	2
CHAPTER 1.....	5
Introduction.....	5
1.1 General introduction.....	5
1.2 Objective.....	8
1.3 Research scope.....	8
1.4 Research methodology.....	9
1.5 Thesis grant chart.....	12
Chapter 2.....	1
Theory.....	1
2.1 Mesoporous silica.....	1
2.1.1 Characteristic of mesoporous silica.....	1
2.1.2 Properties of mesoporous silica.....	1
2.1.3 Variation of pore size of mesoporous silica.....	1
2.1.4 Synthesis of mesocellular foam silica (MCF-Si).....	2
2.1.5 Mesocellular foam carbon (MCF-C).....	4

2.1.5.1 Synthetic of MCF-C.....	4
2.2 Ethanol	5
2.3 Acetaldehyde.....	5
2.4 Ethanol dehydrogenation.....	7
Chapter 3.....	9
Literature review.....	9
3.1 Synthesis of Mesocellular foam carbon.....	9
3.1.1 Mesoporous carbon from other synthetic techniques	9
3.1.2 Mesoporous carbon from sulfuric acid with carbon residue technique ...	10
3.2 Ethanol dehydrogenation.....	11
3.2.1 Carbon catalyst	11
3.2.2 Mesoporous carbon catalyst.....	12
3.2.3 Mesoporous carbon catalyst with dehydrogenation of other substrates.	13
3.3 Catalyst deactivation study in ethanol dehydrogenation.....	13
3.4 Effect of pore sizes on catalytic activity.....	14
CHAPTER 4.....	15
EXPERIMENTAL	15
4.1 Catalysts preparation.....	15
4.1.1 Chemicals and reagents	15
4.1.2 Preparation of mesocellular foam materials as catalysts	16
4.2 Characterization of the mesocellular foam materials.....	17
4.3 Ethanol dehydrogenation testing.....	18
CHAPTER 5.....	23
RESULTS AND DISCUSSION.....	23

Synthesis, characteristics and application of mesocellular foam carbon (MCF-C) as catalyst for dehydrogenation of ethanol to acetaldehyde	24
Part 1: Synthesis, characteristics and application of mesocellular foam carbon (MCF-C) as catalyst for dehydrogenation of ethanol to acetaldehyde	25
5.1 Introduction	26
5.2 Experimental	28
5.2.1 Preparation of mesocellular foam materials	28
5.2.1.1 Mesocellular foam silica (MCF-Si)	28
5.2.1.2 Mesocellular foam silica/carbon (MCF-Si-C)	29
5.2.1.3 Mesocellular foam carbon (MCF-C)	30
5.2.2 Characterization of mesocellular foam materials.....	30
5.2.3 Ethanol dehydrogenation reaction	32
5.2.4 Stability test	33
5.3 Result and Discussion.....	34
5.3.1 Catalyst Characterization.....	34
5.3.1.1 Surface area and pore structure.....	34
5.3.1.2 Textural property and morphology.....	35
5.3.1.3 Crystal structure.....	38
5.3.1.4 Functional groups.....	39
5.3.1.5 Thermogravimetric analysis	40
5.3.1.6 Acidity and acid strength	41
5.3.1.7 Basicity and basic strength	42
5.3.2 Catalytic activity of ethanol dehydrogenation	44
5.3.2.1 Reaction study	44

5.3.2.2 Stability test (Time-on-stream behavior).....	49
5.3.3 Spent catalyst.....	50
Study of deactivation in mesocellular foam carbon (MCF-C) catalyst used in gas-phase dehydrogenation of ethanol.....	53
Part 2: Study of deactivation in mesocellular foam carbon (MCF-C) catalyst used in gas-phase dehydrogenation of ethanol.....	54
5.1 Introduction.....	55
5.2 Materials and method.....	57
5.2.1 Materials (Chemicals).....	57
5.2.2 Catalyst preparation.....	57
5.2.3 Characterization of catalyst.....	58
5.2.4 Catalytic test.....	59
5.3 Results and discussion.....	61
5.3.1 Catalytic behavior.....	61
5.3.1.1 Influence of temperature during time on stream on catalytic behavior of ethanol dehydrogenation.....	61
5.3.2 Characterization on the textural properties of catalysts.....	62
5.3.3 Characterization on the chemical properties of catalysts.....	67
5.3.4 Quantitative analysis of the coke formation.....	70
Effect of TMB/P123 ratios on physicochemical properties of mesocellular foam carbon (MCF-C) as catalyst for ethanol dehydrogenation.....	72
Part 3: Effect of TMB/P123 ratios on physicochemical properties of mesocellular foam carbon (MCF-C) as catalyst for ethanol dehydrogenation.....	73
5.1 Introduction.....	74
5.2. Experimental.....	76

5.2.1 Materials and chemicals.....	76
5.2.2 Characterization	78
5.2.2.1 N ₂ -physisorption.....	78
5.2.2.2 Transmission electron microscopy (TEM).....	78
5.2.2.3 Scanning electron microscopy (SEM) and energy dispersive X-ray spectroscopy (EDX).....	79
5.2.2.4. X-ray diffraction (XRD).....	79
5.2.2.5 Thermogravimetric analysis (TGA).....	79
5.2.2.6 Fourier transform infrared (FT-IR) spectroscopy.....	79
5.2.2.7 Carbon dioxide temperature-programmed desorption (CO ₂ -TPD) 79	
5.2.2.8 Ammonia temperature-programmed desorption (NH ₃ -TPD)	80
5.2.3 Ethanol dehydrogenation process	80
5.2.4 Stability test	81
5.3. Result and Discussion.....	82
5.3.1 Characterization	82
5.3.1.1 N ₂ -physisorption isotherms and textural properties	82
5.3.1.2 Mesophase structures of catalysts.....	84
5.3.1.3. Morphologies of surface and particles.....	86
5.3.1.4 The analysis of crystallinity of MCF-C	89
5.3.1.5 FT-IR studies	90
5.3.1.6 TGA studies	92
5.3.1.7 Surface acidity.....	92
5.3.1.8 Surface basicity	94
5.3.2 Catalytic activity studies.....	97

5.3.2.1 Ethanol dehydrogenation process	97
5.3.2.2 Time-on-stream behavior testing	102
5.3.2.2.1 Spent catalysts	103
Chapter 6.....	107
General conclusion.....	107
6.1 General summary	107
6.2 Conclusion	108
Part 1: Synthesis, characteristics and application of mesocellular foam carbon (MCF-C) as catalyst for dehydrogenation of ethanol to acetaldehyde	108
Part 2: Study of deactivation in mesocellular foam carbon (MCF-C) catalyst used in gas-phase dehydrogenation of ethanol.....	108
Part 3: Effect of TMB/P123 ratios on physicochemical properties of mesocellular foam carbon (MCF-C) as catalyst for ethanol dehydrogenation	109
6.3 Recommendations	110
APPENDIX A.....	111
APPENDIX.....	113
LIST OF PUBLICATIONS	113
B-1 Publications.....	113
B-2 Conference.....	113
References.....	114
REFERENCES	119
VITA.....	121

Lists of Tables

Table 2. 1 Properties of acetaldehyde[51].....	6
Table 4. 1 Operating conditions for gas chromatographs.	20
Table 5. 1 Surface area (BET), average pore size and average pore volume.....	35
Table 5. 2 The amount of each element near the surface of catalyst granule obtained from EDX.....	37
Table 5. 3 Acidity and acid strength of all samples obtained from NH ₃ -TPD.	41
Table 5. 4 Basicity and basic strength of all samples obtained from CO ₂ -TPD.	43
Table 5. 5 Ethanol conversion and acetaldehyde selectivity of all catalysts.....	46
Table 5. 6 Ethanol conversion, selectivity, and yield of acetaldehyde of all catalysts.	48
Table 5. 7 Comparison of catalytic activity of different catalysts for ethanol dehydrogenation to acetaldehyde.	49
Table 5. 8 Surface area (BET), average pore size and pore volume of spent MCF-C and MCF-C catalysts.....	51
Table 5. 9 The amount of each element near the surface of catalyst granule obtained from EDX.....	52
Table 5. 10 Physical properties of the fresh and spent catalyst with different reaction temperatures.....	63
Table 5. 11 Amount of each element adjacent the surface of catalyst granule obtained from EDX.....	66
Table 5. 12 Acidity and acid strength of the fresh and spent catalysts obtained from NH ₃ -TPD.	70
Table 5. 13 Surface area (BET), average pore size and average pore volume.	83

Table 5. 14 The amount of each element near surface of catalyst granule obtained from EDX.	88
Table 5. 15 Acidity and acid strength of all MCF-C catalysts obtained from NH_3 -TPD.	93
Table 5. 16 Basicity and basic strength of all MCF-C catalysts obtained from CO_2 -TPD.	96
Table 5. 17 The specific activity based on basicity and acidity for all MCF-C catalysts.	102
Table 5. 18 The amount of each element near surface of fresh and spent catalyst granule obtained from EDX.	105
Table A1. 1 Ethanol conversion and selectivity of all MCF-C catalysts.....	111



Lists of Figures

Figure 2. 1 Porous structure and TEM image of (a) MCM-41, (b) SBA-15, and (c) MCF [42].	2
Figure 2. 2 Synthesis process of MCF-Si.	4
Figure 2. 3 Synthetic procedure of MCF-C with surfactant residue [48].	5
Figure 2. 4 Mechanism of dehydrogenation reaction over copper (Cu) at 300 °C [57].	8
Figure 4. 1 Flow diagram of catalytic dehydrogenation reaction of ethanol.	21
Figure 5. 1 Nitrogen adsorption/desorption isotherms of all synthesized catalysts.	34
Figure 5. 2 TEM images of MCF-Si, MCF-Si-C, and MCF-C catalysts.	36
Figure 5. 3 Low magnification SEM image of MCF-Si, MCF-Si-C, MCF-C.	37
Figure 5. 4 XRD patterns of all catalysts.	38
Figure 5. 5 FT-IR spectra of all catalysts.	39
Figure 5. 6 Thermogravimetric analysis (TGA) of intermediate materials corresponding to each synthesis step of MCF-C under air atmosphere.	40
Figure 5. 7 NH ₃ -TPD profile of all catalysts.	42
Figure 5. 8 CO ₂ -TPD profile of all catalysts.	44
Figure 5. 9 Ethanol conversion and yield of acetaldehyde over different MCF catalysts toward ethanol dehydrogenation.	45
Figure 5. 10 Stability test (ethanol conversion and yield of acetaldehyde with TOS) for the MCF-C catalyst at 400 °C.	50
Figure 5. 11 Nitrogen adsorption/desorption isotherms of spent MCF-C and MCF-C catalysts.	51
Figure 5. 12 Ethanol Conversion and yield of acetaldehyde of all catalysts with regarding to ethanol dehydrogenation.	61

Figure 5. 13 Nitrogen adsorption/desorption isotherms of all stability testing conditions (MCF-C, MCF-C SP300, MCF-C SP350, and MCF-C SP400).	62
Figure 5. 14 Low magnification SEM image of MCF-C, MCF-C SP300, MCF-C SP350, MCF-C SP400.....	65
Figure 5. 15 XRD pattern of the fresh and spent catalysts.....	67
Figure 5. 16 FT-IR spectra of the fresh and spent catalysts.	68
Figure 5. 17 TPD-NH ₃ profile of the fresh and spent catalysts.....	69
Figure 5. 18 Thermogravimetric analysis (TGA) of material corresponding to each stability testing conditions of MCF-C under air atmosphere.	71
Figure 5. 19 Differential Scanning Calorimetry of the fresh and spent catalysts.	71
Figure 5. 20 Nitrogen adsorption/desorption isotherm of all MCF-C catalysts.	82
Figure 5. 21 TEM images of all MCF-C catalysts.....	85
Figure 5. 22 SEM images of all fresh MCF-C catalysts.....	87
Figure 5. 23 XRD patterns of all MCF-C catalysts.....	90
Figure 5. 24 FT-IR spectra of all MCF-C catalysts.....	91
Figure 5. 25 Thermogravimetric analysis (TGA) of all MCF-C catalysts under air atmosphere.....	92
Figure 5. 26 NH ₃ -TPD profile of all MCF-C catalysts.....	94
Figure 5. 27 CO ₂ -TPD profile of all MCF-C catalysts.....	95
Figure 5. 28 Ethanol Conversion of all MCF-C catalysts on ethanol dehydrogenation.	97
Figure 5. 29 Yield and selectivity of acetaldehyde vs temperature of all MCF-C catalysts on ethanol dehydrogenation.	99
Figure 5. 30 The relationship between the rate of reaction and surface area.....	101
Figure 5. 31 Stability test of all MCF-C catalysts for 12 h on ethanol dehydrogenation.	103

Figure 5. 32 Low magnification SEM image of spent and fresh catalysts of all MCF-C catalysts..... 106



CHAPTER 1

Introduction

1.1 General introduction

Mesocellular foam silica (MCF-Si) [1-5] is one of the most captivating mesoporous materials having the large pore size and spherical shape with interconnected pores. Furthermore, it contains silanol group (-OH) on the surface, which can be appropriately modified by functionalization for improvement of its properties [6-9]. The general application of MCF includes the support for copper as catalyst for methanol synthesis [10, 11] and carrier for immobilization of enzyme in biosensor [12, 13]. Furthermore, it can be used as the support in CO₂ capture and toxic pollutants from air [14-17]. These advantages in characteristics of MCF probably facilitate the diffusion of the target reactant because of its appropriate pore size. In addition, it also likely helps to prevent the collapse of pore structure during high temperature because of well heat transfer released by interconnected pore [18]. However, there are still some disadvantages for chemical properties of MCF such as low acidity and basicity, which are required as active sites for intrinsic catalytic activity on catalytic process including dehydrogenation of ethanol [19].

Accordingly, mesoporous carbon is one of the interesting choices of materials, which possesses mesoporous structure and suitable chemical properties for improving the lack of acidity and basicity properties that are crucial for dehydrogenation of ethanol in this work. Previously, Liu et al. [20] investigated ordered mesoporous carbon in direct dehydrogenation of propane to propylene with high activity and selectivity. Later, Wang et al. [21] reported the use of supported Cu on mesoporous carbon derived from SBA-15 as hard template in dehydrogenation of ethanol to acetaldehyde. It was found that increased selectivity was evident using Cu/mesoporous carbon (MCF-C) compared with that obtained from Cu/SBA-15. It indicated that plenty of silanol groups on SBA-15 favors the minor reaction, which is possible to obtain low selectivity of acetaldehyde [21]. At present, there are many methodologies to synthesize

mesoporous carbon. For example, chemical volatile deposition (CVD) process was used the vaporization technique with reactant as carbon source to cover on the target support [22]. The CVD process was moderately difficult to assure a homogeneous carbon deposition on support surface. Another method is the usage of organic source on the support surface as the hard template and soft template, which are followed by a carbonization. On the other hand, the use of sucrose as an organic source not only rather elaborated, but also plenty of steps for the mesoporous carbon synthesis. Furthermore, the cost of organic reagent as a carbon source is high for the synthetic process. Consequently, simple synthetic route and inexpensive operating cost are more attractive for the synthetic of mesoporous carbon. Therefore, organic template agent is considered for converting to be the carbon source in the synthesis of the mesostructured silica to carbon. The organic template could be transformed into the homogeneous carbon layer in the pores of the silica. Valle-Vig'ón et al. [23] investigated the sulfonated silica-carbon composites which contain a large number of active sites for esterification of maleic anhydride, succinic acid and oleic acid with ethanol. The results showed that these composite materials provide better intrinsic catalytic activity than the commercial ones such as Amberlyst-15. Therefore, the MCF-C is promising as a catalyst for ethanol dehydrogenation to acetaldehyde because it can provide high stability at high reaction temperature operation. It also indicates that enlarge pore sizes and interconnected pores potentially facilitate the transport phenomena of the reactants and products. Moreover, MCF-C can inhibit the formation of byproducts because of its suitable acidity and basicity.

Ethanol is one of the renewable energy sources, which can be easily produced by fermentation of biomass such as sugarcane, corn, wheat, cassava, etc. However, in the unavailability of biomass, ethanol can be produced by catalytic hydration of ethylene via a petrochemical process [24-26]. Ethanol has been widely studied for decades as a potential raw material for production of other value-added chemicals such as ethylene, diethyl ether, acetaldehyde and ethyl acetate [27, 28]. Amongst the ethanol-derived products, acetaldehyde is remarkably interesting as reactants at the beginning of the process in industries for production of ethyl acetate, acetic acid, acetic anhydride and isobutanol [29, 30]. Moreover, it is also used in the food engineering for

as a preservative agent [31]. Currently, there are different reaction routes to produce acetaldehyde in industries including; (1) partial oxidation of ethane using palladium chloride (PdCl_2) catalyst, which is not only an expensive catalyst, but also requires high reaction temperature [32], (2) hydration of acetylene, which has to spend mercury (Hg) to form mercuric complex that is a toxic material for the environmental concern [33] and (3) oxidation of ethylene from petroleum and natural gas. However, the operating cost of the last process is expensive, and it needs high volume of HCl for catalyst regeneration [34]. Hence, the reaction of acetaldehyde production from ethanol dehydrogenation, which is not only uncomplicated, but also uses ethanol as renewable sources and non-toxic process [6-10] is so captivating. There are many catalysts used in ethanol dehydrogenation such as TiO_2 [35], Al_2O_3 [28] SBA-15 [19], and activated carbon [36]. Although there are many studies of catalysts used in ethanol dehydrogenation process, the catalyst properties still need improvement, not only in terms of higher conversion, selectivity or even yield, but also proper thermal stability. There have been only few studies of the acetaldehyde production by ethanol dehydrogenation using mesocellular foam silica (MCF-Si) as the template materials with spherical shape and interconnected pore [37].

Therefore, this work aims to investigate the synthesis, characteristics and the application as the dehydrogenation catalyst of the MCF-Si derived MCF-C for ethanol dehydrogenation to acetaldehyde. In addition, to synthesize these materials, we used the surfactant such as the PEO-PPO-PEO triblock copolymer (Pluronic P123). Pluronic P123 was not only a structure-directing agent for template, but also a carbon source for the MCF-C synthesis. All the synthesized materials were characterized using various techniques and were tested for dehydrogenation of ethanol to measure the catalytic behaviors. Furthermore, the stability of the MCF-C was also studied.

1.2 Objective

1.2.1 To synthesize and characterize the mesocellular foam materials (Silica, Silica/Carbon, Carbon) as well as apply the as the catalysts for ethanol dehydrogenation.

1.2.2 To study the catalyst deactivation of MCF-C on ethanol dehydrogenation to acetaldehyde.

1.2.3 To investigate the effect of pore sizes of MCF-C on the selectivity in ethanol dehydrogenation process.

1.3 Research scope

1.3.1 Synthesis of the mesocellular foam materials as MCF-Si, Mesocellular foam silica/carbon (MCF-Si-C), and MCF-C.

1.3.2 Characterization of mesocellular foam materials with several techniques; N₂-physicorption, Transmission electron microscopy (TEM), Scanning electron microscopy (SEM) and energy dispersive X-ray spectroscopy (EDX), X-ray diffraction (XRD), Fourier transform infrared spectroscopy (FT-IR), Thermalgravimetric analysis (TGA), Ammonia temperature-programmed desorption (NH₃-TPD), and Carbon dioxide temperature programmed desorption (CO₂-TPD).

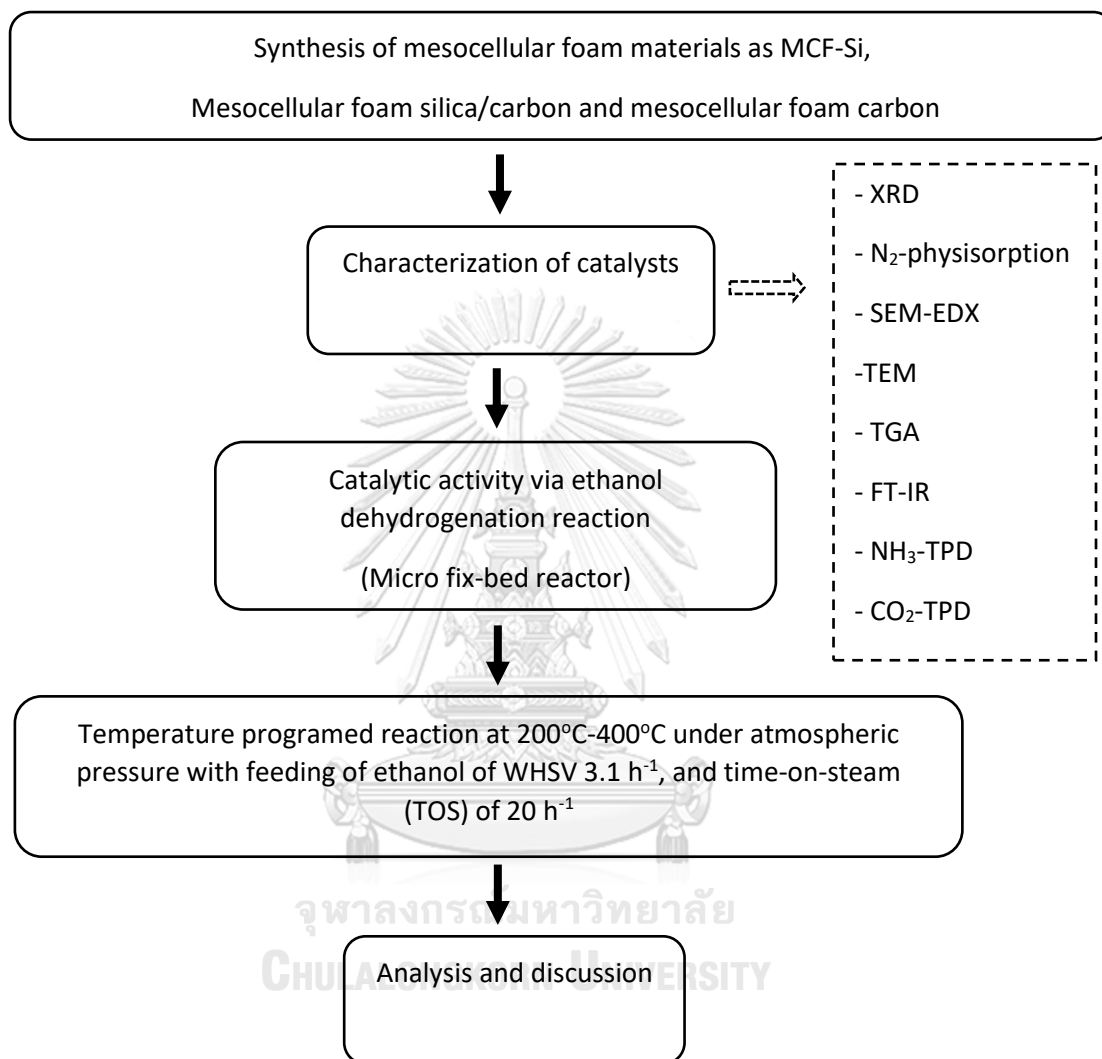
1.3.3 Investigation of the catalytic activity of mesocellular foam carbon materials on ethanol dehydrogenation process in temperature range of 200-400 °C.

1.3.4 Examination of the catalyst deactivation of MCF-C on ethanol dehydrogenation to acetaldehyde via varying the temperature range of 300-400 °C and weight hourly space velocity (WHSV) of 3.1 h⁻¹.

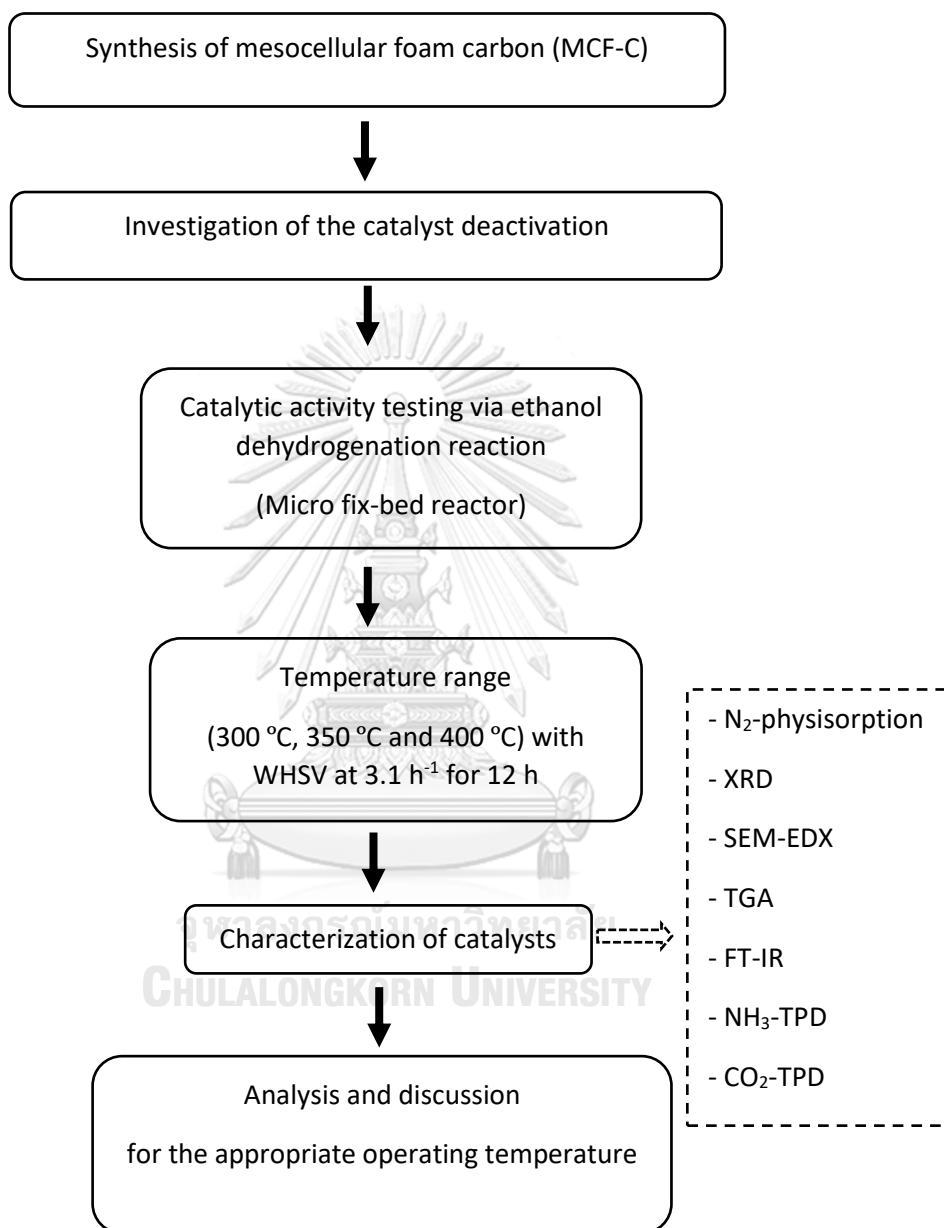
1.3.5 Synthesis of MCF-C with different pore sizes by changing the mass ratio of 1,3,5-trimethylbenzene : Pluronic P123 (TMB:P123 wt.) for 0.5, 1.5, 2.5, 3.5, and 4.5, and the mass ratio of Pluronic P123 : tetraethyl orthosilicate (P123:TEOS wt.) will be constant as 0.5.

1.4 Research methodology

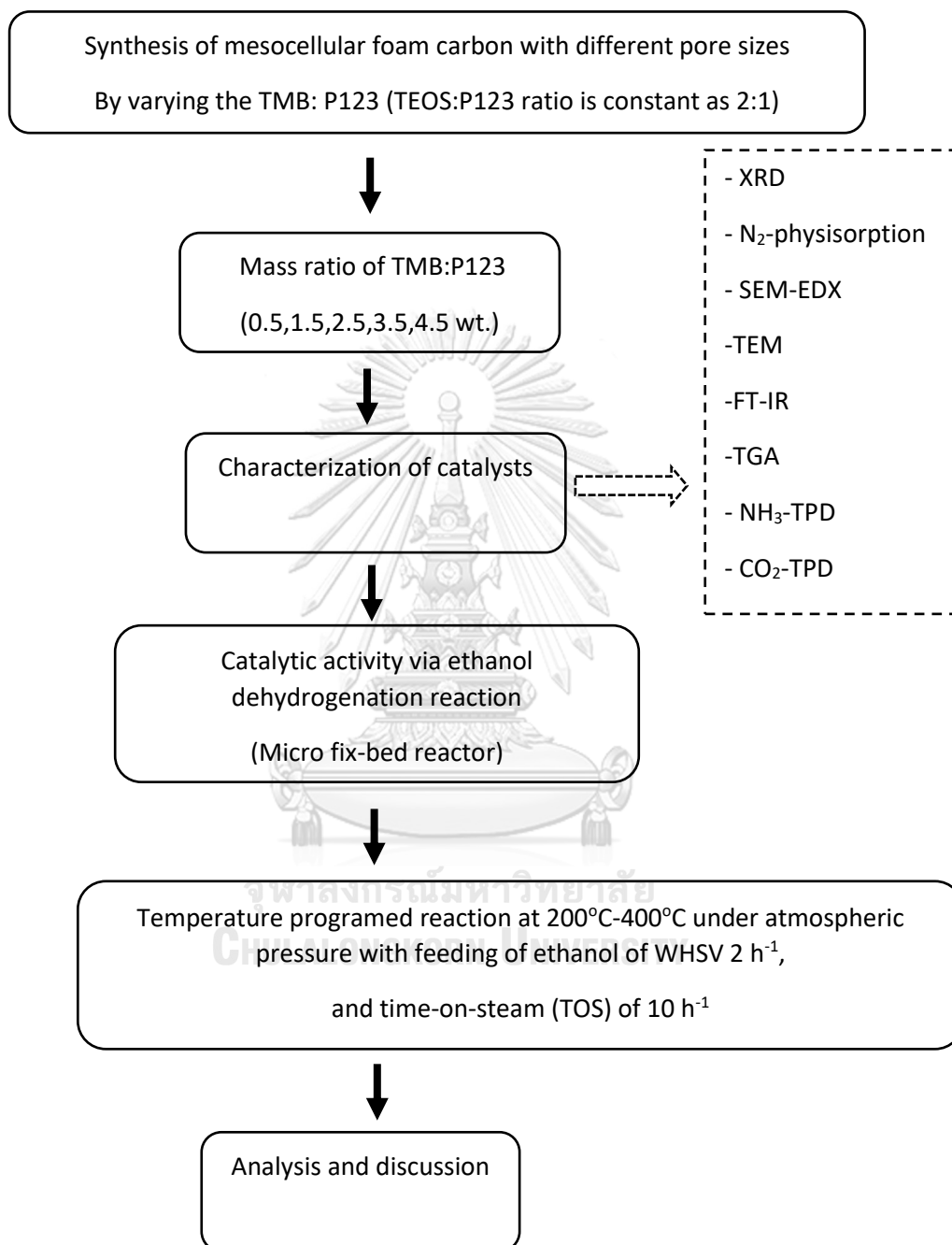
Part I. Synthesis and characterization of mesocellular foam materials. In addition, catalytic activity is performed with ethanol dehydrogenation.



Part II. Study of catalyst deactivation of MCF-C in ethanol dehydrogenation to acetaldehyde on MCF-C.



Part III. Investigation of the effect of pore sizes of mesocellular foam carbon for ethanol dehydrogenation.



Chapter 2

Theory

2.1 Mesoporous silica

2.1.1 Characteristic of mesoporous silica

Mesoporous silica is a type of inorganic materials, which is represented as a high porosity, high surface area about 500-1000 m²/g, and high pore volume [38]. There are several types of mesoporous silica materials, which depend on the pore size and shape of the materials such as MCM-41, SBA-15, and MCF [39]. In general, these materials have been extensively studied and applied for being support in various applications [12, 14]. The International Union of Pure and Applied Chemistry (IUPAC) classified the porous materials using the internal pore width (diameter) as a criterion. Thus, the porous materials can be divided into 3 types; 1. microporous with diameter below 2 nm, 2. mesoporous with diameter in range of 2-50 nm, and 3. macroporous with diameter more than 50 nm [40].

2.1.2 Properties of mesoporous silica

Mesoporous silica is appropriate for the several applications, which need large pore size, high surface area, high porosity, non-toxicity, and biocompatibility. For example, mesoporous silica as SBA-15 with high surface area was used in ethanol dehydrogenation to increase the ethanol conversion [19]. In addition, enlarge pore size of mesoporous silica may affect to the mass transfer of reactant to diffuse inside of the pore, which probably increase contact time between reactant and catalyst [21]. However, there is a disadvantage for some catalytic reaction, which need suitable chemical properties as acidity and basicity.

2.1.3 Variation of pore size of mesoporous silica

Generally, synthesis of mesoporous silica was use in different applications because of its different pore size, surface area and structure. For example, Yu-Shan Chi

and et al. [41] synthesized the MCM-41, MCM-48, and SBA-15, which were reported that the different pore size of 2.9, 2.3, and 5.5 nm, respectively. In addition, these materials were displayed the same structure of rod-like shape. Furthermore, W.Chouyyok and et al. [42] also synthesized the mesoporous materials as MCM-41, SBA-15, and MCF, which were performed the pore sizes as 3.2, 5.4, and 14.6 nm, respectively. The porous structure of these materials was presented at **figure 2.1**. The hexagonal structure and cylindrical shape were shown in MCM-41 and SBA-15, but the pore size of SBA-15 was larger than MCM-41. The structure of MCF represented as the spherical structure. Moreover, it is the largest pore size among these materials, when MCM or SBA were compared. Therefore, the pore size of materials was arranged MCF>SBA-15>MCM-41. Consequently, MCF was probably predicted for good at diffusion because of its large pore size.

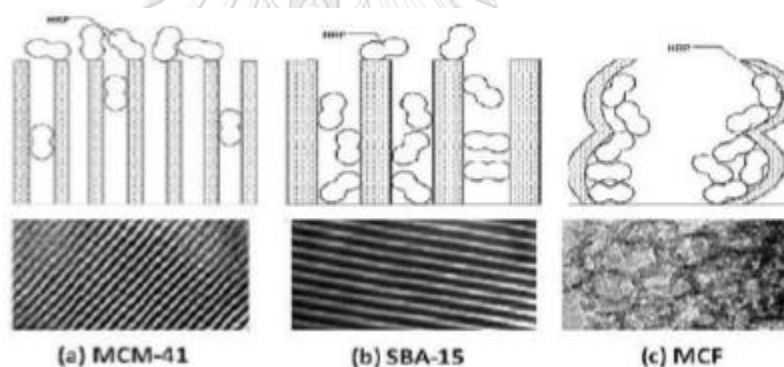


Figure 2. 1 Porous structure and TEM image of (a) MCM-41, (b) SBA-15, and (c) MCF [42].

2.1.4 Synthesis of mesocellular foam silica (MCF-Si)

Normally, the synthesis of mesoporous silica is consisted of 3 mainly steps; 1.Micelle chemistry, 2.Sol-gel process, and 3.template removal [39]. The used chemical substrates are initiated with structure-directing agent, which roles as the template of the materials in order to specify pore structure of mesoporous silica for example cetyltrimethyl ammonium bromine (CTAB), sodium dodecyl sulfonate (SDS), and pluronic P123. Then, the solvent is used to dissolve the reactant as water and ethanol. The organic cosolvent or swelling agent is also used for being expander of the pore of material as 1,3,5-trimethylbenzene. The inorganic substance with silica source is used

to remain the structure of the materials as sodium silicate or tetraethyl orthosilicate. The hydrochloric acid or sodium hydroxide were used to catalyze the synthesis process.

First part of synthesis of MCF is began with structure-directing agent as Pluronic P123, which is dissolved in the solvent solution as water or ethanol that are polar molecules. The P123 as structure-directing agent will systemically connect to its molecule as bulk and settle around the non-polar molecule, after that these bulks molecules will be emerged several structural shapes such as oval, rod or sphere that were depended on the amounts of substances as structure-directing agent in the solvent as water or ethanol. In addition, spherical shape is depended mass ratio of the structure-directing agent to swelling agent, indicating that swelling agent as 1,3,5-trimethylbenzene will play role as the pore expander of rod-like shape to be spherical shape with appropriated mass ratio [43]. Then, the silica source as tetraethyl orthosilicate is added in the previous solution, which is contained the structure-directing, solvent, and swelling agent. The sol-gel process will be arisen when the silica source is adhered on the structure-directing by hydrolysis process with solid particle, which is called sol. The silica network is appeared by aggregation of solid particles, which are become the gel by condensation polymerization process at 40 °C. This process will cause each hole to collide with each other, which affect to create a window within the material. Eventually, the gel is continually dried at 100 °C to make the structure more organized, and followed by template removal process with calcination under air atmosphere or solvent extraction using ethanol in order to dispose the contaminant such as unreacted substrate [43, 44] as **figure 2.2**.

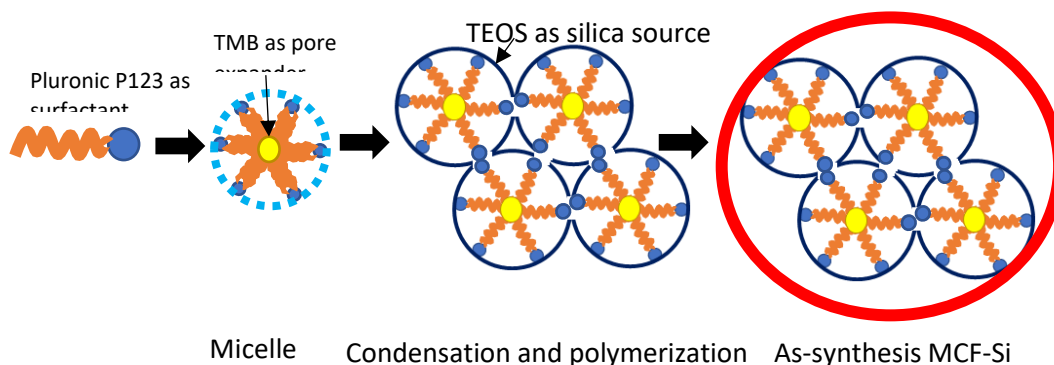


Figure 2. 2 Synthesis process of MCF-Si

2.1.5 Mesocellular foam carbon (MCF-C)

Mesoporous carbon has been fascinated significant attendance because of their use as catalyst support for many reactions, which is a large pore volume, surface area, and pore size [45]. The several kinds of surfactant-template mesoporous silica materials were engaged as the nanoscopic templates for many of the mesoporous carbon synthetic materials. The regular synthetic method for the mesoporous carbon using mesoporous silica as the template. For example, the co-assembly of surfactant and silicates are synthesized to become silica/surfactant-self-assembly nanocomposite. Then, extraction or calcination are employed for elimination of surfactants. After that, the carbon precursor agglomerates into the pore of mesoporous silica materials. Next, the carbonization is applied, which leads to the last step of template removal of silica. Above mentioned method is complex multi-steps and long period of synthesis. Therefore, simplicity and short period of synthetic process is elucidated. At the present time, organic template as structure-directing agent for the silica structure was used as carbon precursor [46].

2.1.5.1 Synthetic of MCF-C

First, the as-synthesized as MCF-Si is treated with sulfuric acid, which plays as a remover of water by dehydration process from Pluronic P123 as structure-directing agent and formation of sulphonic groups, which affects to the crosslinking of the polymeric chains. The carbonaceous material is transformed by these cross-linked

polymer chains in the heat treatment under an inert atmosphere. Finally, the MCF-C is achieved by dissolution of the silica framework from silica/carbon as a hybrid material with hydrofluoric acid sodium hydroxide as **Figure 2.3** [23, 47].

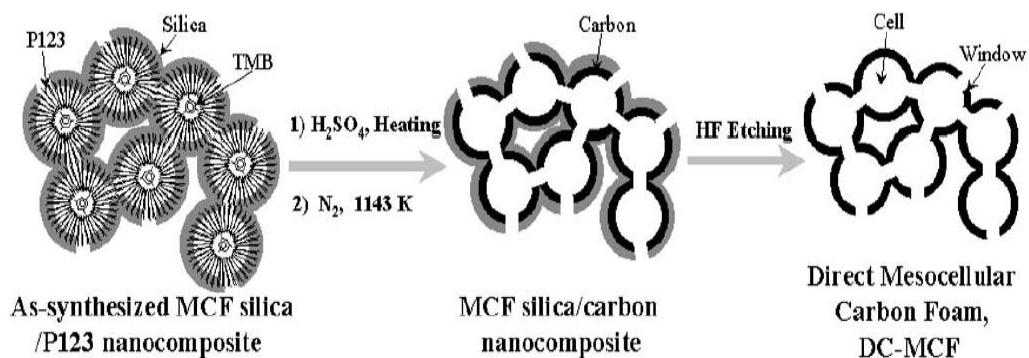


Figure 2. 3 Synthetic procedure of MCF-C with surfactant residue [48].

2.2 Ethanol

Nowadays, agricultural country as Thailand, where has intensely planted the sugarcane, cassava or cone in many parts of the country. The mainly point of planting these crops is the consumption and exportation for selling the other countries. Nevertheless, the overproduction as supply from the agriculture is excessive for the demanding, which affects to the lower prices. Therefore, the problem-solving of the Thai government is the merchandise of the oversupply to the industry for ethanol production. Ethanol is the renewable biomass resource, which is produced from the primary technology using fermentation method of the plant as mentioned above. In general, ethanol is fundamentally consumed in field of petroleum distillates as biofuel additive for transportation fuels. However, the price of ethanol can be increased by the manufacturing to be the value-added via selectively converting into the other chemical products as acetaldehyde, ethylene, diethyl ether or acetic acid [49, 50].

2.3 Acetaldehyde

The general characteristic of acetaldehyde is a colorless liquid or gas with a typical fruity odor. In addition, it is also light molecular weight, low boiling point with formula as CH_3CHO , and flammable substance. In downstream product, acetaldehyde is occasionally used as an intermediate of organic compound. Furthermore, it is also

affected to the humanity, animal or even plant as a mediator in metabolism in order to produce alcohol dehydrogenase via partial oxidation of ethanol. This indicates that the enormous volume of acetaldehyde intervenes the biological process. The physical properties are listed in **Table 2.1**

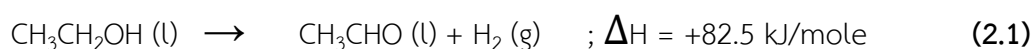
Table 2. 1 Properties of acetaldehyde[51].

Molecular weight	44.05
Boiling point at 101.3 kPa	20.16 °C
Melting point	-123.5 °C
Density	0.785 g/mL at 25 °C
Vapor density (air = 1)	1.52
Flash point	133 °C
Critical temperature t_{crit}	181.50 °C
Critical pressure p_{crit}	6.44 MPa
Molar volume of the gas	23.84 L/mol
Gibbs free energy of formation ΔG from elements	-133.81 kJ/mol

Acetaldehyde was discovered by Wilhelm Scheele between the experimental reaction of black manganese dioxide and sulfuric acid with alcohol. It had been examined by Antoine Francois, comte de Fourcroy, and Louis Nicolas Vauquelin since 1800, and Johann Wolfgang Dobereiner was also found among 1821 and 1832. Finally, Liebig who designated the product ‘‘aldehyde’’ as pure acetaldehyde by oxidation of ethanol with chromic acid. Finally, the previous name as aldehyde was corrected to ‘‘acetaldehyde’’ with a shortness of the full-word of ‘‘ aldehyde dehydrogenatus’’ [51]. There are several pathway in commercial production process such as the hydration of acetylene [52], the partial oxidation of ethane [53], and direct oxidation of ethylene [54], which is known as Wacker-Hoechst process [51]. These some of production routes performed disadvantages point of the process. For example, partial oxidation of ethane has to use an expensive catalyst as PdCl₂, and consume high reaction temperature for operation [53]. Moreover, some reaction process is expensive and eco-unfriendly such as using the mercury in process as the catalyst [52]. Thus, the environmentally friendly process is considerable as ethanol dehydrogenation [19, 55, 56].

2.4 Ethanol dehydrogenation

The reaction that removing of a hydrogen from any molecules in mechanism is defined as dehydrogenation reaction, which is endothermic reaction as following the equation (2.1) 19psource. In addition, aldehyde and ketone can be changed via dehydrogenation reaction of primary alcohol.



Nucleophile addition of basic catalysts affects to the hydrogen moving from the alcohol during the dehydrogenation, indicating that primary alcohol can be change into aldehydes by hydrogen acceptors in the non-existence of oxygen. The primary alcohol and secondary alcohol are converted to an aldehyde and ketone via dehydrogenation reaction, respectively as figure 2.4

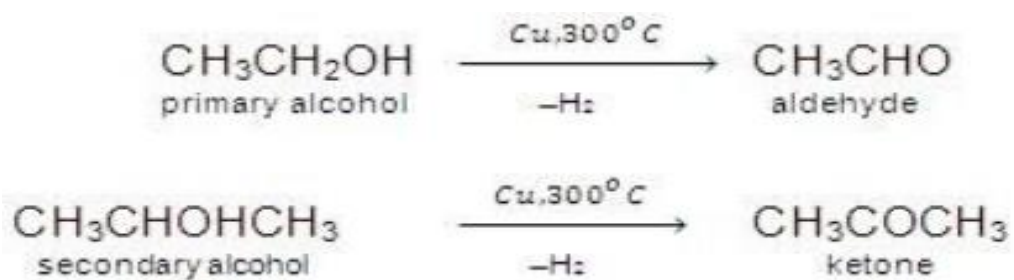


Figure 2. 4 Mechanism of dehydrogenation reaction over copper (Cu) at 300 °C [57].

The different type of catalysts and the specific condition such as space time, pressure, temperature directly affect to the product conversion, selectivity, and yield. In this study, the ethanol dehydrogenation to acetaldehyde is considered.



Chapter 3

Literature review

3.1 Synthesis of Mesocellular foam carbon

The mesoporous carbon can be prepared in the different methods or precursors, which directly affect to the textural characteristics. Herein the reviews of the synthetic methodologies of mesoporous carbon. In addition, not only the short and easy route synthesis of mesoporous carbon are also considered, but also investigated the less operating cost for this thesis.

3.1.1 Mesoporous carbon from other synthetic techniques

Mesoporous silica materials have been intensively used as the template for mesoporous carbon synthesis. Since Hyeon et al. [58] reported that nanocasting technique was achieved with several meso-silica structure materials such as SBA-15 [59], MCM-48 [60], and Mesocellular silica foams [61]. However, the carbon layer of this method did not well perform a uniform layer, which need to be excellent casted the carbon source on the silica template. According to Zhang et al. [62] who reported that chemical volatile deposition (CVD) technique was applied to deposit the carbon on SBA-15, which is one of mesoporous silicas. It was found that this technique was successfully deposited without significant loss in pore volume and surface area, which could be confirm by XRD. On the other, this method was slightly tough to ensure a uniform carbon deposition. Whereas by the second technique was reported by Pang et al. [63] who used the attaching organic moieties technique to synthesize the mesoporous carbon/silica nanocomposites from phenyl-bridged organosilane as carbon source. The evidence suggested that the silica/carbon nanocomposites was demonstrated as a unique pore-wall structure, which existed carbon and silica compositions by XRD and TEM. Moreover, Park et al. [64] also reported that $\text{Na}_2/3\text{Fe}_{1/2}\text{Mn}_{1/2}\text{O}_2$ (NFMO) using dihydroxynaphthalene (DN) as carbon source was

prepared. The result indicated that the thin uniform amorphous carbon layer was completely accomplished on the surface of layered pristine material, which was confirmed by XRD, SEM, and TEM. However, the attaching organic moieties as soft and hard template is likely exhibited a good uniform carbon layer of material, but synthetic route is complicated and multiple steps. Therefore, uncomplicated and low synthetic cost route to attain the silica/carbon materials will be further investigated.

3.1.2 Mesoporous carbon from sulfuric acid with carbon residue technique

Although, there are several synthetic routes of mesoporous carbon material as mentioned technique above, but these synthetic techniques are costly and plenty of steps. Thus, sulfonated mesoporous silica/carbon was investigated instead of the soft-hard template or CVD technique. This technique probably takes the advantage of the residue surfactant, which engaged as structure-directing agent in the synthetic mesoporous silica as the carbon source by aiding only sulfuric acid. In addition, the uniform carbon layer is existed over the pore of silica since the surfactant as structure-direct agent have been fully loaded the silica pores with carbonization. Fuertes et al. [47] reported that the synthesis of carbon-silica composites material was accomplished with the carbonization of surfactant utilized as structure-directing agent in mesostructured silica of KIT-6, SBA-15, and MCM-41. The generation of the carbon source was from the surfactant restricted within the mesoporous silica, which based on using the sulfuric acid as converting agent. The result showed that the structural characteristic of these mesoporous carbon was similar to the mesoporous silica by the confirmation of XRD, which indicated that the agglomeration of carbon did not influence to the structural of silica/carbon composites. This method was indicated an easy synthetic route of mesoporous carbon. According to Lee et al. [46] who synthesized the mesocellular carbon foam from direct carbonization of surfactant as structure-directing agent in the as-synthesized mesostructured silica materials with employing sulfuric acid. The result indicated that the appropriated amount of sulfuric acid is 0.16 ml per gram of material because the structure of carbon performed the most uniform pore distribution with slightly changing of surface area and pore size. The

evidence suggested that the sulfuric acid acted as dehydration catalyst, which had to be carefully controlled to the amount for optimization of pore structure. Moreover, Hyeon et al. [48] also indicated that sulfuric acid could convert the surfactant as P123 triblock copolymer to be carbon precursor by the crosslinking of sulfide bridge in mesostructured silica as SBA-15 or MCF. In addition, the removal of silica template could be used 1 M of hydrofluoric acid (HF) or sodium hydroxide (NaOH) to dissolve the cellular framework silica. Therefore, the converting of mesoporous silica to mesoporous carbon can be possibly achieved using the sulfuric acid as dehydration catalyst, which can change the surfactant as structure-directing agent to become the carbon precursor. This method is represented the effective and easy technique for synthesis the mesocellular foam carbon.

3.2 Ethanol dehydrogenation

Several catalysts for ethanol dehydrogenation have been studied for decade such as Cu [27, 29], γ - Al_2O_3 [28], and $\text{VO}_x/\text{SBA-15}$ [19] etc. On the other hand, the carbon catalyst has not been extensively cultivated as the previous mentioned catalysts.

3.2.1 Carbon catalyst

One of the interesting catalysts for ethanol dehydrogenation is carbon due to their suitable physical and chemical properties. Szymanski et al. [65] reported that polymeric carbon and nickel on polymeric carbon as catalyst were used to catalyze ethanol dehydrogenation. It was found that the activated carbon with nickel(II) and oxidized carbon with nitric acid resulted in good catalytic activity. Moreover, a higher dehydrogenation selectivity could be operated at the high reaction temperature. According to Jasinska et al. [66] who investigated the modified surface of activated carbon with dehydrogenation of ethanol to acetaldehyde. The modified surface of carbon performed a high ethanol conversion about 75 % of reaction temperature at 427 °C. Tveritina et al. [67] also investigated the carbon nanotube (CNT), which used to catalyze the ethanol dehydrogenation. The result showed that the main product

was acetaldehyde with 35 % of ethanol conversion, and 97 % of selectivity of acetaldehyde. Furthermore, Ob-eye et al. [36] studied the ethanol dehydrogenation to acetaldehyde using different metals supported on activated carbon as catalyst. The micro packed-bed reactor was used to operate for this reaction with a temperature range of 250-400 °C. The result indicated that the copper doped on an activated carbon performed the best catalytic activity with 65.3 % of ethanol conversion, and 96.3 % of acetaldehyde selectivity at temperature of 350 °C. The evidence suggested that the significant factor as acidity was increased, when the copper was doped on an activated carbon, which could be demonstrated using the ammonia temperature-programmed desorption (NH₃-TPD). In addition, this result can be pointed that the chemical properties as acidity or basicity of solid catalyst should be appropriated values to catalyze the ethanol dehydrogenation process in order to achieve with high conversion or selectivity.

3.2.2 Mesoporous carbon catalyst

Mesoporous carbon has not been widely studied in field of the ethanol dehydrogenation, which is essential importance in synthetic chemistry and the fine chemical industry. Lu et al. [21] reported that mesoporous carbon supported Cu catalyst performed outstanding product selectivity and conversion with 94 % and 73 %, respectively that was compared with mesoporous silica material as SBA-15. The evidence indicated that the insufficient surface groups as -OH of the mesoporous carbon support could decrease the catalytic activity in the secondary reactions of acetaldehyde. This could directly affect to the excellent product selectivity as acetaldehyde on mesoporous carbon supported Cu. Thus, the external texture of carbon exhibited notable utility in the dehydrogenation of ethanol to acetaldehyde.

3.2.3 Mesoporous carbon catalyst with dehydrogenation of other substrates

Zhao et al. [68] studied the ordered mesoporous carbon nitride nanorods, which was synthesized by nanocasting technique with SBA-15 as template, and hexamethylenetetramine as carbon nitride source. This mesoporous carbon material

was operated in dehydrogenation of ethylbenzene to styrene under oxygen and steam free condition. It was found that the mesoporous carbon performed good catalytic activity. According to Yuan et al. [20] investigated ordered mesoporous carbon catalyst for dehydrogenation of propane to propylene. The result showed that the metal-free ordered mesoporous carbon could demonstrate high activity and selectivity. In addition, it also exhibited an excellent stability.

3.3 Catalyst deactivation study in ethanol dehydrogenation

The deactivation of this catalysts is very important issue since it is related with stability of catalyst. Thus, it seems reasonable to investigate the deactivation behavior of MCF-C catalyst via ethanol dehydrogenation in order to better understand the nature of this catalyst [69]. Nevertheless, the general cause to deactivate most catalysts on ethanol dehydrogenation is derived from coke formation. For this aim, it must be discussed that there is the correlation between the decrease in the catalyst activity and the catalyst deactivation from the occurrence of the coke inside of the catalyst. In addition, this verity is a consequence of the heterogeneous nature of the coke in the catalyst, which is possibly composed of amorphous and filamentous fractions, with the cokes of amorphous structure that have a significant impact on catalyst deactivation owing to the encapsulation in the catalyst [70-72]. Thus, several procedures expected at selecting and adapting catalysts have been considered in the literature to minimize the coke deposition in the catalyst. According to Montero *et al.* [73], they investigated the deactivation of Ni/La₂O₃- α -Al₂O₃ catalyst in ethanol steam reforming (ESR) with different operating condition as either temperature between 500-650 °C or space time up to 0.35 g_{catalyst}h/g_{EtOH}. They reported that catalyst deactivation was merely motivated by coke deposition, remarkably via encapsulating coke inside of the catalyst. In addition, Morales et al. [74] also investigated the difference in deactivation of Au catalyst during transformation when supported on ZnO and TiO₂. The evidence suggested that the catalyst on ZnO demonstrated higher resistance to deactivation caused by coke formation. Therefore, the selection of catalysts in each specific reaction is captivating to exhibit either high activity or resistance to deactivation

caused by coke formation. It is known that the decline in deactivation of catalyst is regularly followed by an increase in the carbon content on the catalyst surface with different conditions.

3.4 Effect of pore sizes on catalytic activity

Synthetic mesoporous materials have been splendid attention cause its application in shape/size-selective catalysis. In addition, it not only performed the unique pore shapes, but is also show the narrow pore size distribution, which may directly affect to the diffusion of the reactant into the pore of materials. Thus, the limited control over the pore size of mesoporous material has been investigated for catalytic activity as ethanol dehydrogenation, which is lack of study in this field. Li et al. [75], they investigated the preparation of Cu-Ce catalysts with different magnitude of pore size, which were used for CO oxidation reaction. The result showed that the enlarge pore size of catalysts was providable for either the formation of the active surface species or the catalytic activity supplemented. In addition, Yuan et al. [76] also investigated the synthesis of catalysts with different pore size by varying the amount of the swelling agent such as 1,3,5- trimethylbenzene for utilizing on hydrodesulfurization reaction. The evidence suggested that the pore size of catalysts could notably affect to the catalytic activity. In contrast, chemical properties of meocellular foam silica as acidity and basicity are still insufficient for dehydrogenation of ethanol to acetaldehyde. Furthermore, N. Pahalagedara et al. [77] investigated the effect of pore size on the catalytic activity using the ordered mesoporous NiAl mixed metal oxides (MMOs) from NiAl layered double hydroxides (LDHs) via a soft template preparation. It was found that the optimum pore diameter of this reaction was 7.7 nm among 3.4-9.4 nm, which excellently performed 99% of ethanol conversion with a 100% selectivity. Therefore, this topic review can indicate the effect of pore size of material on catalytic activity, which possibly enhance the ethanol dehydrogenation.

CHAPTER 4

EXPERIMENTAL

This chapter describes experimental synthesis parts of the catalysts namely Mesocellular foam silica (MCF-Si), Mesocellular foam silica/carbon (MCF-Si-C), Mesocellular foam carbon (MCF-C), which were characterized by N₂-physisorption (BET and BJH), X-Ray diffraction (XRD), scanning electron microscopy (SEM) and energy dispersive X-ray spectroscopy (SEM-EDX), transmission electron microscopy (TEM), Fourier-transform infrared spectroscopy (FT-IR), thermalgravimetric analysis (TGA), ammonia temperature programmed desorption (TPD-NH₃), carbon dioxide temperature programmed desorption (TPD-CO₂). In addition, the catalysts were tested in ethanol dehydrogenation process.

4.1 Catalysts preparation

4.1.1 Chemicals and reagents

1. Pluronic P123 (Sigma-Aldrich, Molar mass ~5800)
2. 1,3,5-trimethyl benzene (TMB), (Sigma-Aldrich)
3. Tetraethyl Orthosilicate (TEOS, 98 % purity), (Sigma-Aldrich)
4. Deionized water (DI water)
5. Ethanol 99.95 % (Sigma-Aldrich)
6. Hydrochloric acid (HCl, 98 % wt.), (Sigma-Aldrich)
7. Sulfuric acid (H₂SO₄, 98 % wt.), Sigma Aldrich)
8. Sodium hydroxide (NaOH), (Sigma-Aldrich)

4.1.2 Preparation of mesocellular foam materials as catalysts

4.1.2.1 Mesocellular foam silica (MCF-Si)

The MCF-Si was prepared with the similar procedure as reported in the previous works [78]. First, 2 g of triblock copolymer Pluronic P123 was used as the template and carbon precursors for the mesoporous carbon. It was dissolved in 65 ml of deionized water and 10 ml of hydrochloric acid at room temperature, and was kept at the same temperature until a homogeneous solution was obtained (ca. 1 h). Then, 1, 3, 5, 7, and 9 g of TMB, as the swelling agent, was added into the previous solution at 40 °C, and was followed by stirring for 2 h. After 2 h, 4 g of TEOS, as the silica source, was added and vigorously stirred at 40 °C for 5 min. The obtained white solution was then aged in the oven at 40 °C for 20 h, and then temperature was ramped at 10 °C/min to 100 °C and kept constant for 24 h. Finally, the obtained white precipitate was consecutively washed by 50 ml of ethanol, and deionized water until the pH of the filtrate was unchanged. The product was dried overnight at ambient temperature. The white powder of MCF-Si was finally obtained.

4.1.2.2 Mesocellular foam silica/carbon (MCF-Si-C)

First, 1 g of MCF-Si obtained from section 4.1.2.1 was mixed with 0.16 ml of sulfuric acid, and stirred for 1 h. Then, the mixture was dried in oven at 100 °C for 12 h. After that, the oven temperature was increased to 160 °C and held for 12 h. The dark brown powder of MCF-Si-C was obtained by calcination at 850 °C under nitrogen flowing for 2 h.

4.1.2.3 Mesocellular foam carbon (MCF-C)

The MCF-C was obtained by etching MCF-Si-C from section 4.1.2.2. It was achieved by using 2 M of NaOH to etch the silica out of the MCF-Si-C at room temperature under low stirring for 1 h. After that, it was washed with deionized water until the pH of the filtrate was constant. Next, it was dried for 24 h at room temperature. Finally, the black powder of MCF-C was obtained.

4.2 Characterization of the mesocellular foam materials

4.2.1 Nitrogen-physorption

The surface area, pore size and pore volume of all samples were measured by nitrogen-physorption using Micromeritics ChemiSorb 2750 Pulse instrument. Determination of Brunauer-Emmet-Teller (BET) isotherm equation was operated at -196 °C, and the samples were degassed with heating in the vacuum oven at ambient temperature to 120 °C for 16 h. In addition, Barrett-Joyner-Halenda (BJH) method based on the Kelvin equation was also applied to determine the pore structure of samples.

4.2.2 Scanning electron microscopy (SEM) and energy dispersive X-ray spectroscopy (EDX)

The morphology of samples was investigated using scanning electron microscopy (SEM), which was identified using the Hitachi S-3400N model. Link Isis Series 300 program EDX was used to analyze the elemental distribution and composition over different catalysts.

4.2.3 Transmission electron microscopy (TEM)

TEM was used to examine the morphology of samples using JEOL JEM-2010 with the thermionic electron type LaB₆ as a source with operating at 200 kV.

4.2.4 X-ray diffraction (XRD)

XRD was used to measure the crystalline framework of samples using a Siemens D 5000 X-ray diffractometer having CuK α ($\lambda = 1.54439 \text{ \AA}$) radiation with Ni filter in the range of 2θ between 10 to 80 with 0.04 resolution. The scan rate was applied at 0.5 sec/step.

4.2.5 Thermogravimetric analysis (TGA)

TGA was performed using TA instrument SDT Q600 analyzer (USA). The sample of 4-10 mg was used in the temperature operation range between 30 to 1000 °C with heating rate of 2 °C/min using air as carrier gas.

4.2.6 Fourier transform infrared (FT-IR) spectroscopy

The functional groups of all samples were analyzed using the FTIR spectroscopy. The observable absorption spectra were obtained using Nicolet 6700 FTIR spectrometer in the wavenumber range of 400 to 4000 cm^{-1} .

4.2.7 Ammonia temperature-programmed desorption (NH_3 -TPD)

The acidity and acid strength of samples were determined using Micromeritics Chemisorb 2750 Pulse Chemisorption System. First, 0.1 g of sample was preheated with helium at 200 °C. Then, ammonia was adsorbed at 40 °C for 1 h. After that, the physisorbed ammonia was desorbed under helium gas flow until the baseline level achieved constant. After that, the chemisorbed ammonia was removed from active sites by increasing the temperature from 30 to 500 °C under a helium flow at 40 ml/min, with a heating rate of 10 °C/min. The thermal conductivity detector (TCD) as a function of temperature was applied to measure the amount of ammonia in effluent.

4.2.8 Carbon dioxide temperature-programmed desorption (CO_2 -TPD)

The basicity and basic strength of samples were measured by CO_2 -TPD using Micromeritics Chemisorb 2750 automated system. The sample powder of 0.1 g was packed into the quartz cell and preheated at 450 °C under a helium flow at 25 ml/min for 1 h to evacuate moisture and impurity. Then, the sample was saturated with CO_2 and evacuated by helium with flow rate of 35 ml/min for 30 min at 40 °C. After that, the temperature-programmed desorption was operated from 40 °C to 500 °C with a heating rate of 10 °C/min. Thermal conductivity detector (TCD) was used to analyze the amount of CO_2 in effluent gas as a function of desorbed temperature.

4.3 Ethanol dehydrogenation testing

4.3.1 Chemical and reagents

1. Absolute ethanol (99.95%), (Merck)
2. Ultra-high purity grade nitrogen (99.999%), (Linde)
3. Ultra-high purity grade argon (99.999%), (Linde)
4. Ultra-high purity grade hydrogen (99.999%), (Linde)

4.3.2 Instrument and apparatus

The ethanol dehydrogenation reaction process is represented in flow diagram of figure 4.1 which consists of a gas controlling system, a syringe pump, a vaporizer, reactor, an electric furnace, a temperature controller and a gas chromatograph.

(1) Gas controlling system: The flow rate of carrier gas (N_2) is adjusted by mass flow controller. The pressure regulator and on-off valve were equipped in this system in order to control gas flow.

(2) Syringe Pump: Liquid ethanol was injected to the vaporizer by the syringe pump.

(3) Vaporizer: Liquid ethanol was vaporized in the vaporizer at a temperature of 120°C .

(4) Reactor: The borosilicate glass tube reactor with inside diameter of 0.7 was used as a reactor. The center of reactor was packed with catalyst on quartz wool layer.

(5) Electric Furnace: the reactor and vaporizer were heated by the electric furnace. The temperature of furnace is controlled by temperature controller with the maximum voltage of 220 volt.

(6) Temperature controller: The temperature of electric furnace was set by the temperature controller in a range between 150°C to 400°C . The temperature controller was connected to a variable voltage transformer and a thermocouple which attached to the reactor.

(7) Gas Chromatograph (GC): Light hydrocarbon such as ethylene, ethanol, acetaldehyde, etc. were analyzed by a gas chromatograph (Shimadzu GC-14A) equipped with flame ionization detector (FID) and DB-5 capillary column. A Shimadzu GC-8A gas chromatograph equipped with thermal conductivity detector (TCD), molecular sieve 5A and Porapak Q column was used to analyze carbon dioxide, carbon monoxide and oxygen in the stream. The operating conditions of GC are shown in the **Table 4.1**.

Table 4. 1 Operating conditions for gas chromatographs.

Gas chromatographs	Shimadzu GC-8A		Shimadzu GC 14B
Detector	TCD	TCD	FID
Column	Molecular sieve 5A	Porapak Q	DB5
Maximum temperature	350°C	150°C	350°C
Carrier gas	He (99.999%)	He (99.999%)	N ₂ (99.999%)
Carrier gas flow	40 cc/min	-	-
Column temperature			
Initial (°C)	60	60	40
Final (°C)	60	60	40
Injection temperature (°C)	100	100	150
Detector temperature (°C)	-	-	150
Current (mA)	80	80	-
Analyzed gas	CO, O ₂ , N ₂	CO ₂ , CH ₄ , C ₂ H ₄	Ethanol, acetaldehyde, ethylene, diethyl ether

4.3.3 Ethanol dehydrogenation reaction

The performance of all MCF catalyst materials was determined using the ethanol dehydrogenation test apparatus using a fixed-bed continuous flow glass tube microreactor. First, 0.1 g of a catalyst sample and 0.05 g of quartz wool bed were packed inside of the central glass tube reactor which was located inside of the electric furnace. The pretreatment at 200 °C under nitrogen flowing for 1 h was operated to remove the moisture on the surface of target catalyst. Then, the liquid ethanol was vaporized at 120 °C with nitrogen gas at 60 ml/min using controlled injection with a single syringe pump using the volumetric flow rate of ethanol feeding at 0.397 ml/h. The gas stream was reached to the reactor with weight hourly space velocity (WHSV) of 3.1 g_{ethanol}/g_{cat}.h. The considerable operating temperature range was 250 to 400 °C

under atmospheric pressure. The gaseous products were analyzed by a Shimadzu (GC-14B) gas chromatograph with flame ionization detector (FID) using capillary column (DB-5) at 150 °C. While the reaction test was operating, the results were recorded at least 3 times for each temperature as figure 4.1.

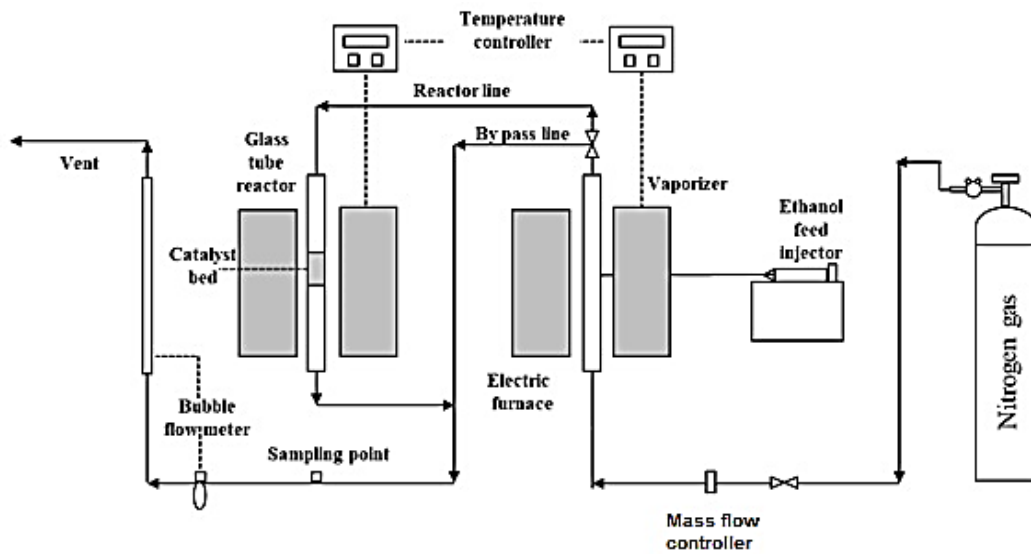


Figure 4.1 Flow diagram of the catalytic dehydrogenation of ethanol.

The values of ethanol conversion, selectivity of acetaldehyde, and yield of acetaldehyde were analyzed using respectively the following equations.

$$\text{Ethanol conversion: } X_{EtOH}(\%) = \frac{n_{EtOH}(in) - n_{EtOH}(out)}{n_{EtOH}(in)} \times 100 \quad (1)$$

$$\text{Selectivity of acetaldehyde: } S_i(\%) = \frac{n_i}{\sum n_i} \times 100 \quad (2)$$

$$\text{Yield of acetaldehyde: } Y_i(\%) = \frac{X_{EtOH} \times S_i}{100} \quad (3)$$

where mol_i is the mole of concerned product and $\sum mol_i$ is the total moles of obtainable products.

4.4 Stability test

The catalyst samples were evaluated for the stability as a function of time on stream (TOS) for 12 h. The experiment apparatus and set-up were similar to those of temperature-programmed reaction studies as mentioned above. The ethanol dehydrogenation reaction was conducted at 400 °C. The product from the reaction was collected every 1 h for 20 h with time on steam.



CHAPTER 5

RESULTS AND DISCUSSION

This chapter is classified to be 3 parts in order to understand the synthesis process of MCF-C catalyst in the first part, and also followed by studying the catalyst deactivation in MCF-C in the second part. In addition, the third part is to investigate the effect of pore size of MCF-C. All parts were operated under ethanol dehydrogenation process.



Synthesis, characteristics and application of mesocellular foam carbon
(MCF-C) as catalyst for dehydrogenation of ethanol to acetaldehyde

Yootapong Klinthongchai, Seeroong Prichanont,

Piyasan Prasertdam and Bunjerd Jongsomjit*

Center of Excellence on Catalysis and Catalytic Reaction Engineering

Department of Chemical Engineering, Faculty of Engineering,

Chulalongkorn University, Bangkok 10330, Thailand

*Corresponding author, email: bunjerd.j@chula.ac.th,

Tel: 62-2186874, Fax: 62-2186877

Journal of Environmental Chemical Engineering, 8 (2020) 103752



จุฬาลงกรณ์มหาวิทยาลัย
CHULALONGKORN UNIVERSITY

Part 1: Synthesis, characteristics and application of mesocellular foam carbon (MCF-C) as catalyst for dehydrogenation of ethanol to acetaldehyde

Abstract

This research focused on synthesis of mesocellular foam carbon (MCF-C) and this catalyst was employed dehydrogenation of ethanol to acetaldehyde. The mesocellular foam silica (MCF-Si) was used as the template of material following by converting the surfactant residue (Pluronic P123) into carbon layers using H_2SO_4 and NaOH etching. The obtained MCF-C exhibited the highest surface area of $995\text{ m}^2/\text{g}$ among these materials, and mesoporous size of 4.2 nm with spherical shape and interconnected pore. Furthermore, total acidity of MCF-C also increased from 427.07 (MCF-Si) to $682.64\text{ }\mu\text{mole}$. In the part of catalytic test, the MCF-C was used in gas-phase ethanol dehydrogenation at 200 to $400\text{ }^\circ\text{C}$. It revealed that the MCF-C exhibited the highest ethanol conversion (ca. 17.5%) at $400\text{ }^\circ\text{C}$ due to its high acidity without significant deactivation of catalyst within 12 h . Besides, its high ethanol conversion, it is worth noting that the acetaldehyde selectivity (ca. 80.3%) was also high, especially at $400\text{ }^\circ\text{C}$. This can be attributed to the proper mesoporous size that can facilitate the diffusion of acetaldehyde without further decomposing at high temperature.

Keywords : mesocellular foam carbon; ethanol dehydrogenation; acetaldehyde, solid catalysts

5.1 Introduction

Mesocellular foam silica (MCF-Si) [1-5] is one of the most captivating mesoporous materials having the large pore size and spherical shape with interconnected pore. Furthermore, it contains silanol group (-OH) on the surface, which can be appropriately modified by functionalization for improvement of its properties [6-9]. The general application of MCF includes the support for copper as catalyst for methanol synthesis [10, 11] and carrier for immobilization of enzyme in biosensor [12, 13]. Furthermore, it can be used as the support in CO₂ capture and toxic pollutants from air [14-17]. These advantages in characteristics of MCF probably facilitate the diffusion of the target reactant because of its appropriate pore size. In addition, it also likely helps to prevent the collapse of pore structure during high temperature because of well heat transfer released by interconnected pore [18]. However, there are still disadvantages for chemical properties of MCF such as low acidity and basicity, which are required as active sites for intrinsic catalytic activity on catalytic process including dehydrogenation of ethanol [19]. Accordingly, mesoporous carbon is one of the interesting choices, which is mesoporous structure and suitable chemical properties for improving the lack of acidity and basicity properties that are crucial for dehydrogenation of ethanol in this work. Previously, Liu et al. [20] investigated ordered mesoporous carbon in direct dehydrogenation of propane to propylene with high activity and selectivity. Later, Wang et al. [21] reported the use of Cu supported on mesoporous carbon derived from SBA-15 as hard template in dehydrogenation of ethanol to acetaldehyde. It was found that increased selectivity was evident using Cu/mesoporous carbon (MCF-C) compared with that obtained from Cu/SBA-15. It indicated that plenty of silanol groups on SBA-15 favors the minor reaction, which is possible to obtain low selectivity of acetaldehyde [21]. According to the research reported by Obe-eye et al. [22], they investigated the production of acetaldehyde using activated carbon with Co loading in ethanol dehydrogenation. The result pointed that 4 wt% of Co loading on activated carbon performed high catalytic activity due to its high acidity and basicity. Therefore, the MCF-C is perhaps promising as catalyst for ethanol dehydrogenation to acetaldehyde because it can provide high stability at high reaction temperature operation. It also indicates that enlarge pore size and interconnected pore potentially

facilitate the transport phenomena of reactants and products between pores. Moreover, it can inhibit the formation of byproducts because of its suitable acidity and basicity.

Ethanol is one of the renewable energy sources, which can be easily produced by fermentation of biomass such as sugarcane, corn, wheat, cassava, etc. However, in the unavailability of biomass resources, ethanol can be produced by catalytic hydration of ethylene via petrochemical process [23-25]. Ethanol has been widely studied for decades as a potential raw material for production of other value-added chemicals such as ethylene, diethyl ether, acetaldehyde and ethyl acetate [26, 27]. Among ethanol-derived products, acetaldehyde is remarkably interesting in field of chemical reactants at the beginning of the process in industries for production of ethyl acetate, acetic acid, acetic anhydride and isobutanol [28, 29]. Moreover, it is also used in the food engineering for storage the food as a preservative agent [30]. Currently, there are different reaction routes to produce acetaldehyde in industries including; (1) partial oxidation of ethane using palladium chloride (PdCl_2) catalyst, which is not only an expensive catalyst, but also uses high reaction temperature for operation [31], (2) hydration of acetylene, which has to spend mercury (Hg) to form mercuric complex that is toxic material for the environmental concern [32] and (3) oxidation of ethylene from petroleum and natural gas. However, the operating cost of this process is expensive, and it needs high volume of HCl for catalyst regeneration [33]. Hence, the noticeable reaction of acetaldehyde production from ethanol dehydrogenation, which is not only uncomplicated, but also used ethanol as renewable sources and non-toxic process [6-10] is so captivating. There are many catalysts used in ethanol dehydrogenation such as TiO_2 [34], Al_2O_3 [27] SBA-15 [19], and activated carbon [35]. Although there are many studies of catalysts used in ethanol dehydrogenation process, it still needs to improve the catalysts, which is not only for higher conversion, selectivity or even yield, but also proper thermal stability. There have been only few studies of the acetaldehyde production by ethanol dehydrogenation using mesocellular foam silica (MCF-Si) as the mesoporous materials with spherical shape and interconnected pore [36]. To the best of our knowledge, no work in the literature

has been yet reported on the use of MCF-C as the catalyst for ethanol dehydrogenation to acetaldehyde.

Thereby, this work aims to investigate the synthesis, characteristics and the application as the dehydrogenation catalyst for ethanol dehydrogenation to acetaldehyde of mesocellular form carbon (MCF-C) derived from the mesocellular form silica (MCF-Si). In addition, to synthesize these materials, it used the surfactant such as the PEO-EO-PEO triblock copolymer (Pluronic P123). It was not only structure-directing agent for template, but it is also used as carbon source for the MCF-C synthesis as well. All synthesized materials were characterized using various techniques and were tested in dehydrogenation of ethanol to measure the catalytic behaviors.

5.2 Experimental

Chemicals

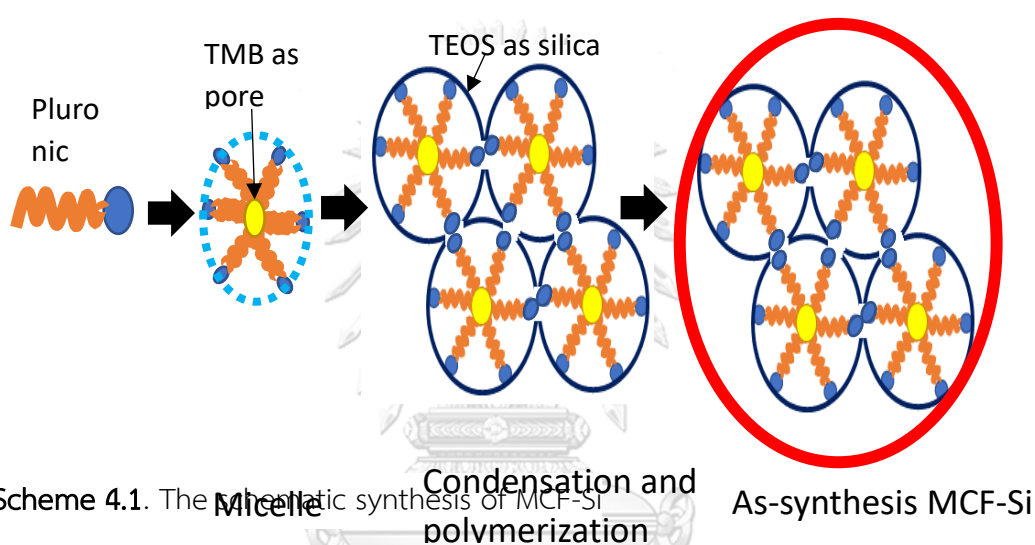
The chemicals were used in this work, which used the analytical grade. Pluronic P123 (Sigma-Aldrich, Molar mass ~ 5800) was used as the surfactant, and hydrochloric acid (HCl (98 wt%), Sigma-Aldrich) was used as a catalyst in the synthesis of MCF-Si. In addition, 1,3,5-trimethylbenzene (TMB, Sigma-Aldrich) was used as the expander of the pore of material. The silica source was from tetraethyl orthosilicate (TEOS; 98% purity, Sigma-Aldrich). Sulfuric acid (H₂SO₄ (98 wt %), Sigma Aldrich) was used as the catalyst of formation of carbon layer. The removing of silica out was used as sodium hydroxide (NaOH, Sigma Aldrich).

5.2.1 Preparation of mesocellular foam materials

5.2.1.1 Mesocellular foam silica (MCF-Si)

The MCF-Si was prepared with the similar procedure as reported by the previous works [37-40]. First, 2 g of triblock copolymer Pluronic P123 was used as the template and carbon precursors for the mesoporous carbon. It was dissolved in 65 ml of deionized water and 10 ml of hydrochloric acid at room temperature, and kept it at that temperature until it became homogeneous solution (ca. 1 h). Then, 5 g of TMB as the swelling agent was added into the previous solution at 40 °C, which was followed by stirring for 2 h. After reaching 2 h, 4 g of TEOS as the silica source was added and vigorously stirred at previous constant temperature for 5 min. The obtained

white solution was aged in the oven at 40 °C for 20 h, and temperature was increased to 100 °C for 24 h with the ramp of 10 °C/min. Finally, the white precipitate was not only consecutively washed by 50 ml of ethanol, but also washed by deionized water until the pH of filtrate was unchanged, and dried overnight at ambient temperature. The white powder of MCF-Si was obtained. The schematic synthesis of MCF-Si is illustrated in **Scheme 1**.



5.2.1.2 Mesocellular foam silica/carbon (MCF-Si-C)

The MCF-Si-C was prepared with the similar procedure as reported by the previous work [41, 42]. First, 1 g of MCF-Si obtained from section 2.1.1 was mixed with 0.16 ml of sulfuric acid with stirring for 1 h. Then, the mixture was dried in oven at 100 °C for 12 h. After that, the oven temperature was increased to 160 °C and held at that temperature for 12 h. The obtained dark brown powder was carried out by calcination at 850 °C under nitrogen flowing for 2 h to obtain MCF-Si-C.

5.2.1.3 Mesocellular foam carbon (MCF-C)

The MCF-C was obtained by etching process of the hybrid composites material as MCF-Si-C of section 2.1.2 [43]. It was achieved by using 2 M of NaOH to etch the silica out of the MCF-Si-C at room temperature with slowly stirring for 1 h. After that, it was washed with deionized water until the pH of the filtrate was constant. In addition, it was dried for 24 h at room temperature. Finally, the black powder of MCF-C was obtained.

5.2.2 Characterization of mesocellular foam materials

Nitrogen-physisorption

The surface area, pore size and pore volume of all samples were measured by nitrogen-physisorption using Micromeritics ChemiSorb 2750 Pulse instrument. Determination of Brunauer-Emmet-Teller (BET) isotherm equation was operated at -196 °C, and the samples were degassed with heating in the vacuum at ambient temperature to 120 °C for 16 h. In addition, Barrett-Joyner-Halenda (BJH) method based on the Kelvin equation was also applied to determine the pore structure of samples [44].

Transmission electron microscopy (TEM)

TEM was used to examine the morphology of samples using JEOL JEM-2010 with the thermionic electron type LaB₆ as a source with operating at 200 kV.

Scanning electron microscopy (SEM)

The morphology of samples was identified using the Hitachi S-3400N model. Link Isis Series 300 program EDX was used to analyze the elemental distribution and composition over different catalysts.

X-ray diffraction (XRD)

XRD was used to measure the crystalline framework of samples using a Siemens D 5000 X-ray diffractometer having CuK_α radiation with Ni filter in the range of 2θ between 10-80 with 0.04 resolution. The scan rate was applied at 0.5 sec/step.

Thermogravimetric analysis (TGA)

TGA was performed using TA instrument SDT Q600 analyzer (USA). The sample of 4-10 mg was used in the temperature operation range between 30 to 1000 °C with heating rate of 2 °C/min using air as carrier gas.

Fourier transform infrared (FT-IR) spectroscopy

The functional groups of all samples were analyzed using the FTIR spectroscopy. The observable absorption spectra were obtained using Nicolet 6700 FTIR spectrometer in the wavenumber range of 400 to 4000 cm^{-1} .

Ammonia temperature-programmed desorption (NH_3 -TPD)

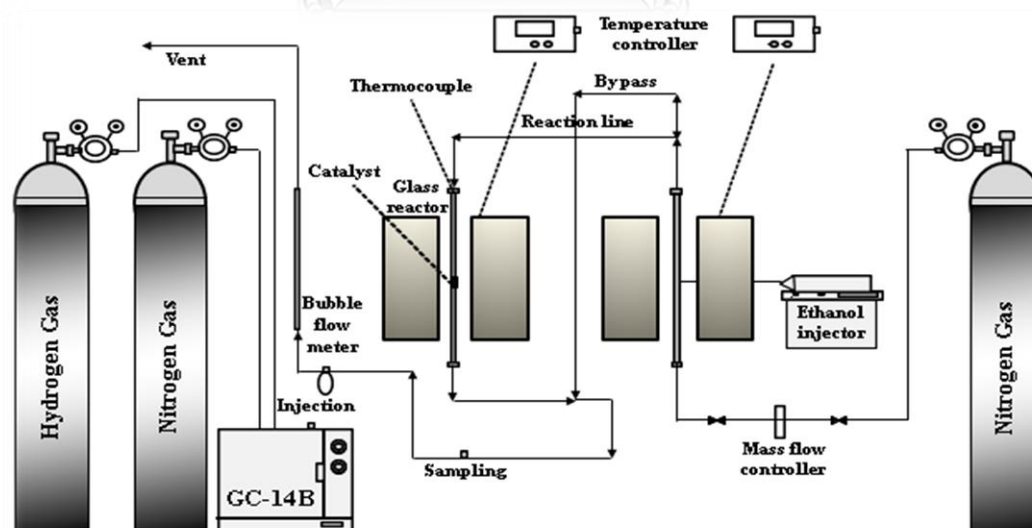
The acidity and acid strength of samples were determined using Micromeritics Chemisorb 2750 Pulse Chemisorption System. First, 0.1 g of sample was preheated with helium at 200 °C. Then, ammonia was adsorbed at 40 °C for 1 h. After that, the physisorbed ammonia was desorbed under helium gas flow until the baseline level was achieved to be constant. After that, the chemisorbed ammonia was removed from active sites by increasing the temperature from 30 to 500 °C under a helium flowing at 40 ml/min, with a heating rate of 10 °C/min. The thermal conductivity detector (TCD) as a function of temperature was applied to measure the amount of ammonia in effluent.

Carbon dioxide temperature-programmed desorption (CO_2 -TPD)

The basicity and basic strength of samples were measured by CO_2 -TPD using Micromeritics Chemisorb 2750 automated system. The sample powder of 0.1 g was packed into the quartz cell and preheated at 450 °C under helium with flow rate of 25 ml/min for 1 h to evacuate moisture and impurity. Then, the sample was saturated with CO_2 and evacuated by helium with flow rate of 35 ml/min for 30 min at 40 °C. After that, temperature-programmed desorption was operated from 40 °C to 500 °C with heating rate of 10 °C/min. Thermal conductivity detector (TCD) was used to analyze the amount of CO_2 in effluent gas as a function of desorbed temperature.

5.2.3 Ethanol dehydrogenation reaction

The performance of all MCF catalyst materials was determined using the ethanol dehydrogenation test apparatus using a fixed-bed continuous flow glass tube microreactor. First, 1 g of catalyst sample and 0.05 g of quartz wool bed were packed inside of the central glass tube reactor, which was located inside of the electric furnace. The pretreatment at 200 °C under nitrogen flowing for 1 h was operated to remove the moisture on the surface of target catalyst. Then, the liquid ethanol was vaporized at 120 °C with nitrogen gas at 60 ml/min using controlled injection with a single syringe pump using the volumetric flow rate of ethanol feeding at 0.397 ml/h. The gas stream was reached to the reactor with weight hourly space velocity (WHSV) of 3.1 $\text{g}_{\text{ethanol}}/\text{g}_{\text{cat}}\cdot\text{h}$. The considerable operating temperature range was 250 to 400 °C under atmospheric pressure. The gaseous products were analyzed by a Shimadzu (GC-14B) gas chromatograph with flame ionization detector (FID) using capillary column (DB-5) at 150 °C. While the reaction test was operating, the results were recorded at least 3 times for each temperature as **Scheme 2**.



Scheme 4.2 Flow diagram of ethanol dehydrogenation system.

The values of ethanol conversion, selectivity of acetaldehyde, and yield of acetaldehyde were analyzed using following these equations (1), (2), and (3), respectively.

$$\text{Ethanol conversion} : X_{EtOH}(\%) = \frac{n_{EtOH(in)} - n_{EtOH(out)}}{n_{EtOH(in)}} \times 100 \quad (1)$$

$$\text{Selectivity of acetaldehyde} : S_i(\%) = \frac{n_i}{\sum n_i} \times 100 \quad (2)$$

$$\text{Yield of acetaldehyde} : Y_i(\%) = \frac{X_{EtOH} \times S_i}{100} \quad (3)$$

where mol_i is the mole of concerned product and $\sum mol_i$ is the total moles of obtainable products.

5.2.4 Stability test

The catalyst samples were evaluated for the stability as a function of time on stream (TOS) for 12 h. The experiment apparatus and set-up were similar to those of temperature-programmed reaction studies as mentioned above. The ethanol dehydrogenation reaction was conducted at 400 °C. The product from the reaction was collected every 1 h for 12 h with time on steam.



5.3 Result and Discussion

5.3.1 Catalyst Characterization

5.3.1.1 Surface area and pore structure

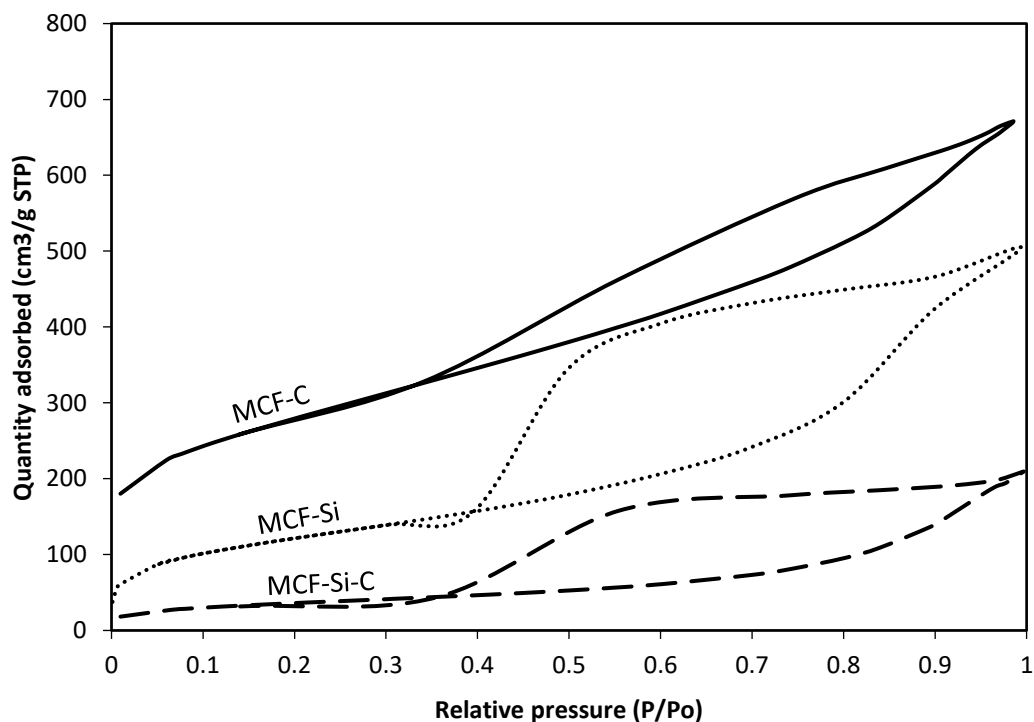


Figure 5. 1 Nitrogen adsorption/desorption isotherms of all synthesized catalysts.

Figure 5.1 shows the adsorption/desorption isotherms of MCF-Si, MCF-Si-C, and MCF-C. All samples represented type IV of hysteresis loop [45]. This result indicated that the mesoporous structure was achieved with these synthetic methods of materials. In addition, the hysteresis loops were of the H2b type, which was indicated restricted pore or pore blocking due to the ink-bottle geometry or restrictions within a porous network. This evidence suggested that the character of these materials likely played important roles of diffusion of reactant, which possibly increased contact time of the reaction between the reactant and the solid catalyst.

Table 5. 1 Surface area (BET), average pore size and average pore volume.

Materials	Surface area (m ² /g)	Average pore size (nm)	Average pore volume (cm ³ /g)
MCF-Si	437	7.1	0.99
MCF-Si-C	133	9.8	0.32
MCF-C	995	4.2	1.13

Table 5.1 shows surface area (BET), average pore size and average pore volume of all samples calculated from BJH model [44]. Among of all MCF materials, MCF-C showed the highest BET surface area (995 m²/g) and the smallest average pore size (4.2 nm), which is still in the mesoporous range (larger than 2 nm). The result indicated that large surface area was not only traded off with small pore size of catalyst, but also from the removal of silica out by etching with NaOH. This is likely suitable for reactants for diffusion into these mesoporous materials.

5.3.1.2 Textural property and morphology

MCF-C was synthesized from MCF-Si as a based component, which was followed by adding the sulfuric acid for converting surfactant residue to be carbon source. Then, MCF-Si-C was converted to the MCF-C by etching with NaOH. **Figure 5.2** shows the comparison of morphologies for all samples obtained from TEM. In fact, differences in morphologies were observed in each part of the synthesis. These results are in accordance with those from N₂ physisorption results. As seen, the MCF-Si originally exhibited a well-defined pore structure, whereas the MCF-Si-C showed the similar structure as the former one, but the MCF-Si-C apparently presented clearer pore size than MCF-Si, indicating that carbon layer was generated after treated with H₂SO₄. The evidence showed that the carbon layer forming could be seen in the MCF-

Si-C, which the walls of the material were apparent more than the pore of the material that meant to be the appearance of carbon layer in the pore.

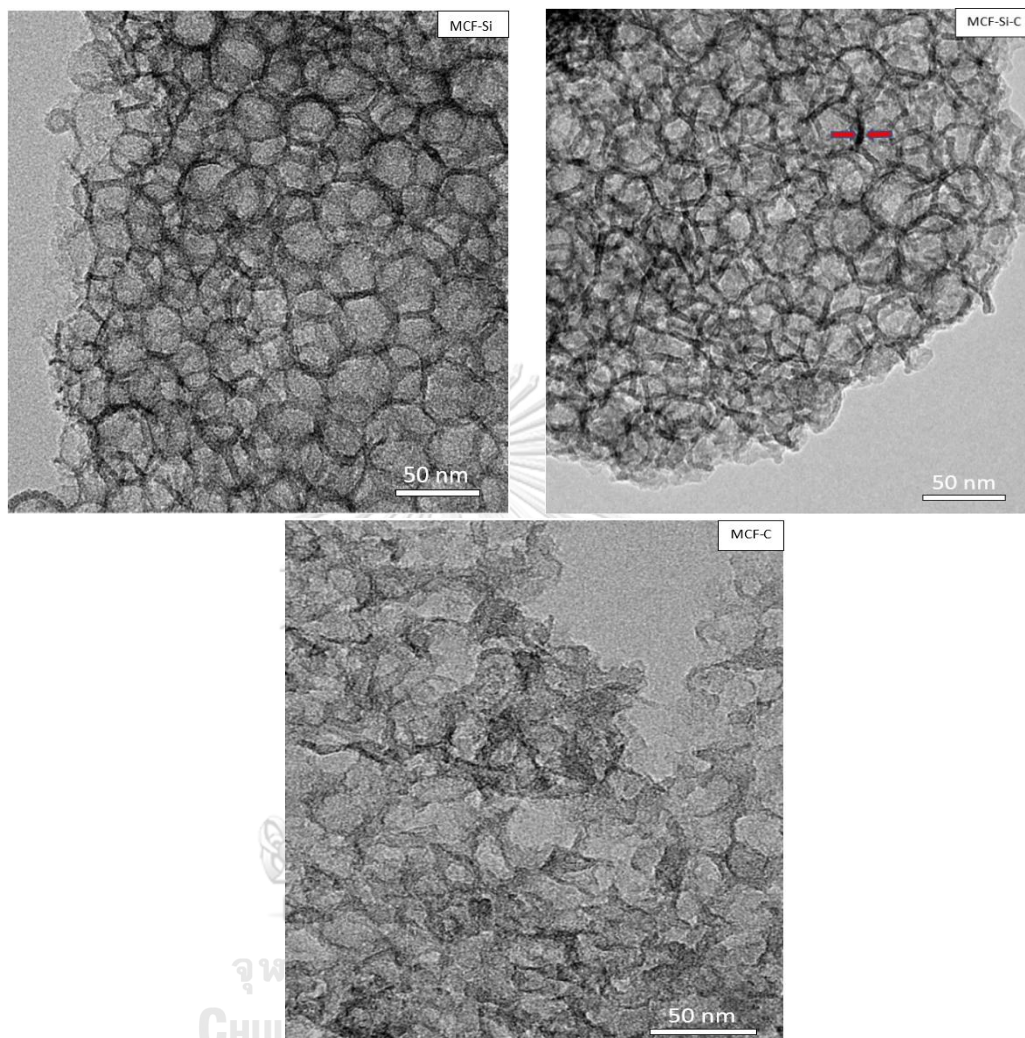


Figure 5. 2 TEM images of MCF-Si, MCF-Si-C, and MCF-C catalysts.

However, after etching of MCF-Si-C by NaOH to obtain the MCF-C, it revealed unwell-defined pore structure of MCF-C due to the collapse of silica wall during etching process. Furthermore, the carbon layer was not thick enough to maintain the well-defined pore structure as seen in this for the MCF-Si and MCF-Si-C. However, some of pore structure in MCF-C can still maintain as conventional pore structure, suggesting that some point of the wall may be thick enough to maintain the spherical structure during the synthesis.

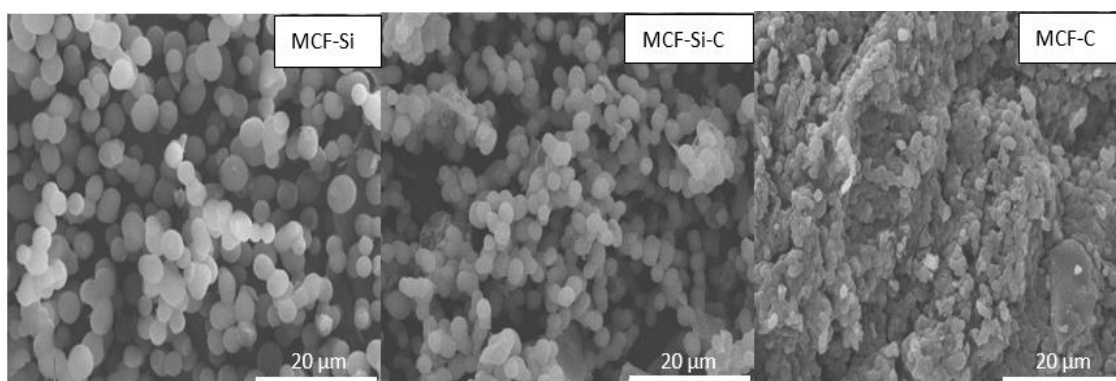


Figure 5.3 Low magnification SEM image of MCF-Si, MCF-Si-C, MCF-C.

Figure 5.3 shows the SEM images of MCF-Si, MCF-Si-C, and MCF-C. An average particle size of MCF-Si and MCF-Si-C are ca. 2.2-2.5 μm ($n = 200$), while the average particle size of MCF-C is ca. 1.25 μm ($n=200$). The reduction of particle size was caused by the etching process resulting in different particles sizes. The morphology of MCF-Si particles was similar to those of MCF-Si-C indicating that sulfuric acid did not affect the outside structure, but it only changed the inside structure. It converted the surfactant to carbon structure by etching with NaOH as seen in MCF-C. Energy dispersive X-ray spectroscopy (EDX) results as seen in **Table 5.2** may be used to confirm the phase change by detecting the atomic percent composition of MCF-Si to MCF-Si-C, and MCF-Si-C to MCF-C. In fact, silicon (Si) was detected in MCF-Si, MCF-Si-C, and MCF-C as 47.17, 45.28, and 0.57 percent, respectively.

Table 5.2 The amount of each element near the surface of catalyst granule obtained from EDX.

Materials	Amount of weight on surface (wt%)		
	Si	O	C
MCF-Si	47.17	42.86	9.96
MCF-Si-C	45.28	31.54	23.17
MCF-C	0.57	7.04	92.38

It was found that the silicon in MCF-C was almost completely removed by NaOH etching having carbon remains at 92.38 wt%. Therefore, the surfactant residue was mostly converted to carbon structure as expected. Moreover, it was also shown that the hybrid of carbon and silicon in MCF-Si-C were at 45.28 wt% and 23.17 wt%, respectively. This is possibly synergy between carbon and silicon of MCF-Si-C in terms of chemical properties to catalyze ethanol dehydrogenation.

5.3.1.3 Crystal structure

The crystal structures of MCF-Si, MCF-Si-C, and MCF-C were determined using powder X-ray diffraction (XRD) as shown in **Figure 5.4**. The low-angle XRD patterns of MCF-Si and MCF-Si-C were similar with dominant peak at 1.55° (red line) indicating that with the presence of carbon layer inside silicon surface [42], the MCF-Si-C can still maintain the similar structure as seen from MCF-Si.

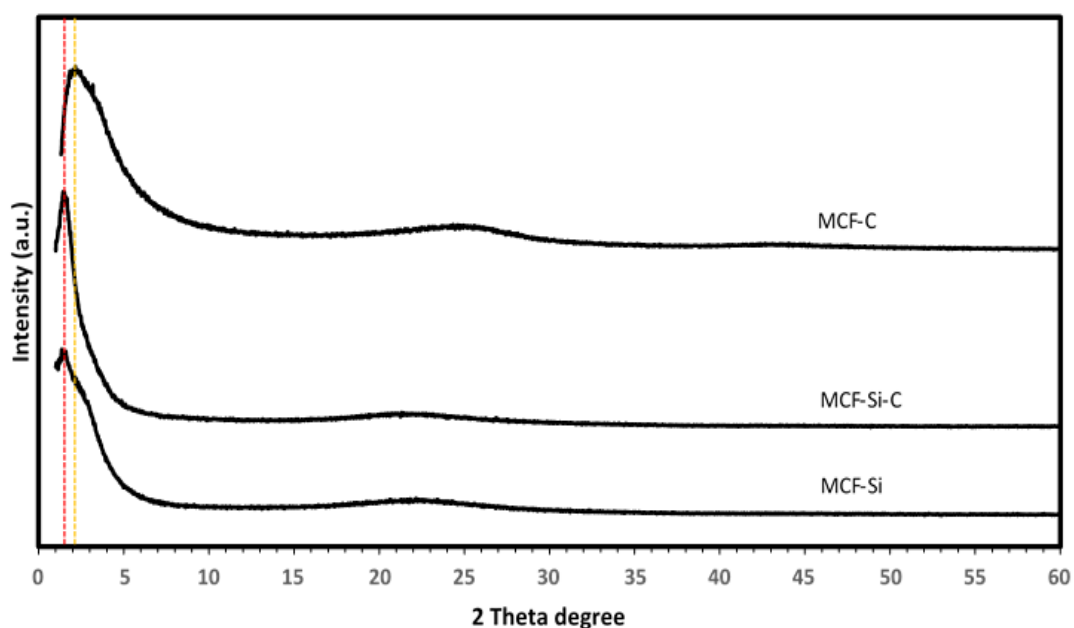


Figure 5. 4 XRD patterns of all catalysts.

On the other hand, the XRD peak of MCF-C was found at 2.48° (orange line). The evidence suggested that the shifting of 2 theta degree of MCF-C was from the phase change of structure since silicon was etched out from this material [41]. Moreover, the distance from spacing between arranged pores or even wall thickness

also possibly changed because of silicon removal. Thus, the presence of silicon is perhaps necessary to preserve the perfect spherical structure.

5.3.1.4 Functional groups

The chemical functional groups in the MCF materials were identified using FT-IR technique to examine the changes in steps of synthesis of MCF-C as shown in **Figure 5.5**

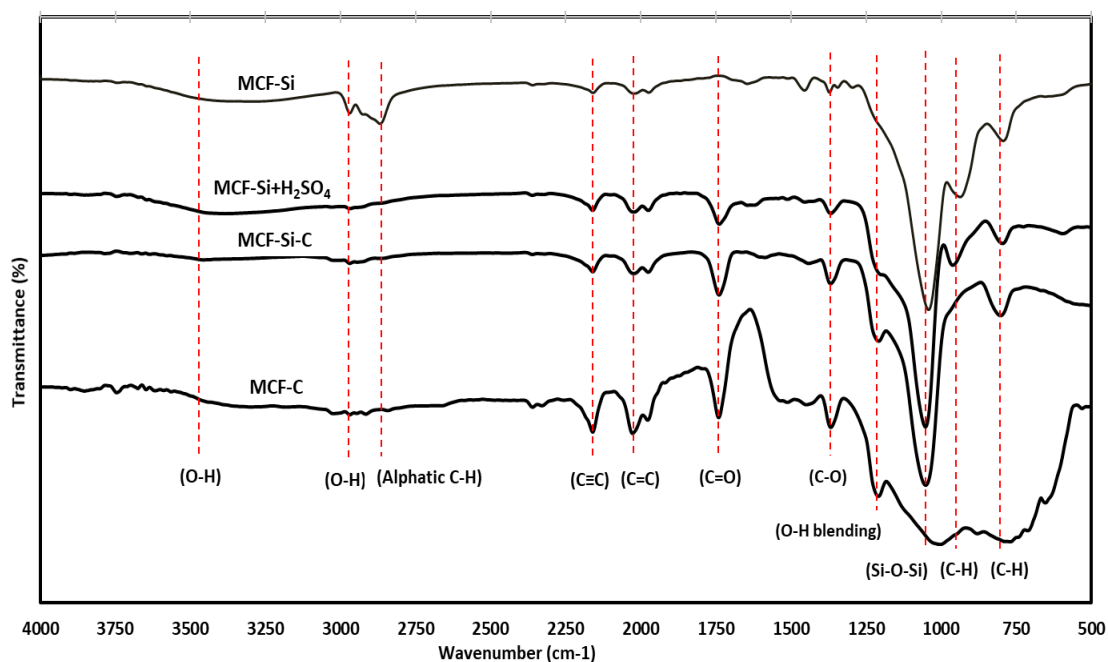


Figure 5. 5 FT-IR spectra of all catalysts.

The silanol group was detected on broad IR band located at 2950-3500 cm^{-1} for O-H stretching vibrational mode in MCF-Si, MCF-Si+H₂SO₄, MCF-Si-C, and MCF-C [46]. The result showed that the peak of O-H stretching apparently decreased from MCF-Si to MCF-C, suggesting that O-H on surface of all materials was consumed to form the carbon layer. Furthermore, the aromatic ring was found in the IR band at 795 cm^{-1} due to C-H vibrations out of plane, which was possibly classified as benzene rings [47]. The increased peaks of IR band at 1373, 1975 and 2023 cm^{-1} were assigned to C-O, C=O and C=C stretching vibrations, respectively [35, 46]. These IR peaks of all MCF materials were probably presented for residue surfactants, and the existence of C=C was not only occurred in the sulphonation process for connection of each residue surfactant molecules, but also emerged in the dehydration process. This evidence suggested that

the residue surfactant was converted to carbon layer from MCF-Si to MCF-C using sulfuric acid. Moreover, the silica of MCF-Si, MCF-Si+H₂SO₄, MCF-Si-C was represented in IR band at 1000-1060 cm⁻¹ as Si-O-Si symmetric stretching vibrations [46]. However, it only slightly appeared in MCF-C because of the removal of silica by NaOH.

5.3.1.5 Thermogravimetric analysis

One of powerful techniques to observe the changes during material synthesis for each step including MCF-Si, MCF-Si+H₂SO₄, MCF-Si-C, and MCF-C, is the thermogravimetric analysis (TGA) that was operated under the air atmosphere as shown in Figure 5.6

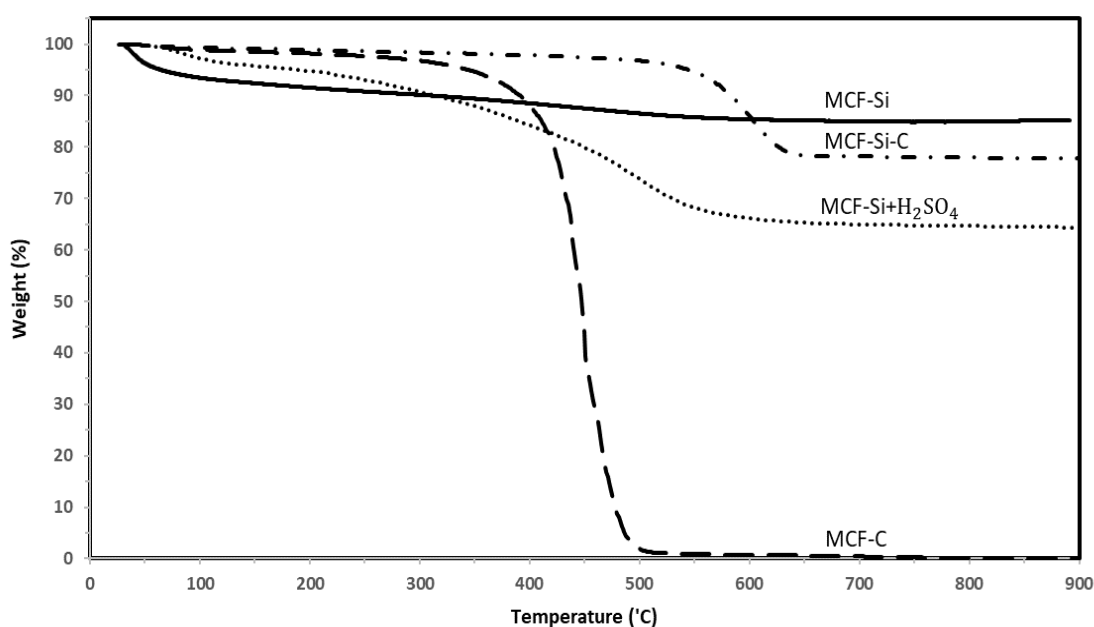


Figure 5. 6 Thermogravimetric analysis (TGA) of intermediate materials corresponding to each synthesis step of MCF-C under air atmosphere.

The temperature profile of all materials showed that the weight loss near to 100 °C, especially MCF-Si, owing to dehydration. The weight loss of MCF-Si after 100 °C was probably attributed to the removal of surfactant as Pluronic P123, which was approximately 8.44 % [41]. MCF-Si+ H₂SO₄, which was sulfuric acid treatment with MCF-Si, represented the weight loss about 33.36 %. The evidence suggested that the hydroxyl group as silanol group (O-H) of Pluronic P123 reacted with sulfuric acid in the form of H₂O, which was related to dehydration and sulphonation catalytic process [41]. In case of composites materials between silicon and carbon as MCF-Si-C, the weight

loss of this material was about 21.1 %, which could be carbon source in the composites between Si and C. The dissolution of silica template by NaOH etching as MCF-C was around 96.6 % of weight loss at 450 °C, indicating that the etching process by NaOH was mostly accomplished as also corresponding to the results from SEM-EDX.

5.3.1.6 Acidity and acid strength

The examination of acidity and acid strength of MCF-Si, MCF-Si-C, and MCF-C was determined using NH₃ temperature-programmed desorption (NH₃-TPD) with operating at temperature range of 30 °C to 500 °C by integration of desorption peaks of ammonia. The results of amount of acid sites (μmole/g) are presented in **Table 5.3**

Table 5. 3 Acidity and acid strength of all samples obtained from NH₃-TPD.

Samples	Amount of acid site (μmole NH ₃ /g cat.)*		
	Weak acid sites	Medium-strong acid sites	Total acid sites
MCF-Si	13.33	413.74	427.07
MCF-Si-C	109.37	384.75	512.06
MCF-C	87.69	586.89	682.64

*Amounts of acid sites of catalyst were determined by NH₃-TPD (use of Fityk program calculation).

Furthermore, the NH₃-TPD profiles are also defined that weak acid sites have desorption peaks at low temperature ca. below 200 °C, and medium to strong acid sites desorb ammonia between 200-500 °C [48]. It was found that the MCF-C exhibited the highest total acid sites among all samples as seen in **Table 5.3**, accordingly, it is likely related to the highest amount of Brønsted acid sites, especially medium to strong acid sites, which can be observed at **Figure 5.7**. Furthermore, the presence of carbon

in MCF-Si-C can also increase the surface acidity of this material by nature of the support [22]. Therefore, the major improvement in the ethanol dehydrogenation to acetaldehyde catalyzed by the MCF-C is essentially captivating.

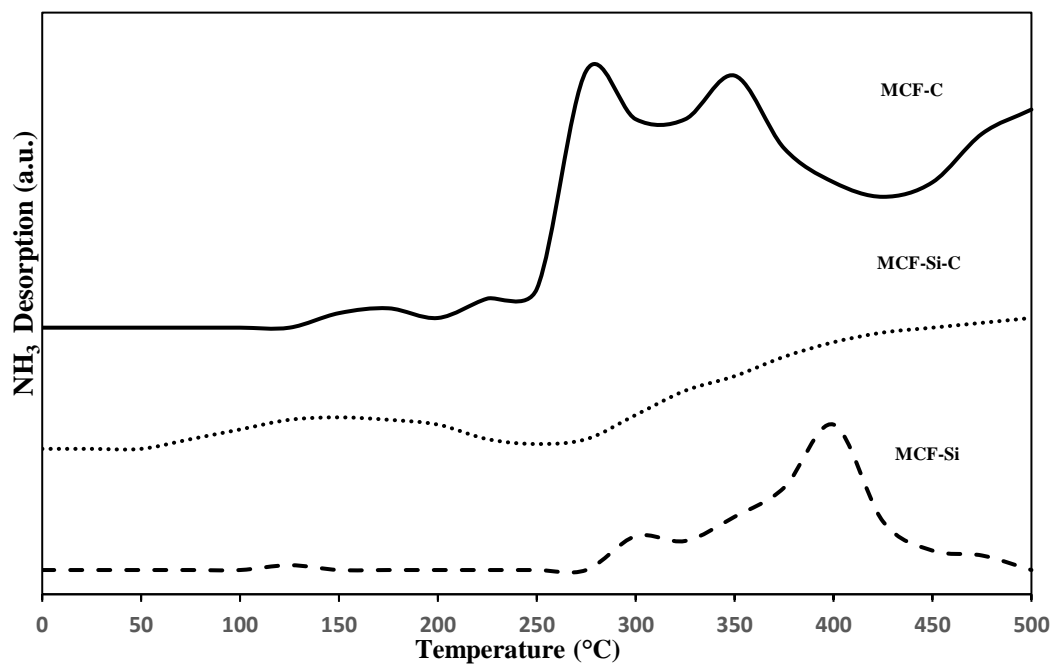


Figure 5. 7 NH₃-TPD profile of all catalysts

5.3.1.7 Basicity and basic strength

The CO₂-TPD was used to emphasize the total basicity of the catalysts with operating condition at temperature range of 40 °C to 500 °C by integration of desorption peaks of carbon dioxide as shown in Table 5.4. The result show that total basicity was increased when the carbon layer occurred.

Table 5. 4 Basicity and basic strength of all samples obtained from CO₂-TPD.

Sample	Number of base site (umole CO ₂ /g cat.)*		
	Weak base sites	Medium-strong base sites	Total base sites
MCF-Si	0.24	97.24	97.48
MCF-Si-C	194.91	-	194.91
MCF-C	48.26	873.47	927.74

*Amounts of basic sites of catalyst were determined by CO₂-TPD (use of Fityk program calculation).

In addition, MCF-C shows the highest basicity among these catalysts, which was followed by MCF-Si-C and MCF-Si, respectively. It was known that basicity is one of the factors, which could affect ethanol dehydrogenation [22, 49]. The CO₂-TPD profile of all catalysts (**Figure 5.8**) were presented as broad desorption peak, which can be divided into three different regions such as weak basic sites (below 200 °C), moderate basic sites and strong basic sites (200-500 °C). It was found that the MCF-C performed both the weak and moderate to strong sites, which were dissimilar to MCF-Si or MCF-Si-C that exhibited only the weak or the moderate to strong sites peak. Therefore, the significant increase of the basicity on surface of MCF-C might promote the ethanol conversion. In contrast, the basicity and acidity on surface catalyst should be balance for converting ethanol to acetaldehyde.

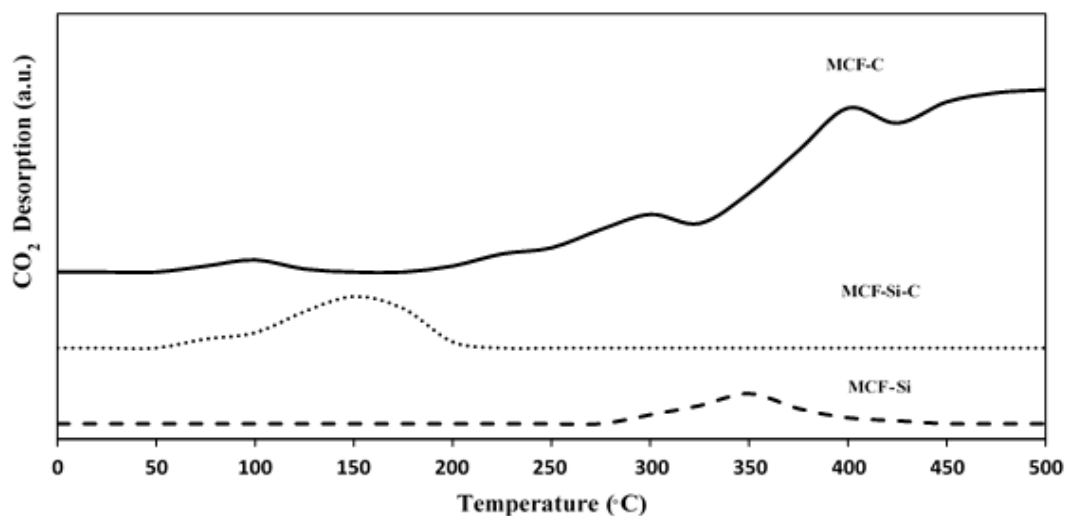


Figure 5. 8 CO₂-TPD profile of all catalysts.

5.3.2 Catalytic activity of ethanol dehydrogenation

5.3.2.1 Reaction study

The performance of all MCF catalysts can be examined using the ethanol dehydrogenation reaction, in which acetaldehyde is present as a major product from this reaction. This reaction study was operated at different reaction temperatures between 200 to 400 °C and atmospheric pressure. The ethanol conversion and the acetaldehyde yield are presented in **Figure 5.9**.

In fact, ethanol conversion of all catalysts apparently increased with increasing reaction temperature as expected and the deactivation of catalyst did not occur via these reaction temperatures. On the other words, the reaction rate of this endothermic reaction obeys the rule of Arrhenius equation [50]. The ethanol conversion of MCF-C was found to be the highest having the values of ca. 5.9 and 17.5 % at 350 and 400 °C, respectively. The evidence suggested that increased ethanol conversion in dehydrogenation probably involved the acidic sites on the catalyst surface.

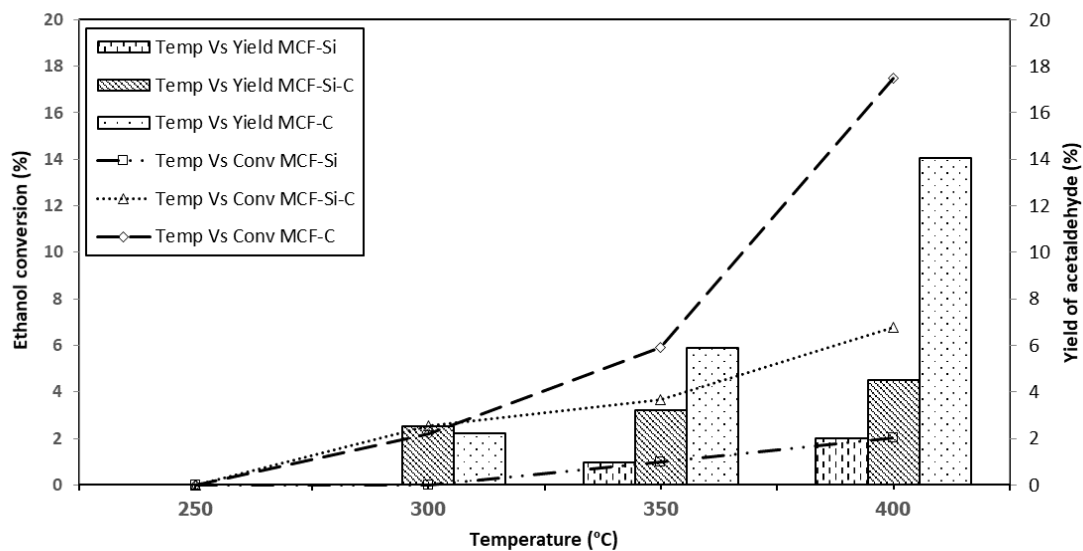
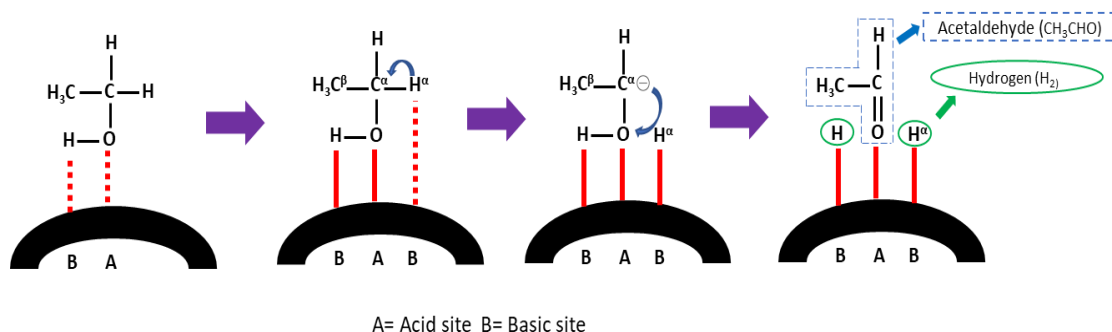


Figure 5. 9 Ethanol conversion and yield of acetaldehyde over different MCF catalysts toward ethanol dehydrogenation.

Thus, MCF-C was suitable because it exhibited the highest acidity and accessibility with appropriate porous structure. Considering, the composite material (MCF-Si-C), it also showed higher ethanol conversion than that of MCF-Si for all reaction temperature. This possibility is because MCF-Si-C had higher acidity than MCF-Si. It is confirmed that the presence of carbon in mesoporous material can enhance acidity of catalyst because of the natural property of carbon [51]. Furthermore, the physical properties including the surface area and porous structure are also one of the most important factors affecting for diffusion control of the reactant and product. This should be considered in the ethanol dehydrogenation over the MCF-C catalyst since high catalytic activity for this catalyst was also caused by high surface area and mesoporous structure as seen in **Table 5.1**. The plausible mechanism of ethanol dehydrogenation process on the acid and basic site is shown in **Scheme 5.3** for better understanding.



Scheme 5.3 The plausible mechanism of ethanol dehydrogenation process on the acid and basic site.

This mechanism is likely described by adsorption of ethanol molecule on acid and basic sites of MCF-C surface to O and H atoms, respectively. Then, $C^{\alpha}-H^{\alpha}$ bond cleavage of a surface ethoxy species to form acetaldehyde, which is followed by two surface-bonded hydrogens desorb to form gas phase hydrogen. Finally, the regeneration of active site on surface materials will be ready for the further reaction.

Table 5. 5 Ethanol conversion and acetaldehyde selectivity of all catalysts.

Materials	Temperature (°C)	Ethanol conversion (%)	Acetaldehyde selectivity (%)
MCF-Si	250	-	-
	300	-	-
	350	0.99	100
	400	2.02	100
MCF-Si-C	250	-	-
	300	2.53	100
	350	3.67	87.1
	400	6.79	66.7
MCF-C	250	-	-
	300	2.22	100
	350	5.91	100
	400	17.48	80.2

Besides ethanol conversion, the selectivity of acetaldehyde of all MCF catalysts was also high (ca. 88.33%), especially at high temperature as shown in **Table 5.5**. In most cases, it was found that the increase in reaction temperature led to the decrease in acetaldehyde selectivity due to the decomposition of acetaldehyde [49, 52]. It is worth noting that all MCF catalysts can maintain the high selectivity of acetaldehyde even at high reaction temperature mostly due to the limitation of further reaction in this type of porous structure. Furthermore, MCF-C not only resulted in high ethanol conversion, but also showed the high selectivity of acetaldehyde at high temperature, which indicated good potential catalysts for ethanol dehydrogenation to acetaldehyde. In addition, the side or by-product during reaction is represented in **Table 5.6**, which indicates that the by-product including ethylene was found in MCF-Si-C and MCF-C with low selectivity at 350 °C and 400 °C. Nevertheless, selectivity of ethylene apparently decreased, whereas, selectivity of acetaldehyde essentially increased from MCF-Si-C to MCF-C at 400 °C. This evidence suggested that the hybrid materials as MCF-Si-C did not provide the higher activity as much as MCF-C.

In our previous work as reported by Obe-eye et al. [35], it revealed that increased acidity and basicity can facilitate the catalytic activity for ethanol dehydrogenation over activated carbon-based catalysts in both ethanol conversion and acetaldehyde selectivity. In addition, Lu et al. [21] reported that mesoporous carbon can be employed in ethanol dehydrogenation, and resulted in high activity and selectivity to acetaldehyde. In order to compare the catalyst performance MCF-C with other researches, the catalytic activities of several catalysts for ethanol dehydrogenation to acetaldehyde are concluded in **Table 5.7**. Although without the metal loading, ethanol conversion and acetaldehyde selectivity of MCF-C are quite high. As a result, MCF-C is a promising catalyst for ethanol dehydrogenation to acetaldehyde. Its key advantages include simplicity of the synthesis, possible usage used without any noble metal, low cost, and optional pre-reduction step prior to reaction.

Table 5. 6 Ethanol conversion, selectivity, and yield of acetaldehyde of all studied catalyst.

Materials	Temperature (°C)	Selectivity (%)			Ethanol conversion (%)	Yield of acetaldehyde (%)
		Ethylene	Acetaldehyde	Ethyl acetate		
MCF-Si	250	-	-	-	-	-
	300	-	-	-	-	-
	350	-	100	-	0.99	0.99
	400	-	100	-	2.02	2.02
MCF-Si-C	250	-	-	-	-	-
	300	-	100	-	2.53	2.53
	350	12.9	87.1	-	3.67	3.2
	400	33.29	66.71	-	6.79	4.53
MCF-C	250	-	-	-	-	-
	300	-	100	-	2.22	2.22
	350	-	100	-	5.91	5.91
	400	9.66	80.28	10.06	17.48	14.03

Table 5. 7 Comparison of catalytic activity of different catalysts for ethanol dehydrogenation to acetaldehyde.

Catalysts	Reaction Temperature (°C)	Ethanol Conversion (%)	Acetaldehyde Selectivity (%)	Ref.
MCF-C	400	17.48	80.28	This work
Mg-Al-450	350	45.8	64.9	[49]
V4b-MCM-41	300	95	40	[53]
Au-TiO ₂	125	95	60	[54]
Cu/ACC	250	15	96.3	[48]
CeO ₂ /ACC	250	3	13.3	[55]
Cu/MC	280	83	95.1	[21]

5.3.2.2 Stability test (Time-on-stream behavior)

The stability test was applied to examine the performance of catalyst. The MCF-C was chosen for this investigation due to its highest ethanol conversion and yield of acetaldehyde. The reaction was performed at 400 °C with time-on-stream for 20 h as shown in **Figure 5.10**. Ethanol conversion and yield of acetaldehyde were found to slightly changed about 19.18 % and 12.21 %, respectively. This indicated that the highly uniform and large pore size of mesopore structure could promote the mass transfer inside of the pore.

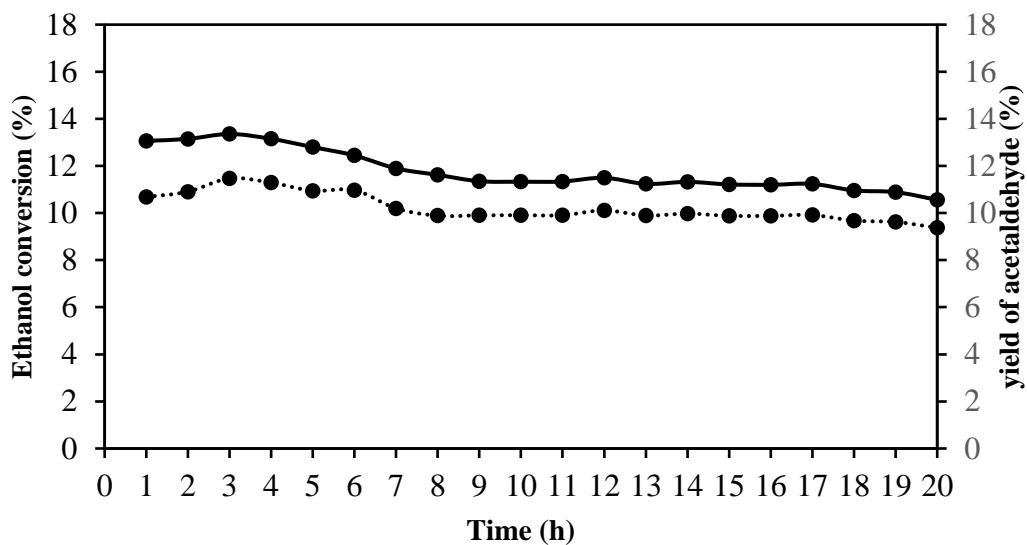


Figure 5. 10 Stability test (ethanol conversion and yield of acetaldehyde with TOS) for the MCF-C catalyst at 400 °C.

5.3.3 Spent catalyst

The spent MCF-C catalyst MCF-C after reaction testing at 400 °C for 20 h was characterized using BET, and SEM-EDX and compared with the catalyst before reaction test. **Figure 5.11** represents the adsorption/desorption isotherms of MCF-C and MCF-C (spent). The nitrogen isotherms of both catalysts exhibit type IV with hysteresis loop, but the isotherms were not exactly the same [45]. However, it is possible that the changing of nitrogen isotherm of MCF-C (spent) from MCF-C was the collapse in some part of mesoporous structure after long period of reaction test.

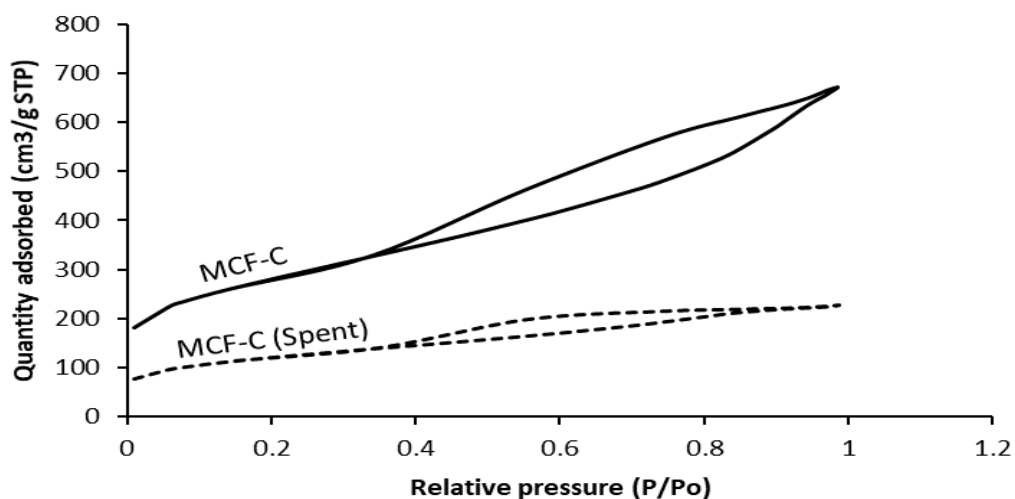


Figure 5. 11 Nitrogen adsorption/desorption isotherms of spent MCF-C and MCF-C catalysts.

In addition, the hysteresis loops of MCF-C (spent) was approximate to be the H4 type, which indicated that the structural shape of MCF-C (spent) became narrow slit-like pore [45], which possibly affected the diffusion of reactant due to the decreasing of the pore size (4.16 to 3.63 nm), the pore volume (1.13 to 0.39 cm³/g), and the surface area (994.56 to 582.66 m²/g) of spent catalyst as seen in **Table 5.8**.

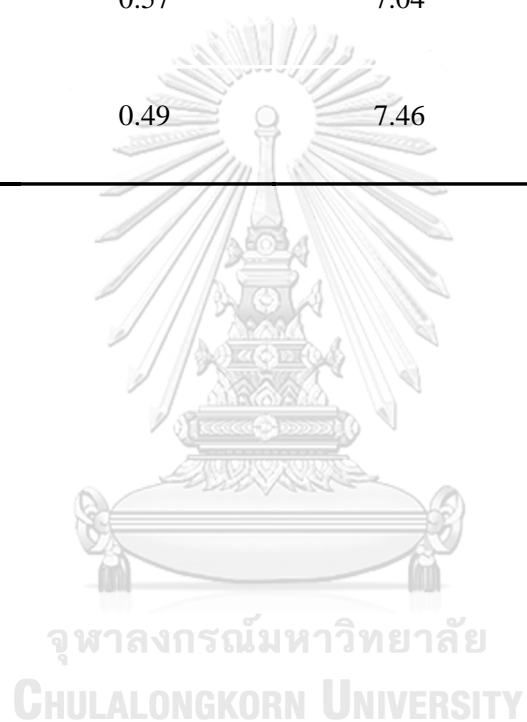
Table 5. 8 Surface area (BET), average pore size and pore volume of spent MCF-C and MCF-C catalysts.

Material	Surface area (m ² /g)	Average Pore size (nm)	Average Pore volume (cm ³ /g)
MCF-C	994.56	4.16	1.13
MCF-C (Spent)	582.66	3.63	0.39

Nevertheless, the appearance of coke might occur and agglomerate inside the pore among long period of reaction test, which may lower the catalytic activity. The SEM-EDX was used to investigate coking by determining different percentage of carbon between MCF-C and MCF-C (spent) as shown in **Table 5.9**. The results show that the carbon percentages are scarcely different, indicating that MCF-C (spent) probably did not contain the coke after the reaction testing. Therefore, MCF-C could be judged as one of the potentially stable catalysts for ethanol dehydrogenation to acetaldehyde.

Table 5. 9 The amount of each element near the surface of catalyst granule obtained from EDX.

Materials	Amount of weight on surface (wt%)		
	Si	O	C
MCF-C	0.57	7.04	92.38
MCF-C (spent)	0.49	7.46	92.05



Study of deactivation in mesocellular foam carbon (MCF-C) catalyst used in
gas-phase dehydrogenation of ethanol

Yoottpong Klinthongchai, Seeroong Prichanont,

Piyasan Prasertdam and Bunjerd Jongsomjit*

Center of Excellence on Catalysis and Catalytic Reaction Engineering

Department of Chemical Engineering, Faculty of Engineering,

Chulalongkorn University, Bangkok 10330, Thailand

*Corresponding author, email: bunjerd.j@chula.ac.th,

Tel: 62-2186874, Fax: 62-2186877



Part 2: Study of deactivation in mesocellular foam carbon (MCF-C) catalyst used in gas-phase dehydrogenation of ethanol

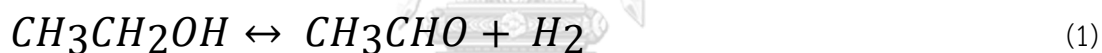
Abstract

In this present study, the mesocellular foam carbon (MCF-C) was spent in gas-phase dehydrogenation of ethanol under mild conditions. The deactivation of catalyst was investigated toward different conditions. First, the MCF-C catalyst having spherical shape with interconnected pore, enlarge pore size, high surface area and high acidity was prepared, characterized, and tested in ethanol dehydrogenation system via gas phase. Effects of reaction condition including different reaction temperatures of 300, 350, and 400 °C with feeding flow rate of weight hourly space velocity (WHSV) at 3.1 h⁻¹ on the deactivation behaviors were determined. The results indicated that the operating temperature at 400 °C significantly retained the lowest change of ethanol conversion and yield of acetaldehyde with value of ca.15.38 % and 5.24 % for 12 h due to the lowest deactivation of the catalysts. After running reaction, the physical properties as pore size, surface area, and pore volume of spent catalysts were decreased owing to the coke formation, which possibly blocked the pore that directly affected to the difficult diffusion of reactant and caused to be lower in catalytic activity, especially operating temperature of 300 °C with the lowest ethanol conversion. In addition, SEM-EDX techniques can confirm the occurrence of coke formation on the particles of catalysts. Furthermore, a slight decrease in acidity as measured by NH₃-TPD was observed owing to consumption of reactant at surface of catalyst or chemical change on surface caused by coke formation. Therefore, it can remarkably choose the suitable operating temperature to avoid deactivation of catalyst, and then optimize the ethanol conversion or yield of acetaldehyde.

Keyword : catalyst deactivation; mesocellular foam carbon; solid catalyst; acetaldehyde; ethanol dehydrogenation

5.1 Introduction

The renewable energy has high impact to the world in the last decade, especially in many countries, in order to use the renewable clean fuel with eco-friendly environment such as bioethanol. As known, one of the crucial bioethanol production processes is the fermentation of sugars as the major sources from sugar cane and starch, which is uncomplicated process in the production [1-5]. At present, ethanol is not only interesting in fields of alternative fuel or even blending of alcohols with gasoline or biodiesel fuels [6], but also as attentive feedstock to produce essential origination chemicals for chemical industries such as acetic acid, ethyl acetate, butanol, acetaldehyde, etc. [7]. In this research, we emphasized our consideration on the feasibility in direct production of acetaldehyde from ethanol via catalytic dehydrogenation, which is considered as cleaner foresight technology. Some researchers previously investigated the reaction of ethanol dehydrogenation to acetaldehyde [8, 9], and this reaction undergoes using proper catalysts as follows (eq. 1):



In fact, there are different types of carbon catalysts used in dehydrogenation process. Previously, Liu *et al.* [10] reported that ordered mesoporous carbon catalyst essentially catalyzed the dehydrogenation of propane to propylene with high activity. Later, Ob-eye *et al.* [11] also reported that ethanol dehydrogenation to acetaldehyde apparently occurred using activated carbon-promoted with cobalt (Co) having very high selectivity to acetaldehyde. It is also recognized that the mesocellular foam carbon (MCF-C) is one of the robust carbon catalysts, which can be employed in ethanol dehydrogenation in order to produce acetaldehyde. This is owing to its appropriate physicochemical properties such as desired pore characteristics and acid-base properties as reported in our previous study [12]. In addition, the structure of MCF-C is well defined as the interconnected pore and large pore size, which not only provided higher diffusion, but also accorded high activity as conversion or even selectivity. Besides, the deactivation of this catalysts is very important issue since it is related with stability of catalyst. Thus, it seems reasonable to investigate the deactivation behavior

of MCF-C catalyst via ethanol dehydrogenation in order to better understand the nature of this catalyst [12]. Nevertheless, the general cause to deactivate most catalysts on ethanol dehydrogenation is derived from coke formation. For this aim, it must be discussed that there is the correlation between the decrease in the catalyst activity and the catalyst deactivation from the occurrence of the coke inside of the catalyst. In addition, this verity is a consequence of the heterogeneous nature of the coke in the catalyst, which is possibly composed of amorphous and filamentous fractions, with the cokes of amorphous structure that have a significant impact on catalyst deactivation owing to the encapsulation in the catalyst [13-15]. Thus, several procedures expected at selecting and adapting catalysts have been considered in the literature to minimize the coke deposition in the catalyst. According to Montero *et al.* [16], they investigated the deactivation of Ni/La₂O₃- α -Al₂O₃ catalyst in ethanol steam reforming (ESR) with different operating condition as either temperature between 500-650 °C or space time up to 0.35 $\frac{\text{g}_{\text{catalyst}}}{\text{g}_{\text{EtOH}} \cdot \text{h}}$. They reported that catalyst deactivation was merely motivated by coke deposition, remarkably via encapsulating coke inside of the catalyst. In addition, Morales *et al.* [17] also investigated the difference in deactivation of Au catalyst during transformation when supported on ZnO and TiO₂. The evidence suggested that the catalyst on ZnO demonstrated higher resistance to deactivation caused by coke formation. Therefore, the selection of catalysts in each specific reaction is captivating to exhibit either high activity or resistance to deactivation caused by coke formation. It is known that the decline in deactivation of catalyst is regularly followed by an increase in the carbon content on the catalyst surface with different conditions. To the best of our knowledge, no work in the literature has been yet reported on the deactivation behaviors MCF-C catalyst used in gas-phase ethanol dehydrogenation to acetaldehyde.

Accordingly, this research is emphasized on the effects of operating conditions such as reaction temperature and weight hourly space velocity (WHSV) on the formation of coke under mild condition. According to the study, gas-phase ethanol dehydrogenation over MCF-C catalyst was carried out in a micro fixed-bed reactor, which is possibly reasonable for the scaling-up, capacitates thermal uniformity of the catalytic bed, and moderates the deactivation via coke deposition as well. The spent

catalysts under specified condition were collected after each run and characterized by nitrogen-physisorption, X-ray diffraction (XRD), scanning electronic microscopy (SEM), thermogravimetric analysis (TGA), ammonia temperature-programmed desorption (NH₃-TPD) and Fourier transform infrared spectroscopy (FT-IR) in order to observe the changes of catalysts after being used.

5.2 Materials and method

5.2.1 Materials (Chemicals)

Pluronic P123 (Sigma-Aldrich, Molar mass \sim 5800) was used as the surfactant or template, and hydrochloric acid (HCl (98 wt%), Sigma-Aldrich) was used to catalyze in the synthesis of MCF-Si for forming the structure of materials. Furthermore, 1,3,5-trimethylbenzene (TMB, Sigma-Aldrich) was used as the swelling agent, which can expand the pore of material. The silica source was from tetraethyl orthosilicate (TEOS; 98 % purity, Sigma- Aldrich). Sulfuric acid (H₂SO₄ (98 wt % , Sigma Aldrich) was employed as the provider of the formation of carbon layer. The etching of silica was used as sodium hydroxide (NaOH, SigmaAldrich).

5.2.2 Catalyst preparation

Mesocellular foam carbon (MCF-C) was synthesized using mesocellular foam silica (MCF-Si) as based material [12]. First, 2 g of Pluronic P123 as triblock copolymer was dissolved in 10 ml of hydrochloric acid with 65 ml of deionized water by stirring until it became homogeneous solution (ca. 1 h) at ambient temperature. After that, 5 g of 1,3,5-trimethyl benzene (TMB) as the pore expander was added into the prior solution at 40 °C, and continuously stirred for 2 h to obtain milky solution. After approaching 2 h, tetraethyl orthosilicate (TEOS) used as the silica source was consecutively added into the previous solution, and then kept rapidly stirring at the same temperature for 5 min. Consequently, the milky solution was transferred into Teflon bottle, which was followed by aging at 40 °C for 20 h. After reaching 20 h, the temperature was increased to 100 °C with the ramping rate of 10 °C/min. The white solution was filtered with 50 ml of ethanol and 100 ml of deionized water, and then dried overnight at room temperature. The white precipitate of MCF-Si was ready to be used as the based material for MCF-C synthesis. To obtain MCF-C, 1 g of MCF-Si was

mixed with 0.16 ml of sulfuric acid, and also stirred it for 1 h. After that, it was dried in the oven at 100 °C for 12 h. Then, the temperature was increased to 160 °C for 12 h. The black powder was calcined at 850 °C under nitrogen flowing for 2 h with ramping rate of 1 °C/min. Next, the etching process was applied using 2 M of NaOH to eliminate the silica from the material at ambient temperature with stirring for 1 h. In addition, it was followed by washing with deionized water until the pH of filtrate was exactly unchanged, and dried overnight at room temperature. Finally, the MCF-C was ready to use.

5.2.3 Characterization of catalyst

Nitrogen-physisorption

Nitrogen-physisorption was used to measure the pore size, surface area, and pore volume of samples using Micromeritics ChemiSorb 2750 Pulse instrument. Measuring of Brunauer-Emmet-Teller (BET) isotherm equation was performed at -196 °C, and the samples were degassed with heating in the vacuum at ambient temperature to 120 °C for 16 h. In addition, Barrett-Joyner-Halenda (BJH) method based on the Kelvin equation was also employed to evaluate the pore structure of samples [18].

Scanning electron microscopy (SEM)

The morphology of specimens was identified using the Hitachi S-3400N model. Link Isis Series 300 program EDX was applied to analyze the elemental distribution and composition over different catalysts.

X-ray diffraction (XRD)

XRD was used to estimate the crystalline framework of samples using a Siemens D 5000 X-ray diffractometer having $\text{CuK}\alpha$ radiation with Ni filter in the range of 2θ between 1 to 60 with 0.04 resolution. The scan rate was applied at 0.5 sec/step.

Thermogravimetric analysis (TGA)

TGA was operated using TA instrument SDT Q600 analyzer (USA). The sample of 4-10 mg was used in the temperature operation range between 0 to 1000 °C with heating rate of 2 °C/min using air as carrier gas.

Fourier transform infrared (FT-IR) spectroscopy

The functional groups of specimens were analyzed using the FTIR spectroscopy. The signal absorption spectra were obtained using Nicolet 6700 FTIR spectrometer in the wavenumber range of 400 to 4000 cm^{-1} .

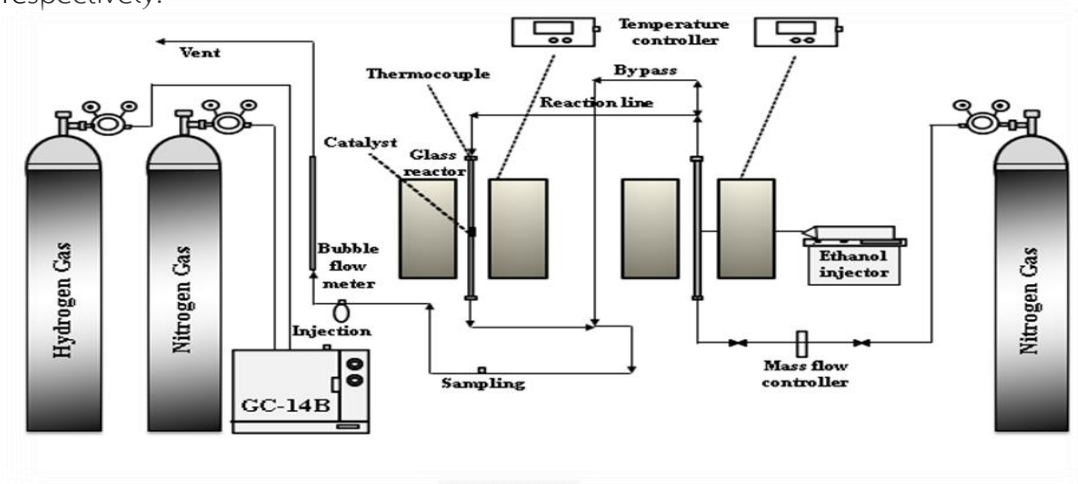
Ammonia Temperature-programmed desorption (NH_3 -TPD)

The acidity and acid strength of catalysts were examined applying Micromeritics Chemisorb 2750 Pulse Chemisorption System. First, 0.1 g of catalyst was preheated with helium at 200 °C. Then, ammonia was adsorbed at 40 °C for 1 h. After that, the physisorbed ammonia was desorbed under helium gas flow until the baseline level was reached to be constant. The chemisorbed ammonia was removed from active sites by raising the temperature from 30 to 500 °C under a helium flowing at 40 ml/min, with a heating rate of 10 °C/min. The thermal conductivity detector (TCD) as a function of temperature was adapted to estimate the amount of ammonia in effluent.

5.2.4 Catalytic test

The kinetic behavior of catalyst was determined using the ethanol dehydrogenation test apparatus using a fixed-bed continuous flow glass tube microreactor. Starting with 1 g of catalyst sample (MCF-C) and 0.05 g of quartz wool bed were packed inside of the central glass tube reactor, which was placed inside of the electric furnace. The pretreatment at 200 °C under nitrogen flowing for 1 h was conducted to remove the humidity on the surface of target catalyst. Then, the liquid ethanol was vaporized at 120 °C with nitrogen gas at 60 ml/min using controlled injection with a single syringe pump with the volumetric flow rate of ethanol feeding at 0.397 ml/h. To obtain the spent samples (deactivation catalysts), the gas stream was fed into the reactor with weight hourly space velocity (WHSV) in the desired

feeding of $3.11 \text{ g}_{\text{ethanol}} / \text{g}_{\text{cat}} \cdot \text{h}$. Furthermore, the considerable operating temperature range was at 300, 350, and 400 °C under atmospheric pressure. The gaseous products were analyzed by a Shimadzu (GC-14B) gas chromatograph with flame ionization detector (FID) using capillary column (DB-5) at 150 °C. While the reaction test (**Scheme 1**) was operated, the results were repeatedly recorded at least 3 times for each temperature. After running different operating temperatures of 300, 350, and 400 °C, the spent catalysts were denoted to MCF-C SP300, MCF-C SP350, and MCF-C SP400, respectively.



Scheme 5.1 Flow diagram of ethanol dehydrogenation system.

The values of ethanol conversion, selectivity of acetaldehyde, and yield of acetaldehyde were diagnose using these following equations (1), (2), and (3), respectively.

$$\text{Ethanol conversion} : X_{\text{EtOH}}(\%) = \frac{n_{\text{EtOH}}(\text{in}) - n_{\text{EtOH}}(\text{out})}{n_{\text{EtOH}}(\text{in})} \times 100 \quad (1)$$

$$\text{Selectivity of acetaldehyde} : S_i(\%) = \frac{n_i}{\sum n_i} \times 100 \quad (2)$$

$$\text{Yield of acetaldehyde} : Y_i(\%) = \frac{X_{\text{EtOH}} \times S_i}{100} \quad (3)$$

5.3 Results and discussion

5.3.1 Catalytic behavior

5.3.1.1 Influence of temperature during time on stream on catalytic behavior of ethanol dehydrogenation

The effect of different temperature between 300 to 400 °C during time on stream of 12 h on the deactivation behavior of catalysts was investigated and the results are illustrated in **Figure 5.12**.

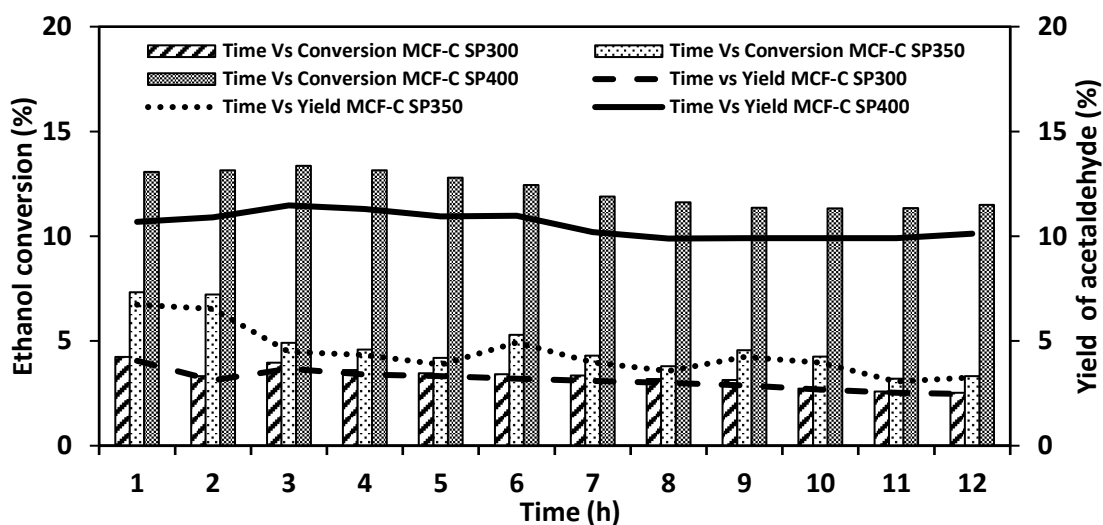


Figure 5. 12 Ethanol Conversion and yield of acetaldehyde of all catalysts with regarding to ethanol dehydrogenation.

In the first hour of the reaction test, the operating temperature at 400 °C exhibited the highest ethanol conversion of ca. 13.06 % followed by the ones at 350 °C (ca. 6.32 %), and 300 °C (ca. 3.24 %). The evidence suggested that within the first hour of operating time, the increased ethanol conversion from 300 to 400 °C was dependent on the increased temperature since dehydrogenation is endothermic reaction corresponding to the principle of Arrhenius equation [19-21]. In addition, yield of acetaldehyde also simultaneously increased from 3.05 to 10.68% with increasing of ethanol conversion from 300 °C to 400 °C. During the 12 h of reaction, the ethanol conversion with operating temperature of 400 °C slowly declined with time on stream from the first hour until 7 h, but it hardly changed from 7th h to 12th h having the value of ca. 11.89 to 11.49%. Yield of acetaldehyde at this temperature insignificantly varied during the 12 h of reaction. This suggested that the ethanol dehydrogenation at

400 °C for 12 h was essentially stable up on the obtained values of ethanol conversion or yield of acetaldehyde. However, with lower operating at temperatures of 350 °C and 300 °C for 12 h, ethanol conversion decreased with values of ca. 7.32 to 3.3 % and 4.24 to 2.52 %, respectively. From these results, it was revealed that MCF-C catalyst tended to rapidly deactivate at lower temperature i.e. 300-350 °C. This evidence suggested that the decrease of catalytic activity with long period of operation was likely occurred owing to the possible coke formation, which probably affected the active sites on the surface of catalysts, particularly the reaction temperature at 300 °C. The finding was quite surprising and ,thus, more characterization techniques were crucial for investigation the coke formation on the spent catalyst

5.3.2 Characterization on the textural properties of catalysts

Differences on the textural properties between the fresh and spent MCF-C catalyst were elucidated using N₂ physisorption and SEM/EDX measurement. In fact, all characterization techniques were conducted for the fresh MCF-C catalyst and spent catalysts after being used for 12 h in the reaction tests under three operating temperatures including 300, 350 and 400 °C. Thus, there were four catalyst samples in each technique to consider.

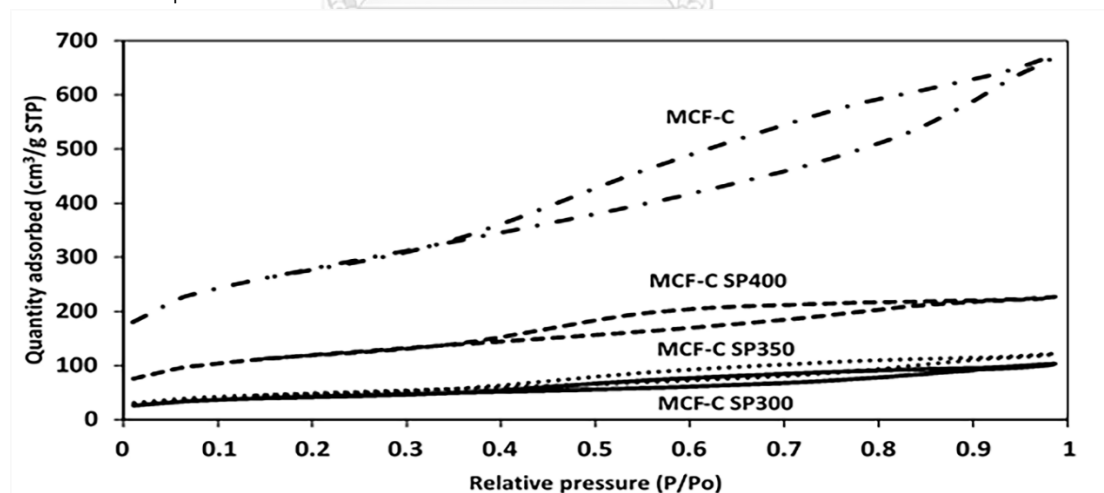


Figure 5. 13 Nitrogen adsorption/desorption isotherms of all stability testing conditions (MCF-C, MCF-C SP300, MCF-C SP350, and MCF-C SP400).

First, the adsorption/desorption isotherms obtained from the N₂ physisorption of fresh and other three spent catalysts are illustrated in **Figure 5.13**. As seen, all catalysts exhibit the type IV (IUPAC classification) of mesoporous structure with

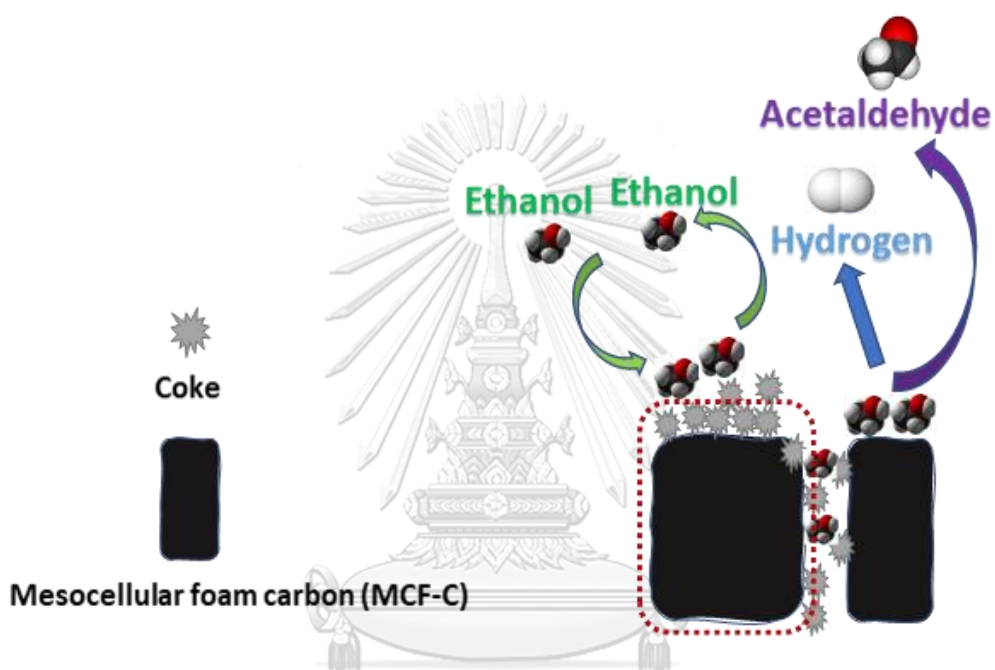
hysteresis loop [22]. This indicates that under these specified dehydrogenation conditions; the MCF-C catalyst was apparently stable. Nevertheless, the fresh MCF-C catalyst displayed the hysteresis loop of H2b type having a spherical pore shape [22], whereas MCF-C SP300, MCF-C SP350, and MCF-C SP400 demonstrated the hysteresis loop of H4 type with the narrow slit-like pore shape [22]. This result probably suggested that coke formation likely occurred and deposited inside the pore, especially at low operating temperature such as MCF-C SP300 due to its conformation of almost nonexistence of the hysteresis loop. In other words, MCF-C SP300 exhibited the highest coke formation, which was not reasonable to operate the ethanol dehydrogenation at this temperature. Furthermore, the pore size, surface area, and pore volume of all spent catalysts also decreased from the fresh catalyst after the test for 12 h as seen in **Table 5.10**, which confirmed that coke was probably deposited in the pore of the catalyst.

Table 5. 10 Physical properties of the fresh and spent catalyst with different reaction temperatures.

Materials	Surface area (m ² /g)	Average pore size (nm)	Average pore volume (cm ³ /g)
MCF-C	994.51	4.96	1.13
MCF-C SP300	312.86	4.1	0.17
MCF-C SP350	439.36	4.19	0.36
MCF-C SP400	782.16	4.27	0.75

In addition, this evidence indicated that the coke formation at low temperature of 300 °C likely blocked the pathway of diffusion of reactant to the surface catalyst, which directly affected to catalytic ability of MCF-C on ethanol dehydrogenation as seen in **Scheme 5.2**. Thus, one of the crucial factors causing lower catalytic activity was the coke formation owing to the effect from pore blocking. In order to verify the

coke formation, SEM is one of the most powerful techniques to explore the textural property of fresh and spent catalysts as seen in **Figure 5.14**. From the SEM images of spent catalysts, it is revealed that the particle size of these catalysts does not significantly differ from fresh catalyst by having the values of ca. 1.26-1.32 μm ($n=100$). This indicated that the different operating temperatures and coke formation had no effect on the particle size of these spent catalysts.



Scheme 5.2 Coke formation on the surface catalysts.

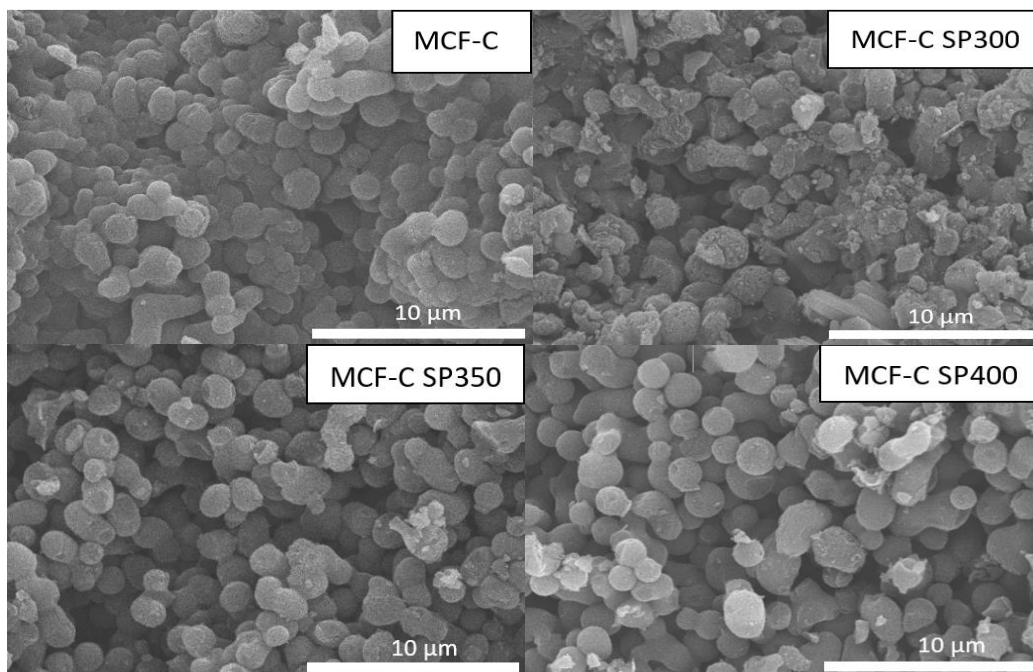


Figure 5. 14 Low magnification SEM image of MCF-C, MCF-C SP300, MCF-C SP350, MCF-C SP400.

However, the emergence of the coke particles, which possibly adhered and encapsulated in all spent catalysts, could be observed. Moreover, the apparent quantity of coke dispersion on MCF-C SP300 was high compared with other operating temperatures (MCF-C SP350 and MCF-C SP400, respectively). It was found that the high aggregation of the coke contents at the external surface of spent catalysts was observed at low temperature of 300 °C, which was corresponding to the low catalytic activity of ethanol dehydrogenation at this temperature.

Table 5. 11 Amount of each element adjacent the surface of catalyst granule obtained from EDX.

Materials	Amount of weight on surface (wt%)		
	C	O	Si
MCF-C	93.26	6.33	0.41
MCF-C SP300	65.61	33.56	0.83
MCF-C SP350	76.45	22.63	0.92
MCF-C SP400	87.39	11.75	0.86

Accordingly, the reasonable operating temperature on ethanol dehydrogenation to acetaldehyde would be 400 °C due to the lowest deactivation of the catalyst. Besides, SEM-EDX from **Table 5.11** demonstrates the atomic percent compositions of fresh and spent catalysts. The data displayed that there is the decrease of the carbon contents from the fresh MCF-C catalyst from 93.26 wt% to the spent catalyst at 300 °C with the lowest carbon contents of 65.61 wt%. The decrease of carbon content on the surface was due to the replacement with oxygen element, which occurred during ethanol dehydrogenation reaction. On the other hand, oxygen contents in spent catalysts increased in the order of MCF-C SP400 < MCF-C SP350 < MCF-C SP300. This phenomenon was probably due to the formation of products or by-products, which cannot migrate from the inside of the catalyst because of the pore blockage from the carbon encapsulation leading to inhibition of internal mass diffusion [23].

5.3.3 Characterization on the chemical properties of catalysts

X-ray diffraction (XRD) patterns of all samples are shown in **Figure 5.15** in order to examine the difference of phase change of the crystal structures.

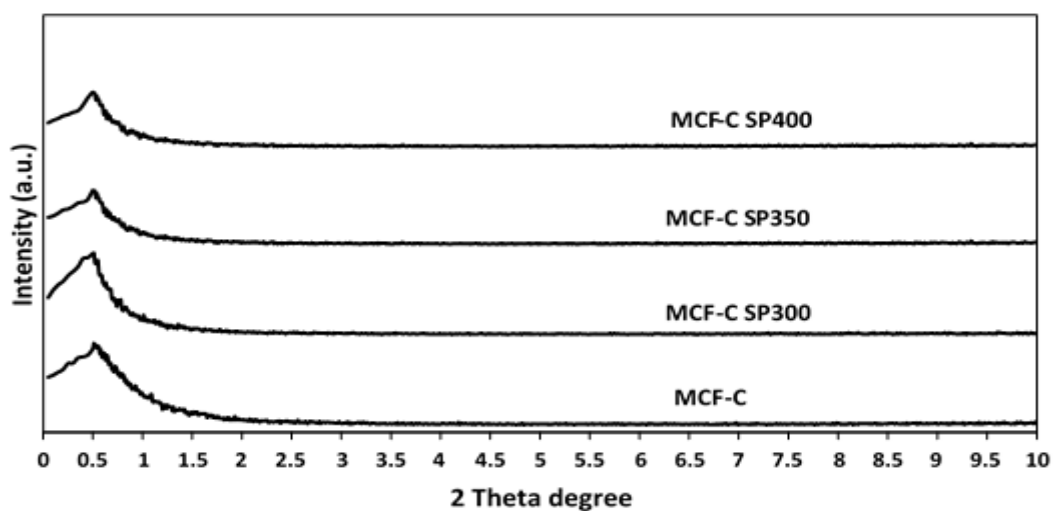


Figure 5. 15 XRD pattern of the fresh and spent catalysts.

All catalyst samples exhibited identical XRD peak located at 1.06 ° as the major crystalline phase using low-angle XRD, which is similar to the previous study [12]. Nevertheless, the peak of MCF-C SP300 at the top was slightly broader than other catalysts indicating that the coke formation might softly affected the crystal structure.

To identify the changes in chemical functional groups, FT-IR technique was employed on MCF-C, MCF-C SP300, MCF-C SP350, and MCF-C SP 400 as seen in **Figure 5.16**.

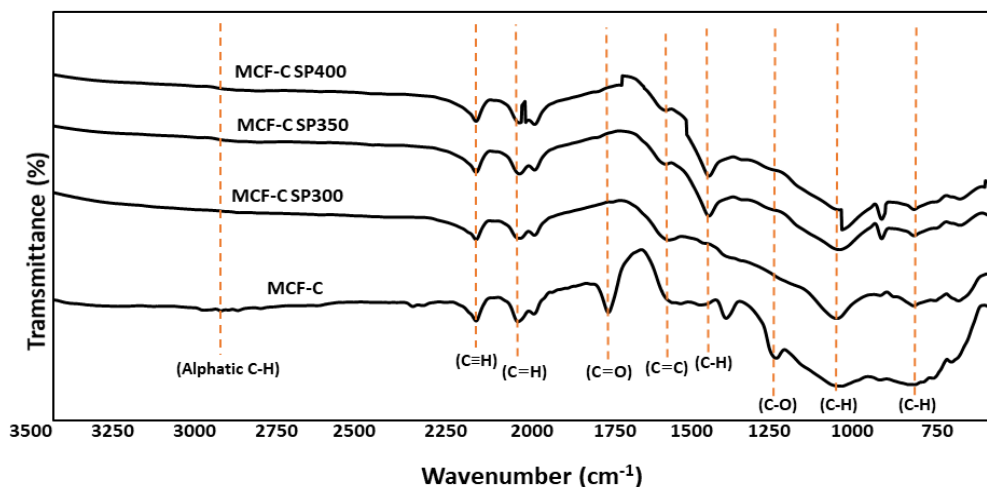
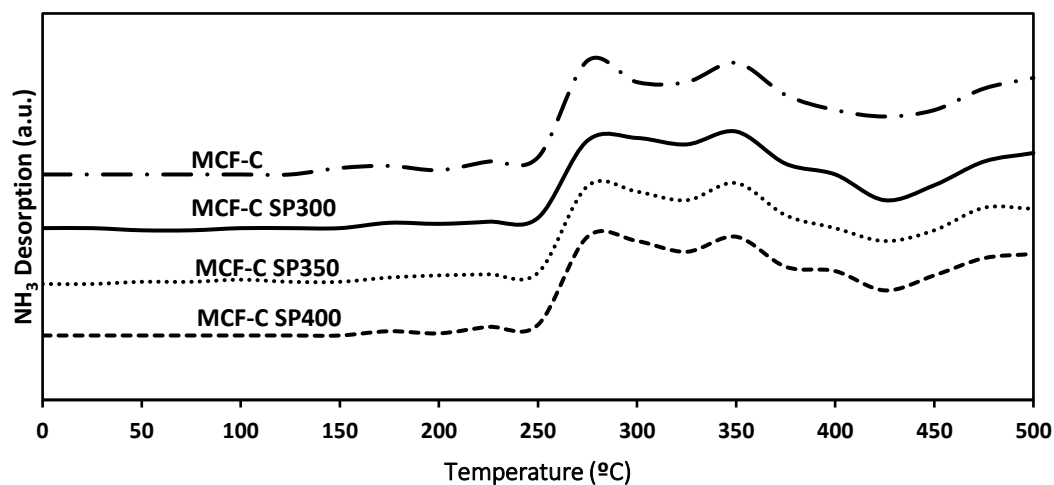


Figure 5. 16 FT-IR spectra of the fresh and spent catalysts.

The IR spectrum of fresh MCF-C catalyst was well accorded with that reported in the literature [12], having eight IR active elementary bands encountered at 759 cm^{-1} (C-H vibrations), 1020 cm^{-1} (C-H vibrations), 1239 cm^{-1} (O-H blending), 1550 cm^{-1} (C=C stretching vibrations), 1755 cm^{-1} (C=O stretching vibrations), 2040 cm^{-1} (C=C stretching vibrations), 2150 cm^{-1} (C \equiv C stretching vibrations), and 2970 cm^{-1} (aliphatic C-H) [11, 24-26]. For all the spent catalysts, the peaks in the region of $750\text{-}800\text{ cm}^{-1}$ (C-H vibrations) was observed suggesting coke formation, especially in the MCF-C SP300 catalyst. In addition, it was also found that the peak in the region of $1000\text{-}1100\text{ cm}^{-1}$ (C-H vibrations) increased with decreasing operating temperature. This also suggested that the presence of the coke was likely initiated when the operation temperature was low i.e. $300\text{ }^{\circ}\text{C}$.

One of the major factors that affects the catalytic properties is acidity and acid strength [12, 27, 28]. Thus, ammonia temperature-programmed desorption ($\text{NH}_3\text{-TPD}$) was applied to evaluate the acidity of the catalyst surface. There are two types of the acidic classification as weak acidic sites with desorption peaks under the temperature



of ca. 200 °C, and medium to strong acid sites with desorption peaks between 200-500 °C [29, 30]. The NH₃-TPD profiles for all the catalysts are presented in **Figure 5.17**.

Figure 5. 17 TPD-NH₃ profiles of the fresh and spent catalysts.

The results indicate that NH₃-TPD profiles of all the spent catalysts are similar with the one obtained from the fresh catalyst at the weak acid site regime. However, the changes in medium and strong acid sites regime were observed. As seen, the MCF-CSP300 exhibits the lowest amounts of medium and strong acid sites comparing to other catalysts. In fact, the decrease in acidity can be proved by calculation of the amount of acid sites ($\mu\text{mole/g}$) as listed in **Table 5.12**. It was found that MCF-C SP300 exhibited the lowest acidity with the value of ca. 767.32 $\mu\text{mole NH}_3/\text{g cat}$, whereas that from the MCF-C as fresh catalyst was 866.61 $\mu\text{mole NH}_3/\text{g cat}$. This indicated that the presence of coke formation resulted in decreased acidity via obscuring on the coverage of active sites, which was probably changed to be inactive sites [31-33]. Therefore, to avoid coke formation, ethanol dehydrogenation should be operated at high temperature of 400 °C for MCF-C catalysts.

Table 5. 12 Acidity and acid strength of the fresh and spent catalysts obtained from NH₃-TPD.

Catalysts	Amount of acid site ($\mu\text{mole NH}_3/\text{g cat.}$)*		
	Weak acid sites	Medium-strong acid sites	Total acid sites
MCF-C	43.45	823.16	866.61
MCF-C SP300	27.68	739.64	767.32
MCF-C SP350	31.22	764.95	796.17
MCF-C SP400	35.96	779.56	815.52

*Amounts of acid sites of catalyst were calculated by NH₃-TPD (employ of Fityk program evaluation).

5.3.4 Quantitative analysis of the coke formation

Thermal gravimetric analysis (TGA) was used to investigate the coke formation by observing the weight loss, which was operated under air atmosphere as shown in **Figure 5.18**. TG curves of the fresh MCF-C catalyst exhibit 95.7 % weight loss at 450 °C, indicating the characteristic of the mesocellular foam carbon as reported in previous study [12]. After the reaction was tested for 12 h, all spent catalysts including MCF-C SP300, MCF-C SP350, and MCF-C SP showed sharply declined weight losses at the temperature of ca. 370 °C, which differed from the fresh MCF-C catalyst. Based on TGA, all spent catalysts contained the aliphatic and aromatic coke [34].

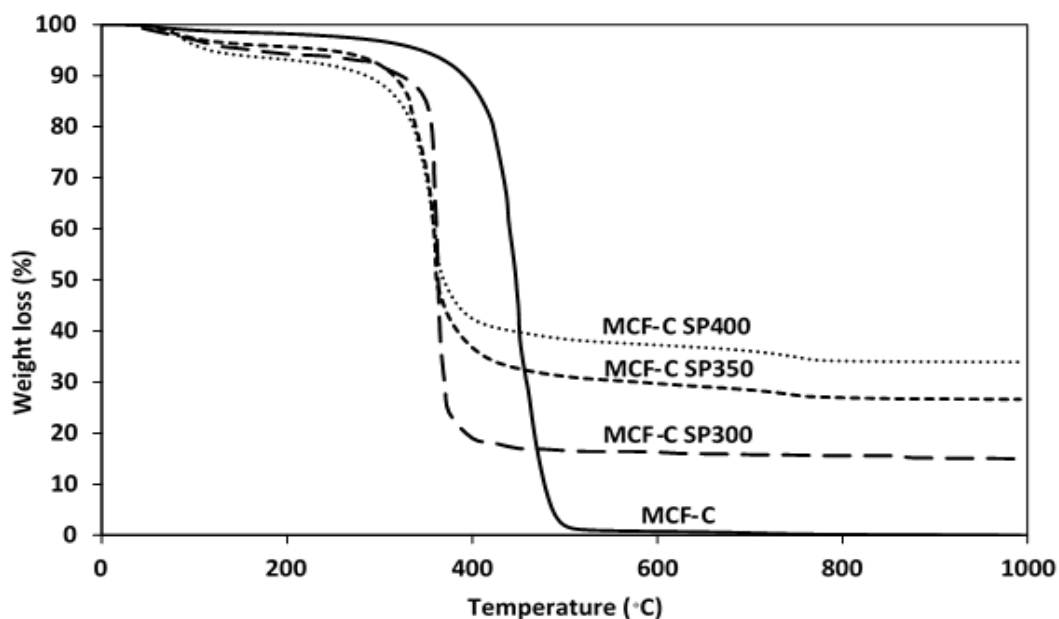


Figure 5. 18 Thermogravimetric analysis (TGA) of material corresponding to each stability testing conditions of MCF-C under air atmosphere.

Furthermore, the highest percentage of weight loss of TGA curves was found on MCF-C SP300 with value of ca. 77.3 % followed by MCF-C SP350 and MCF-C SP400, respectively. This indicates that MCF-C SP300 exhibited the largest amount of coke formation resulting in decreased pore volume. In addition, this result can be confirmed with differential scanning calorimetry (DSC) technique showing increased area below curve, which is related to higher coke content as shown in **Figure 5.19**.

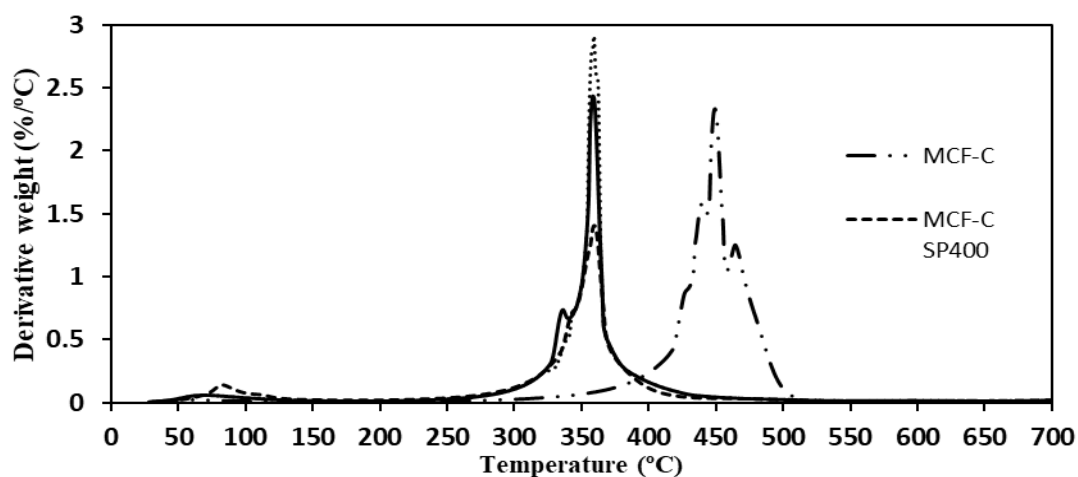


Figure 5. 19 Differential thermal analysis of the fresh and spent catalysts.

Effect of TMB/P123 ratios on physicochemical properties of mesocellular
foam carbon (MCF-C) as catalyst for ethanol dehydrogenation

Yoottapong Klinthongchai, Seeroong Prichanont,

Piyasan Prasertdam and Bunjerd Jongsomjit*

Center of Excellence on Catalysis and Catalytic Reaction Engineering

Department of Chemical Engineering, Faculty of Engineering,

Chulalongkorn University, Bangkok 10330, Thailand

*Corresponding author, email: bunjerd.j@chula.ac.th,

Tel: 62-2186874, Fax: 62-2186877

Materials Today Chemistry



จุฬาลงกรณ์มหาวิทยาลัย
CHULALONGKORN UNIVERSITY

Part 3: Effect of TMB/P123 ratios on physicochemical properties of mesocellular foam carbon (MCF-C) as catalyst for ethanol dehydrogenation

Abstract

The preparation of mesocellular foam carbon catalysts with different ratios of TMB/P123 is represented for investigation in catalytic activity via ethanol dehydrogenation to acetaldehyde. The TMB was employed as swelling agent and P123 acted as template-structuring. The physicochemical properties of synthesized catalysts were determined using BET, TEM, SEM-EDX, XRD, FT-IR, TGA, CO₂-TPD and NH₃-TPD. The evidence suggested that various ratios of TMB/P123 can differently control the meso-structure including the pore size, specific surface area and pore volume. Particularly, MCF-C 3.5 catalyst (TMB/P123 of 3.5) enhanced the catalytic via ethanol dehydrogenation. Interestingly, effectively controllable pore structure of catalysts is beneficial for the desorption of selective product such as acetaldehyde leading to remarkably increased yield of acetaldehyde. Furthermore, the MCF-C 3.5 evidently exhibited outstanding stability at temperature of 400 °C for 12 h. Thus, it can be reasonably selected the ratio of TMB/P123 as 3.5, which is dominantly facilitated either high diffusion of reactant or high stability without losing of the traditional structure compared with other ratios of TMB/P123

Keywords : mesocellular foam carbon; ethanol dehydrogenation; acetaldehyde, pore size

5.1 Introduction

The desire for industrial chemicals in the world is consecutively escalating with the sudden growth of industry [1]. Nowadays, the renewable energy products are gently explicated to chemical feedstock. Ethanol is one of captivated renewable energy products owing to either environmentally friendly or great mobilization value. The agriculture source as sugar cane, corn, straw, bagasse, wheat, and cassava can be normally utilized to produce ethanol by fermentation of biomass process [2, 3]. On contrary, the technology of ethanol production has been drastically developed that it directly affects to higher excess production capacity as a major problem, which has been supremely crucial [4]. Consequently, it has been attended to convert the ethanol to be higher value of the chemical products, such as acetaldehyde, ethyl acetate, and acetic acid [5, 6]. Noticeably, ethanol is precipitately turning into a strong relation between chemicals, biomass, and renewable energy. Acetaldehyde is respected to an essential intermediate organic synthesis. Thus, it plays an important role in the chemical industry due to be appropriate in chemical function in order to produce fruit flavor, wine flavor or even synthesis of pesticide. At the present, the majority methods to produce acetaldehyde are ethylene oxidation and acetylene hydration [7, 8]. However, these acetaldehyde production methods are employing nonrenewable energy products, eco-unfriendly method, and high operating cost. Thereby, the improvement of the acetaldehyde production process has befitted a priority. One of the captivated green processes for acetaldehyde production is ethanol dehydrogenation owing to its use the renewable energy source as employing the ethanol, and uncomplicatedly operate [9-11]. Previously, Gabarino *et al.* [6] investigated the ethanol dehydrogenation to acetaldehyde over copper/zinc aluminate catalysts. They found that $\text{Cu/ZnAl}_2\text{O}_4$ had potential for ethanol dehydrogenation to acetaldehyde with high selectivity at low conversion, but lower selectivity at high temperature. This is because it competed with the more preferred dehydration reaction of ethanol to ethylene. In addition, Obe-eye *et al.* [12] also investigated the acetaldehyde production from ethanol dehydrogenation using activated carbon with Co loading. The evidence suggested that activated

carbon with Co loading could achieve a good catalytic activity due to its high acidity on active site of catalyst, however, lower in the selectivity was observed at higher temperature. In addition, hydrogen (H_2) can be also produced from ethanol dehydrogenation process, which is one of the most energetic renewable process to generate the other energies as electricity power [13, 14]. Furthermore, ethanol dehydrogenation process to produce acetaldehyde and hydrogen is also one of the great advantages related to dehydrogenative oxidation of ethanol route [15]. Notwithstanding, the improvement of the selectivity either low or high operating temperature was passionate in ethanol dehydrogenation. Moreover, the core of this green process is still the design and investigation of great performance catalysts, which were needed at environmentally and eco-friendly catalyst in the production of acetaldehyde. Thus, One of the most attractive catalysts is mesocellular foam silica, which is a mesoporous material, large pore size, and spherical shape with interconnected pore [16, 17]. Incidentally, it essentially exists silanol group (-OH) on their surface, which can be properly adapted via functionalization for improvement of its chemical properties [18, 19]. In addition, one of the outstanding characteristics of mesocellular foam silica is the potentiality of the pore sizing by changing the ratio of swelling agent to surfactant, which directly affects to expand or shrink the pore materials [20, 21]. According to Schmidt *et al.* [22], they investigated the mesocellular siliceous foams with uniform large pore size that was desirable for chemical reactions. It was found that the change in ratio of swelling agent to surfactant was possibly affected to the pore size of materials. Furthermore, Ying *et al.* [23], who examined the spherical siliceous mesocellular foam particles for high-speed size exclusion chromatography via changing the ratio of swelling agent to surfactant. The evidence suggested that higher ratio of swelling agent to surfactant was respected to the higher pore size, which exhibited better separation capability than a commercial silica. Therefore, the choice of different ratios of swelling agent to surfactant is superiorly interesting to apply as the catalysts, which can be capably controlled the pore structure and specific area in order to facilitate higher diffusion of reactant and catalytic activity [24, 25]. For instance, Li *et al.* [26] investigated the preparation of highly active Cu-

Ce catalysts with different magnitude of pore size, which were used for CO oxidation reaction. The result showed that the enlarge pore size of catalysts was providable for either the formation of the active surface species or the catalytic activity supplemented. In addition, Yuan *et al.* [27] also investigated the synthesis of catalysts with different pore size by varying the amount of the swelling agent such as 1,3,5- trimethylbenzene for utilizing on hydrodesulfurization reaction. The evidence suggested that the pore size of catalysts could notably affect to the catalytic activity. In contrast, chemical properties of mesocellular foam silica as acidity and basicity are still insufficient for dehydrogenation of ethanol to acetaldehyde. Mesocellular foam carbon is one of the most potential catalysts obtained from the synthesis of mesocellular foam silica-based with adding sulfuric acid, which can provide higher acidity and basicity than mesocellular foam silica [28]. To the best of our knowledges, no work in the literature has not been yet reported that the preparation of mesocellular foam carbon catalyst with using different ratios of the swelling agent (pore expander) to the surfactant (carbon source) for ethanol dehydrogenation to produce acetaldehyde.

Accordingly, this research aims to investigate either the effect of TMB/P123 ratio in the mesocellular foam carbon (MCF-C) synthesis, which was derived from the mesocellular foam silica and the catalytic activity on ethanol dehydrogenation for acetaldehyde production. All catalysts were characterized using several techniques such as nitrogen physisorption, TEM, SEM-EDX, XRD, FT-IR, TGA, NH₃-TPD, and CO₂-TPD. In addition, these catalysts were tested for cultivation the catalytic behavior in ethanol dehydrogenation.

5.2. Experimental

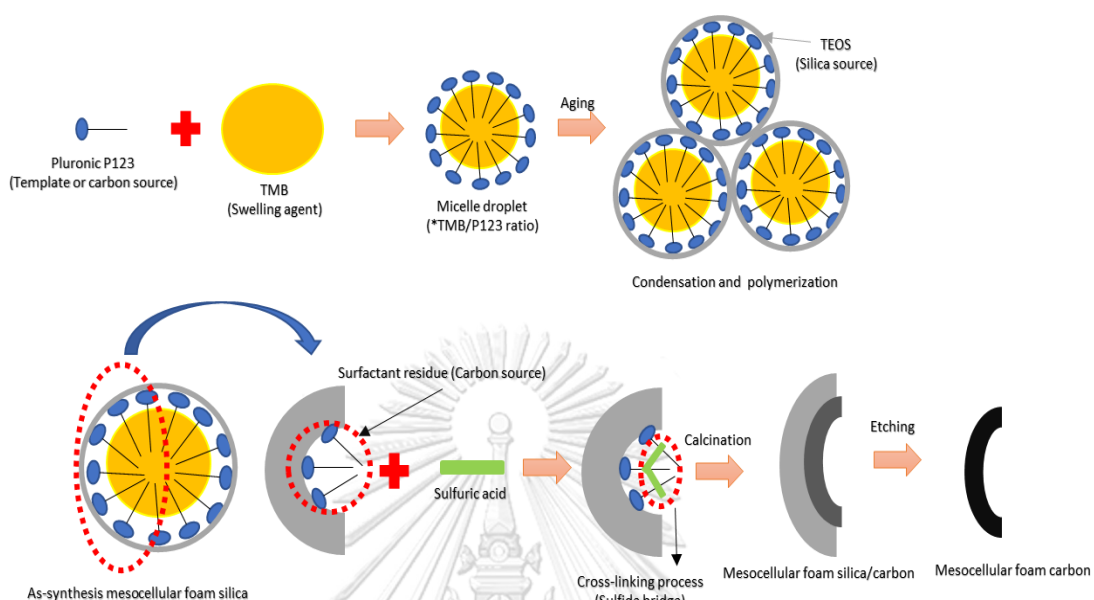
5.2.1 Materials and chemicals

All chemicals in this research were employed using analytical grade. Pluronic P123 (Sigma-Aldrich) was used either as the template or carbon source, and hydrochloric acid (HCl; 98 wt%, Sigma-Aldrich) was used to catalyze the synthesis process. The expander of the porous materials was 1,3,5-trimethylbenzene (TMB, Sigma-Aldrich). Tetraethyl orthosilicate (TEOS; 98% purity, Sigma-Aldrich) was the silica source. The catalyst used for formation of carbon layer was sulfuric acid [H₂SO₄ (98wt%,

Sigma-Aldrich]. Sodium hydroxide (NaOH, Sigma-Aldrich) was used to remove the silica in the materials.

Mesocellular foam carbon (MCF-C) was synthesized from mesocellular foam silica as the template [28]. The amount of 2 g of the surfactant as Pluronic P123 (triblock copolymer) was employed as the template of materials, which was dissolved in 10 ml of HCl with 65 ml of deionized water via stirring until it turned into homogeneous solution for 1 h at temperature of 25 °C. Then, the main step of the MCF-C synthesis was the varying of expander or swelling agent as 1,3,5-trimethyl benzene (TMB) with value of 1,3,5,7, and 9 g corresponding to different ratio of TMB/P123 denoted as MCF-0.5, MCF-1.5, MCF-C 2.5, MCF-C 3.5, and MCF-C 4.5, which were added into the prior solution at 40 °C, and consistently stirred for 2 h to gain milky solution. After that, the silica source as TEOS was added into the earlier solution followed by rapidly stirring with keeping the same temperature for 5 min. By the time, milky solution was migrated into the Teflon bottle. In addition, it was aged at 40 °C for 20 h, and was followed by increasing temperature to 100 °C with ramping rate of 10 °C/min. The milky solution was filtered with 100 ml of deionized water and 50 ml of ethanol, and accordingly dried it overnight at ambient temperature. The white sediment of mesocellular foam silica with different ratios of TMB/P123 were ready to be used as template for MCF-C synthesis by converting the residue of the surfactant to become carbon source. Therefore, MCF-C was transformed using 1 g of mesocellular foam silica, which was mixed with 0.16 ml of sulfuric acid, and continuously stirred it for 1 h at ambient temperature. Then, it was consecutively dried at 100 °C for 12 h. After that, increased the temperature to 160 °C and held at that temperature for 12 h. The obtained black powder was calcined at 850 °C under nitrogen flowing for 2 h by means of 1 °C/min as ramp rate. The etching part was followed by using 2 M of NaOH, which was mixed and slowly stirred with 1 g of black powder to remove the silica from the material for 6 h at ambient temperature. After reaching of 6 h, it was washed by using deionized water until the pH of filtrate was precisely unchanged, and subsequently dried for 24 h at ambient temperature as shown in **scheme 1**. Eventually, the catalysts preparation as MCF-C with different ratios of TMB/P123 could be readily

obtained, used for characterization and tested for catalytic activity in ethanol dehydrogenation.



Scheme 1. The schematical synthesis of MCF-C.

5.2.2 Characterization

5.2.2.1 N₂-physorption

The physical characteristics such as surface area, pore size, and pore volume of the catalysts were determined by a multipoint BET analysis method via nitrogen adsorption/desorption isotherms at -196 °C. The catalysts were degassed by heating in vacuum at ambient temperature to 120 °C for 12 h before operating the adsorption. Barret-Joyner-Halenda (BJH) method was also applied to determine the pore structure of catalysts based on the Kelvin equation.

5.2.2.2 Transmission electron microscopy (TEM)

The characteristic of internal structure of catalysts was determined using TEM for investigation with JEOL JEM-2010 with the thermionic electron type LaB₆ as a source via operating at 200 kV.

5.2.2.3 Scanning electron microscopy (SEM) and energy dispersive X-ray spectroscopy (EDX)

The external catalyst morphology was examined by SEM with Hitachi S-3400 N model. The deposition of catalysts was taken on carbon tape for SEM investigation. In addition, micrographs were applied at the accelerating voltage of 30 kV. The elemental distributions on surface of the catalysts were performed by Link Isis Series 300 program EDX.

5.2.2.4. X-ray diffraction (XRD)

The investigation of the crystalline framework of catalysts was applied by XRD with a Siemens D 5000 X-ray diffractometer having CuK α radiation via Ni filter in the range of 2θ between 10 to 80 with 0.04 resolution having the scan rate at 0.5 sec/step.

5.2.2.5 Thermogravimetric analysis (TGA)

TGA was operated with TA instrument SDT Q600 analyzer (USA). The amounts of catalysts of 4-10 mg were employed in the temperature operation range between 30 to 1000 °C with heating rate of 2 °C/min under air as carrier gas.

5.2.2.6 Fourier transform infrared (FT-IR) spectroscopy

The functional groups on bulk catalysts were examined using the FT-IR spectroscopy. The evident absorption spectra were attained using Nicolet 6700 FT-IR spectrometer in the wavenumber range of 400 to 4000 cm^{-1} .

5.2.2.7 Carbon dioxide temperature-programmed desorption (CO₂-TPD)

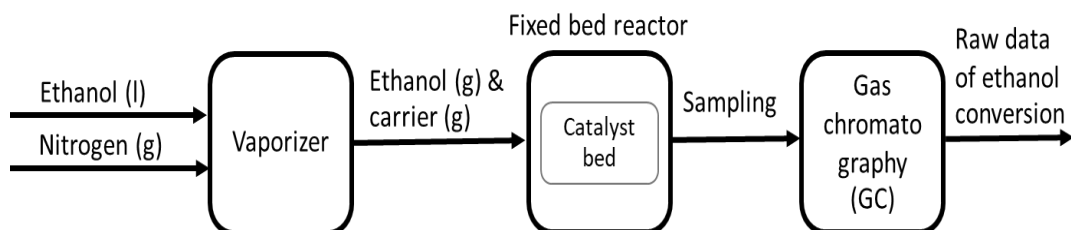
CO₂-TPD was employed to measure the basicity of the catalysts using Micromeritics Chemisorb 2750 automated system. The catalyst powder of 0.1 g was loaded into the quartz cell and also preheated at 450 °C under helium gas using flow rate of 25 ml/min for 1 h to remove moisture and impurity of catalyst sample. After that, CO₂ was used to saturate in the catalyst sample and then evacuated using helium gas with flow rate of 35 ml/min for 30 min at 40 °C. Next, TPD was performed from 40 °C to 500 °C with ramping rate of 10 °C/min. The analysis of the amount of CO₂ in effluent gas as a function of desorbed temperature was employed the thermal conductivity detector (TCD).

5.2.2.8 Ammonia temperature-programmed desorption (NH₃-TPD)

NH₃-TPD was used to measure the acidity of the catalysts using Micromeritics Chemisorb 2750 Pulse Chemisorption System. The catalysts power of 0.1 g was packed to preheat with helium at 200 °C. Then, ammonia was followed adsorbing at 40 °C for 1 h. Then, the physisorbed ammonia was consecutively desorbed under helium gas flow until the baseline level was reached to be constant. Next, the chemisorbed ammonia was evacuated from active sites via increasing of the temperature from 30 to 500 °C under helium gas with the flow rate of 40 ml/min, and the heating rate of 10 °C/min. The amount ammonia in effluent was measure by employing the thermal conductivity detector (TCD) as a function of temperature.

5.2.3 Ethanol dehydrogenation process

To investigate the catalyst behavior of each catalysts, ethanol dehydrogenation reaction was applied using a fixed-bed continuous flow glass tube microreactor. At first, either 1 g of catalysts or 0.05 g of quartz wool bed were loaded inside of the middle glass tube reactor, which was placed inside of the electric furnace. The nitrogen gas was fed into the microreactor for pretreatment at 200 °C for 1 h, which was performed to evacuate the moisture on the surface of target catalyst. After that, the ethanol was vaporized at 120 °C with nitrogen gas with flowing rate of 60 ml/min employing controlled injection with a single syringe pump, which used the volumetric flow rate of ethanol feeding of 0.397 ml/h. Next, the gas stream was achieved to the reactor with weight hourly space velocity (WHSV) of 3.1 $\frac{\text{g}_{\text{ethanol}}}{\text{g}_{\text{cat}} \cdot \text{h}}$. The attentive operating temperature range was 250 to 400 °C under atmospheric pressure. The gaseous products were determined using a Shimadzu (GC-14B) gas chromatograph by flame ionization detector (FID) and capillary column (DB-5) at 150 °C. While the reaction test was performed, the data results were recorded at least 3 times for each temperature as **Scheme 4.2**.



Scheme 4.2 Flow diagram of ethanol dehydrogenation system.

The magnitudes of ethanol conversion, selectivity of acetaldehyde, and yield of acetaldehyde were determined using following these equations (1), (2), and (3), serially.

$$\text{Ethanol conversion} : X_{EtOH}(\%) = \frac{n_{EtOH}(in) - n_{EtOH}(out)}{n_{EtOH}(in)} \times 100 \quad (1)$$

$$\text{Selectivity of acetaldehyde} : S_i(\%) = \frac{n_i}{\sum n_i} \times 100 \quad (2)$$

$$\text{Yield of acetaldehyde} : Y_i(\%) = \frac{X_{EtOH} \times S_i}{100} \quad (3)$$

where mol_i is the mole of regarded product and $\sum mol_i$ is the total moles of achievable products.

5.2.4 Stability test

All MCF-C catalyst samples were investigated for the stability performance as a function of time on stream (TOS) for 12 h. This experimental operating and set-up were employed with the similarity to those of temperature-programmed reaction studies as ascribed above. The stability conditions of ethanol dehydrogenation reaction were proceeded at 400 °C. The outlet products from reactor were consolidated every 1 h for 12 h with time on stream.

5.3. Result and Discussion

5.3.1 Characterization

5.3.1.1 N₂-physisorption isotherms and textural properties

The nitrogen adsorption-desorption isotherms were effectively used to identify the type of pore characteristic of catalysts samples, which were varied depending on different TMB/P123 ratios employed during the synthesis of MCF-C catalysts are depicted in **Figure 5.20**.

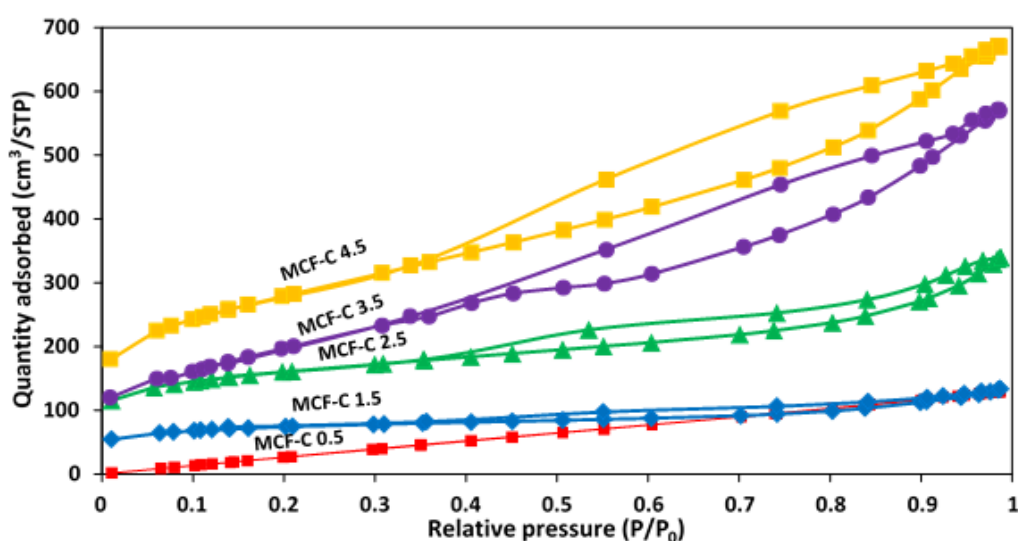


Figure 5. 20 Nitrogen adsorption/desorption isotherm of all MCF-C catalysts.

The difference in amount of TMB could be pointed in explicit structural transformation of nitrogen isotherm for each of the catalysts prepared. The nitrogen isotherms of MCF-C 4.5, MCF-C 3.5, and MCF-C 2.5 exhibit the type IV with H2(b) type hysteresis loops (IUPAC) indicating that the pore size of these catalysts having the high ratio of TMB/P123 from 3.5 to 4.5 possibly signified the presence of mesoporous structure and narrow pore owing to ink-bottle shape with interconnected cell as the porous network [28, 29]. Besides, the slope of hysteresis loops of MCF-C 4.5, MCF-C 3.5, and MCF-C 2.5 abruptly increase at P/P_0 value of 0.35 due to the capillary condensation in the pore structure [30]. In contrary, there were softly variations in the movement and flat degree of the hysteresis loops suggesting that the pore size and consistency were slightly similar with the tradition template as mesocellular foam silica [28]. This revealed that the higher amount of TMB did not significantly influence the

meso-structure of the catalysts. Furthermore, the addition of TMB promoted significant changes in the characteristic of large pore size mesoporous materials with enlarge compartment connected via pores recognized as windows [31]. Meanwhile, the nitrogen isotherm of MCF-C 1.5 still exhibited the combination of types IV (major) and I (minor) of hysteresis loop, and MCF-C 0.5 performed the combination of types I (major) and IV (minor), according to the IUPAC. These results were denoted that the isotherm characteristics was present in both microporous and mesoporous structures [32]. In addition, it was evidently discovered that at this low ratio of TMB/P123 was partially displayed the characteristic of mesoporous due to the insufficient amount of TMB for expanding the pore, which possibly indicated either the typical rod-like materials or hexagonal structure for MCF-C 0.5 [33]. Moreover, the characteristic of isotherm of the MCF-C 1.5 probably had both structures of incomplete spherical and cylindrical shapes due to the combination of isotherms that likely facilitate the diffusion owing to the synergetic of these two structures. Simultaneously, the textural properties, including the data for BET surface, BJH pore size, and pore volume, were also correlated as seen in **Table 5.13**

Table 5. 13 Surface area (BET), average pore size and average pore volume.

Materials (TMB/P123 ratio)	Surface area (m ² /g)	Pore size (nm)	Pore volume (cm ³ /g)
MCF-C 0.5	413	3.4	0.17
MCF-C 1.5	558	4.5	0.25
MCF-C 2.5	759	5.7	0.82
MCF-C 3.5	863	9.5	1.03
MCF-C 4.5	524	15.0	1.38

It was suggested that the increase of TMB/P123 ratios from 0.5 to 4.5 were significantly influenced on the extensive pore size of carbon structure. Fundamentally, this phenomenon can be described for the basis of the fact that TMB acted as a nonpolar compound which can dissolve the internal template of the triblock copolymer assemblies. Therefore, it expands the volume of the hydrophobic part leading to the expansion of the pore size due to the addition of the swelling agent,

according to be miscible with the synthetic mesocellular foam carbon with various ratios of TMB/P123. In addition, the increased amount of TMB evidently facilitated the optimization of BET surface of materials from 413 to 863 m²/g with the TMB/P123 ratios from 0.5 to 3.5. However, it abruptly decreased to 524 m²/g when increased TMB/P123 ratio to 4.5. It was likely that the increase of TMB dosage provides higher surface area, but it decreases with increased TMB/P123 ratio up to 4.5 due to its trading off between surface area and pore size. This led to the saturation point of meso-structured carbon synthesis process. Therefore, it is remarkable that by altering the amount of TMB, it apparently results not only in variations in terms of their morphology and mesophase, but it also promotes the individuality in the hysteresis loops curves. Moreover, the higher ratio of TMB/P123 as 2.5 to 4.5 was notably conducted to be successfully synthesized the meso-structural carbon catalysts due to the appropriate amount of TMB, which did not only remain the mesocellular foam carbon structural, but also extend the pore size in order to provide higher diffusion of reactant and higher catalytic activity on ethanol dehydrogenation.

5.3.1.2 Mesophase structures of catalysts

In order to identify the transformation of the structural of the mesophase of catalysts via increasing amounts of swelling agent i.e. TMB, the catalysts prepared were investigated using TEM as shown in **Figure 5.21**. The figure indicates the TEM micrographs of the catalysts with different ratios of TMB/P123 between 0.5, 1.5, 2.5, 3.5, and 4.5. It was found that the increase in ratios of TMB/P123 obviously caused a phase transformation from disorder and unclear foam-like structure to the more explicit foam-like structure of mesopores of the catalysts from MCF-C 0.5 to MCF-C 4.5. However, the slight changes in the pore structures as seen from MCF-C 1.5 and MCF-C 2.5 were due to increasing of TMB dosage, which could impart either the obvious spherical pore shape or more ordered mesopore structure.

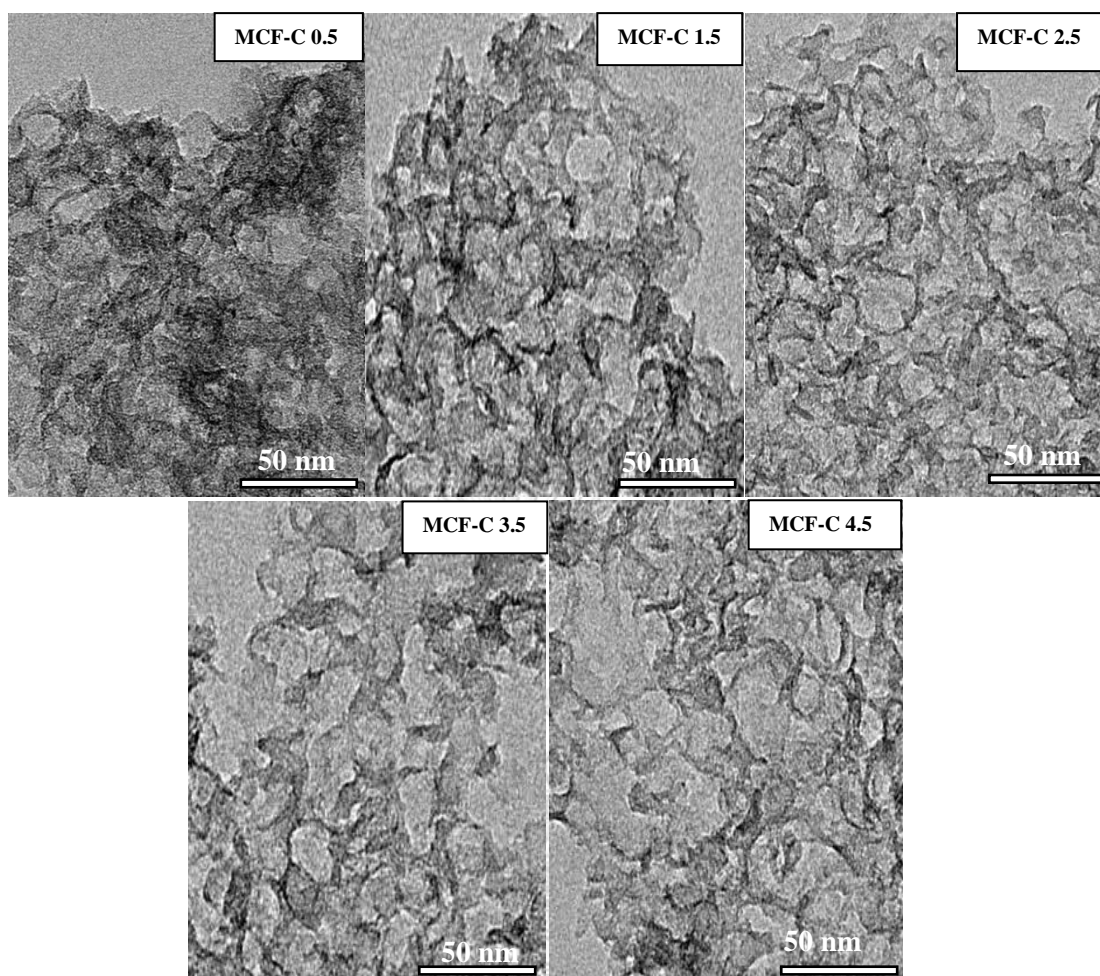


Figure 5. 21 TEM images of all MCF-C catalysts.

On the contrary, the higher TMB/P123 ratio greatly changed the carbon wall as MCF-C 3.5 and MCF-C 4.5 were synthesized. The evidence pointed that the large amount of TMB possibly influenced the collapse of the carbon wall owing to the high volume of TMB, which massively expand the micelle template and enlarged pore size [21]. In addition, the higher ratios of TMB/P123 did not affect the consumption of the residue surfactant, which reacted with sulfuric acid, and did not affect the etching process of the silica.

Basically, the conclusion should be made whereby the ratio of TMB/P123 of MCF-C 0.5 and MCF-C 1.5 from the synthetic process caused a dramatic transformation in the mesophase with the enlargement of pore size as disorder structure, which was formed to be more order and foam-like structure. In the meantime, the addition of ratios of TMB/P123 at 2.5, 3.5, and 4.5 led to obtain complete foam-like structures,

which were intensely involved in the tradition structure as mesocellular foam silica materials. The transformed mesophase of catalysts from disordered and unclear pore to sponge-like structure [20] and clearer pore of MCF-C slightly arose by mixed phased with an increase in the ratios of TMB/P123 employed.

5.3.1.3. Morphologies of surface and particles

To investigate the morphology as external surface of mesocellular foam carbon with variation in the ratio of TMB/P123 that remarkably affected the physical appearance of the mesostructured carbon catalysts, the explicit transformation in the morphology is noticed as seen in **Figure 5.22**. The SEM image of MCF-C 0.5 showed the rod-like structure in bundle arrangement [20], which was distinguished when low TMB/P123 ratio was employed. In contrast, this typical rod-like structure was notably disturbed to irregular spherical particles when adding more TMB dosage to become MCF-C 1.5. In addition, the low ratios of TMB/P123 hardly affected the surfactant residue amount for converting to the carbon source in meso-structure carbon synthesis process indicating that the TMB reagent just only provided more enlarge pore size of the materials, but it did not increase the carbon content. However, the agglomeration of the spherical particles was remarkable when the ratio of TMB/P123 was further increased. The uncommon spheres were observed in an aggregated phase in the case of MCF-C 1.5 and, its morphology was observed to transform from the rod-like shape to the spherical shape. Principally, whenever swelling agent was supplemented into the synthetic mixtures, the 'oil as an expander' swelled the polypropylene oxide (PPO block), which is hydrophobic in character of its reagent [34].

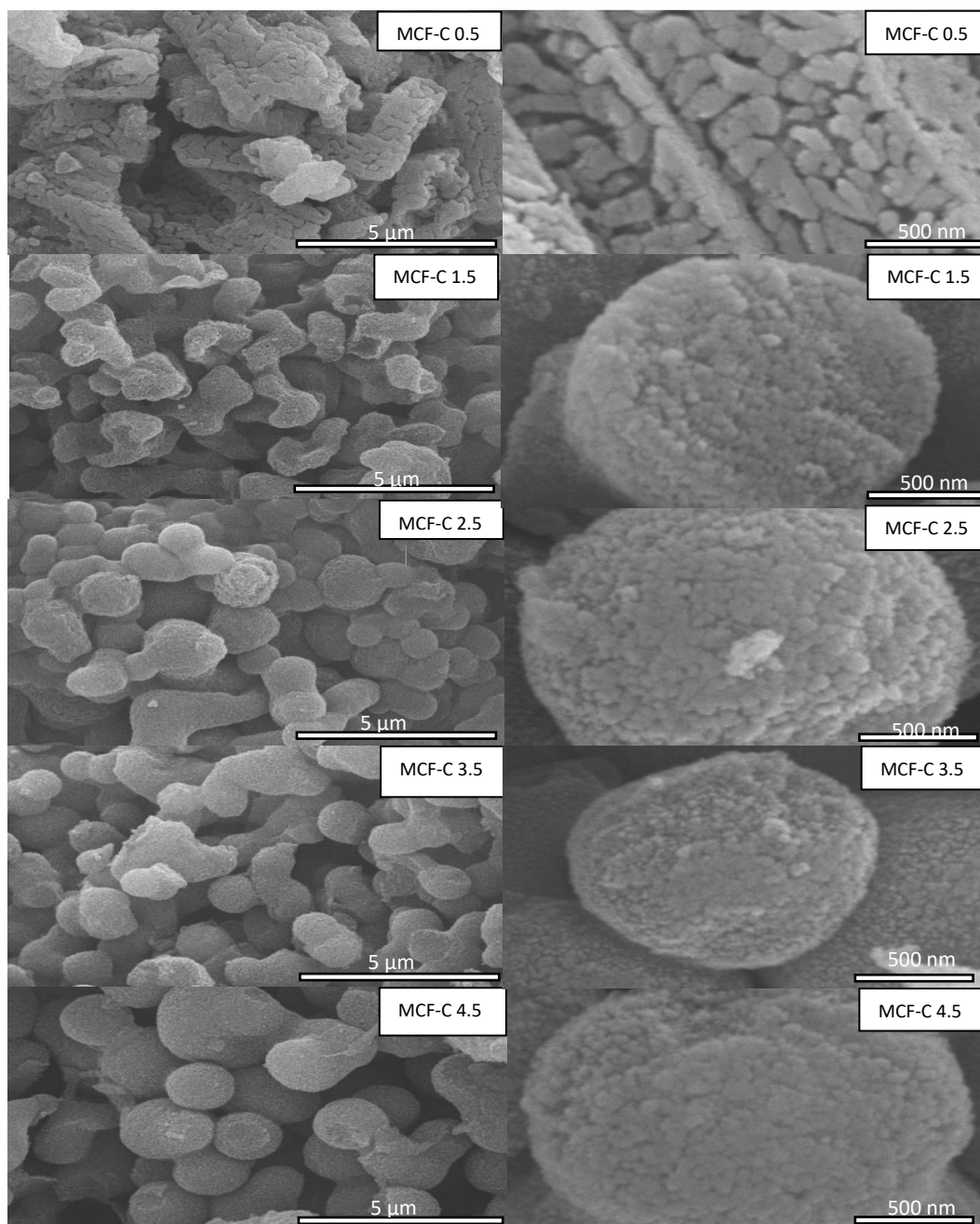


Figure 5. 22 SEM images of all fresh MCF-C catalysts.

Nevertheless, according to the quantity of added oil was interrelated low, thus the transformation of MCF-C 0.5 and 1.5 were only partial rather than complete as its higher ratio of TMB/P123 to form the spherical shape as its expected.

A plenary spheres shape might only be achieved when the ratio of TMB/P123 was increased up to 2.5, 3.5, and 4.5. At this phase, more complete spherical particles were accomplished. Simultaneously, the ratios of TMB/P123 of MCF-C 2.5, 3.5, and 4.5 scarcely influenced the particle size with the obtained diameters of ca. 2.1-2.3 μm ($n = 200$) suggesting that it was no reduction of particle size with the high ratio of TMB/P123 owing to the saturation of particles size among adding the higher swelling agent. Meanwhile, the energy dispersive X-ray spectroscopy (EDX) was applied to detect the amounts of atomic percent composition of all ratios of TMB/P123 as C, O, and Si, respectively as seen in **Table 5.14**.

Table 5. 14 The amounts of each element near surface of catalyst granule obtained from EDX.

Catalyst	Amount of element on surface (wt%)		
	C	O	Si
MCF- C 0.5	85.2	11.6	3.2
MCF- C 1.5	88.5	10.3	1.2
MCF- C 2.5	90.8	8.4	0.8
MCF- C 3.5	91.4	7.9	0.7
MCF- C 4.5	90.7	8.4	0.9

The evidence suggested that carbon contents of each material were slightly different with values varied 85.2 to 90.7 wt % due to the constant amounts of surfactant. In addition, the noticeable presence of silicon in the lower ratio of TMB/P123 as MCF-C 0.5 and MCF-C 1.5 was observed. It indicated that the etching process for removing the silica out of the template might be hindered due to the limited diffusion of NaOH to the inner core of the small pore-size particles.

Therefore, it was predicated that the role of TMB was coherently obvious as a swelling agent and it possibly influenced the transformation of the rod-like morphology to discontinuous spherical, and complete spherical shape. In addition, a reasonable

ratio of TMB/P123 might play a significant role in transforming from the rod particles to spherical particles of MCF-C materials whilst as excessive magnitudes of it was harmful to the aim of obtaining perfect spherical shape structure.

5.3.1.4 The analysis of crystallinity of MCF-C

In order to further examine the crystal structure of all materials, X-ray diffraction (XRD) was applied as seen in **Figure 5.23**. X-ray diffractograms of all catalysts introduced low angle reflection characteristic of ordination at the mesoscale. Ordinarily, an XRD pattern of each catalyst was found to correspond to the micellar cubic phase as the spherical micelles [35]. In addition, XRD pattern of MCF-C 0.5 at the low angle region ($2\theta = 0.5^\circ$) demonstrates the dominant broad peak indicating the existence of the carbon structure [36, 37].



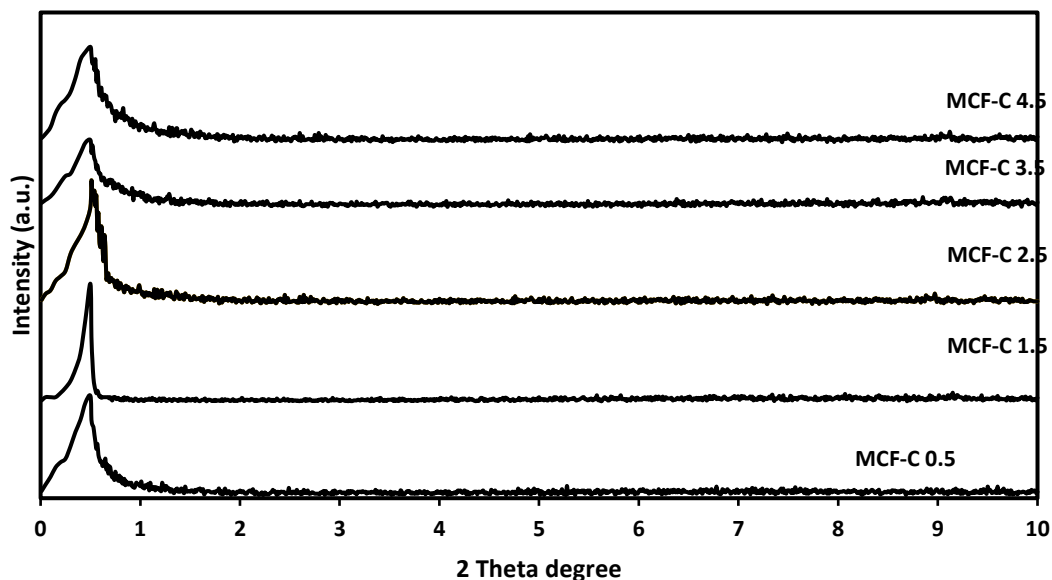


Figure 5. 23 XRD patterns of all MCF-C catalysts.

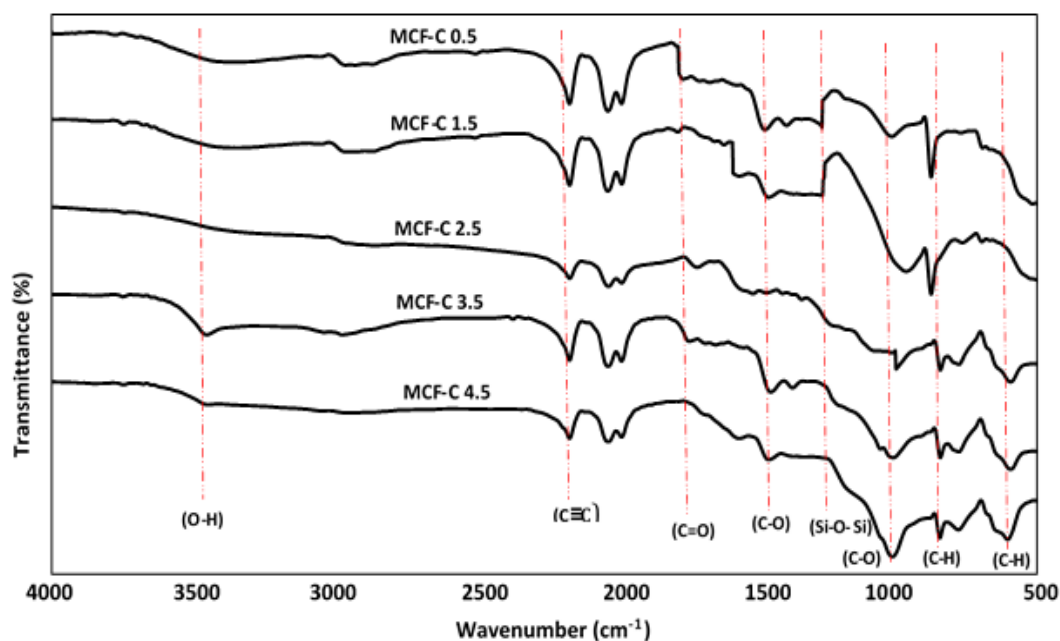
Meanwhile, when TMB was added to the ratio of TMB/P123 to 1.5, the phase change with a sharp peak in order to form the mesophases of foam-like structure with the high volume of the swelling agent with the divergence of the structural arrangement. However, at the high ratios of TMB/P123, there was no change of 2 theta degree, but these peaks of MCF-C 2.5, 3.5, and 4.5 possibly became back to the broad peaks. The possibility was demonstrated that the high volume of TMB dosage could facilitate to enlarge pore size, but it was evidently signified the more disordered structure due to the uncontrollable effect of etching the silica out when the pore size was greater. Thereby, the ratio of TMB/P123 could affect the ordered or disordered structure of mesophase, but there was none of evident effects of the carbon layer of the materials upon increasing of TMB dosage.

5.3.1.5 FT-IR studies

The natural chemistry of all MCF-C surfaces was investigated using an infrared technique. FT-IR spectra for the materials with different ratios of TMB/P123 were compared to investigate the effect of TMB volume as shown in **Figure 5.24**. All MCF-C materials apparently exhibited the characteristic of carbon materials from FT-IR

bands at ~ 625 and ~ 850 cm^{-1} corresponding to C-H vibrations out of plane, which was probably referred to the benzene rings representing a carbon source [38, 39]. In addition, the symmetric vibrations of the Si-O-Si were evidently remained (1250 cm^{-1}) for MCF-C 0.5 and MCF-C 1.5, which confirmed the EDX data of the Si existence. Furthermore, all the ratios of TMB/P123 were apparently perceived at 3500 cm^{-1} representing O-H stretching vibrational mode, indicating the presence of silanol group [36, 40]. The evidence suggested that even at the adding TMB dosage with higher ratio of TMB/P123, it was explicitly balanced the silanol group, which could provide either the retainable chemical characteristic of MCF-C or the facilitated functionalization of other chemicals for approving the chemical surface. Furthermore, the OH formation on all the MCF-C surface could remarkably energize the Brønsted acid sites during the catalytic reaction step [39, 41], which were significantly important influences on the acidic character of the carbon catalysts for ethanol dehydrogenation process.

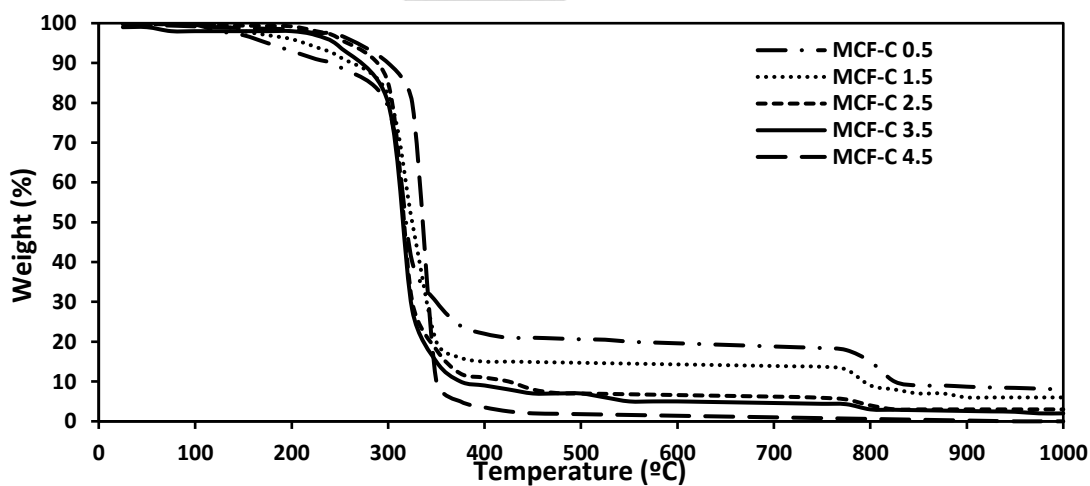
Figure 5. 24 FT-IR spectra of all MCF-C catalysts.



5.3.1.6 TGA studies

The thermogravimetric analysis is one of the techniques to investigate the weight loss patterns of MCF-C with different TMB/P123 as shown in **Figure 5.25**. Weight losses were observed at 325-350 °C with the sharply decline peak. This indicates the existing of carbon composition in all MCF-C materials [42], which remarkably indicates successful conversion of the surfactant to carbon structure in all of the TMB/P123 ratios. Meanwhile, the MCF-C 4.5 exhibits the highest weight loss at 350 °C. This showed that the highest volume of TMB added could be converted into the highest carbon composition with value of ca. 97 %, which might as well influence the chemical properties in either acidity or basicity. Thus, the neat ratio of TMB/P123 should be notably considerable with the appropriate functional process. In this case, MCF-C 3.5 was a reasonable candidate as a catalyst for the ethanol dehydrogenation, which was compared to other MCF-C materials owing to its highest carbon composition.

Figure 5. 25 Thermogravimetric analysis (TGA) of all MCF-C catalysts under air atmosphere.



5.3.1.7 Surface acidity

Ammonia temperature-programmed desorption (NH_3 -TPD) was properly utilized to evaluate the surface acidity and the strength of acid sites of each ratio of MCF-C considered. The NH_3 -TPD was integrated the desorption peaks of ammonia under operating temperature range between 30-500 °C. The two main regions of acidity are isolated desorption ammonia peaks for weak acid sites at the low temperature (<

200 °C), whereas medium to strong acid sites are at the higher temperature range (200-500 °C) [9, 41]. The magnitudes of the acid sites ($\mu\text{mole/g}$) of all the catalysts are summarized in **Table 5.15**. The evidence suggested that all MCF-C materials exhibited high total acid sites due to the chemical character of carbon [12, 28], which might help enhancing the efficient of ethanol dehydrogenation to acetaldehyde.

Table 5. 15 Acidity and acid strength of MCF-C catalysts obtained from NH_3 -TPD.

Catalyst	Amount of acid site ($\mu\text{mole NH}_3/\text{g cat.}$) ^a		
	Weak acid sites	Medium-strong acid sites	Total acid sites
MCF-C 0.5	39.4	479.7	519.1
MCF-C 1.5	61.5	496.1	557.6
MCF-C 2.5	79.3	546.9	626.2
MCF-C 3.5	92.2	552.5	644.7
MCF-C 4.5	84.2	524.3	608.5

^a Amounts of acid sites of catalysts were determined by NH_3 -TPD (use of Fityk program calculation).

Compared to all other MCF-C, MCF-C 3.5 exhibited the highest amount of total acid sites having value of 644.64 $\mu\text{mole NH}_3/\text{g cat.}$, which possibly suggested the highest Brønsted acid sites [43]. Moreover, it also evidently exhibited the NH_3 -TPD profile of MCF-C 3.5 with either the highest weak acid sites or medium to strong acid sites as seen in **Figure 5.26**. It indicated that this TMB/P123 ratio is likely appropriate for ethanol dehydrogenation to acetaldehyde, which highly corresponded to the two acidic regions. The significant indication was that the variation of the TMB/P123 ratio provided the obvious increase of acidity, but the appropriate ratio of TMB/P123 needed to be identify by ethanol dehydrogenation in order to optimize the catalytic activity.

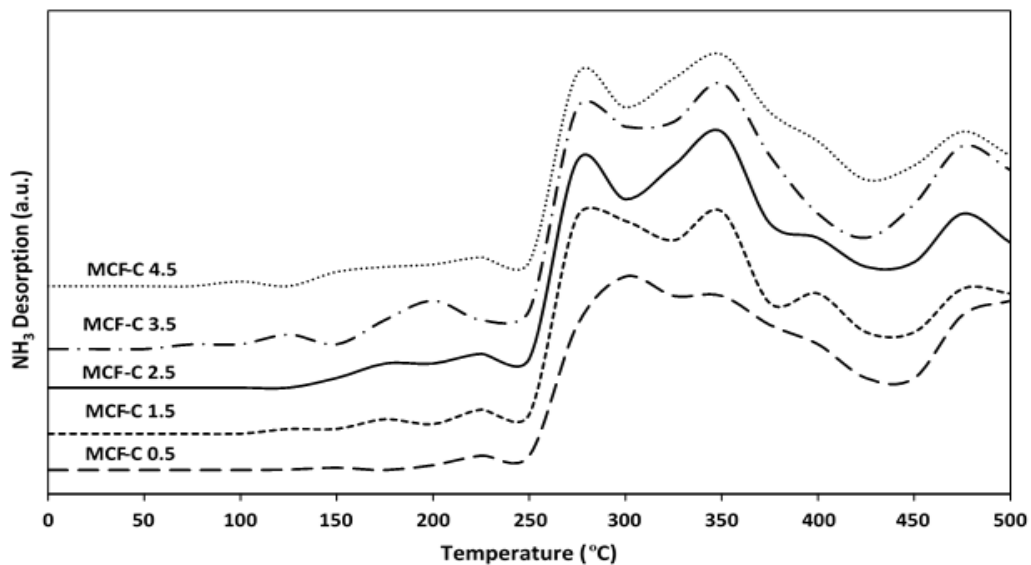


Figure 5. 26 NH₃ -TPD profile of all MCF-C catalysts.

5.3.1.8 Surface basicity

To investigate the surface basicity and base strength for all the materials, CO₂-TPD was employed to determine the total basicity via the calibration factor, which was determined from the integration of the area under CO₂ desorption curve in order to convert into moles of CO₂ evaded [44]. There are two major regions of basicity from CO₂ desorption, which could be classified into the weak basic site region in the temperature below ca.200 °C and the medium to strong basic site region at the temperature of 200 to 500 °C. The CO₂-TPD profiles of all materials are shown in **Figure 5.27**, it partly exhibited the small and broad peak of CO₂ desorption under temperature of 200 °C according to CO₂ from bicarbonate species, which was possibly mentioned to the weak acid sites due to formation via the reaction of CO₂ with silanol group (OH) adsorbed.

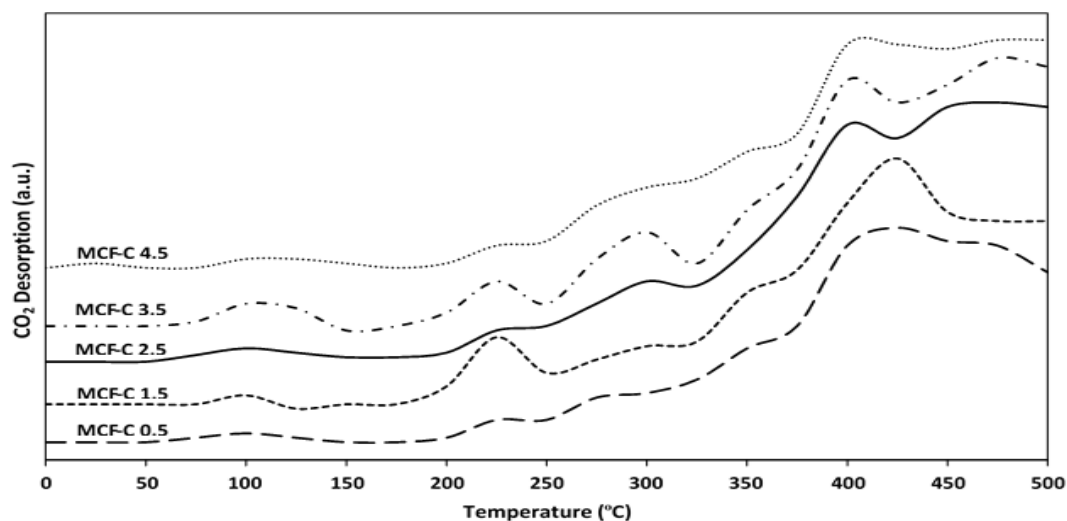


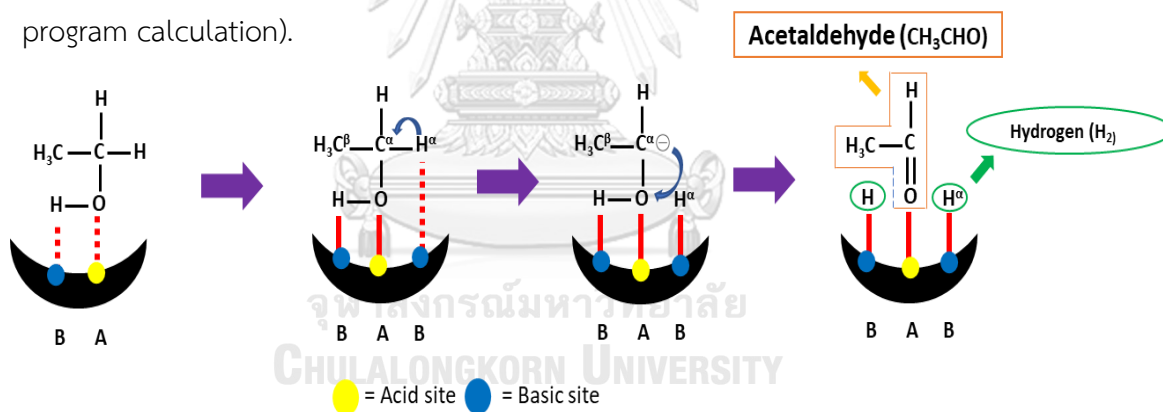
Figure 5. 27 CO₂ -TPD profile of all MCF-C catalysts.

In addition, MCF-C 3.5 exhibited the highest peak, which corresponded to the FT-IR with the highest existing of OH group. Meanwhile, at the temperature above 200 °C also strongly exhibited the high density of desorption peaks for all the materials, which probably provided the high value of medium to strong basic sites corresponding to **Table 5.16**. These results indicated that MCF-C 3.5 exhibited the highest value of total base sites of 916 $\mu\text{mole CO}_2/\text{g cat.}$, but it was not obviously different in total base site comparing to the other ratios of TMB/P123. This suggested that the various TMB dosages in MCF-C synthetic process insignificantly affected to the surface basicity. However, the appropriate change of TMB dosage was still important in order to optimize the highest catalytic activity on ethanol dehydrogenation to acetaldehyde, which apparently favor the high basicity [32, 45]. Furthermore, the feasible mechanism of ethanol dehydrogenation process on the acid and basic sites is shown in **Scheme 4.3** [32, 45]. Firstly, adsorption of ethanol molecule on the acid and basic sites of the MCF-C surface to O and H atoms. After that, C ^{α} -H ^{α} bond directly cleavage to a surface ethoxy species in order to form acetaldehyde, which is next accompanied by two surface-bonded hydrogens desorption to form hydrogen in a gas phase. Lastly, the regeneration of active sites occurs and ready for further reaction.

Table 5. 16 Basicity and basic strength of all MCF-C catalysts obtained from CO₂-TPD.

Catalysts	Number of base site (umole CO ₂ /g cat.) ^b		
	Weak base sites	Medium-strong base sites	Total base sites
MCF-C 0.5	21.3	762.7	784
MCF-C 1.5	32.5	802.7	835.2
MCF-C 2.5	42.7	854.4	897.1
MCF-C 3.5	51.1	865.2	916.3
MCF-C 4.5	36.3	822.8	859.1

^b Amounts of basic sites of catalysts were determined by CO₂-TPD (use of Fityk program calculation).



Scheme 4.3. The feasible mechanism of dehydrogenation of ethanol process on the acid and basic sites.

5.3.2 Catalytic activity studies

5.3.2.1 Ethanol dehydrogenation process

The mesocellular foam carbon catalysts with the difference in ratio of TMB/P123 were applied for investigating the behavior on ethanol dehydrogenation focusing on acetaldehyde as a major product. Basically, the reaction temperature directly influences the driving force of the reaction system in order to improve the catalytic activity as the conversion is endothermic [46]. The investigated operating temperatures were 200-400 °C under atmospheric pressure. The activity results for ethanol conversion of all TMB/P123 ratio are represented in **Figure 5.28**. The initiated operating temperature was 200 °C, while the conversion of ethanol continuously increased with increased temperatures from 250 to 400 °C for all the ratios of TMB/P123. The implication of the increase in ethanol conversion was thermodynamically related with the endothermic behavior of dehydrogenation reaction, which contributed to the high heat retainable in the products. Meanwhile, the MCF-C 3.5 evidently exhibited the highest ethanol conversion amongst other ratios of TMB/P123 with value of ca. 18.6 % at 400 °C.

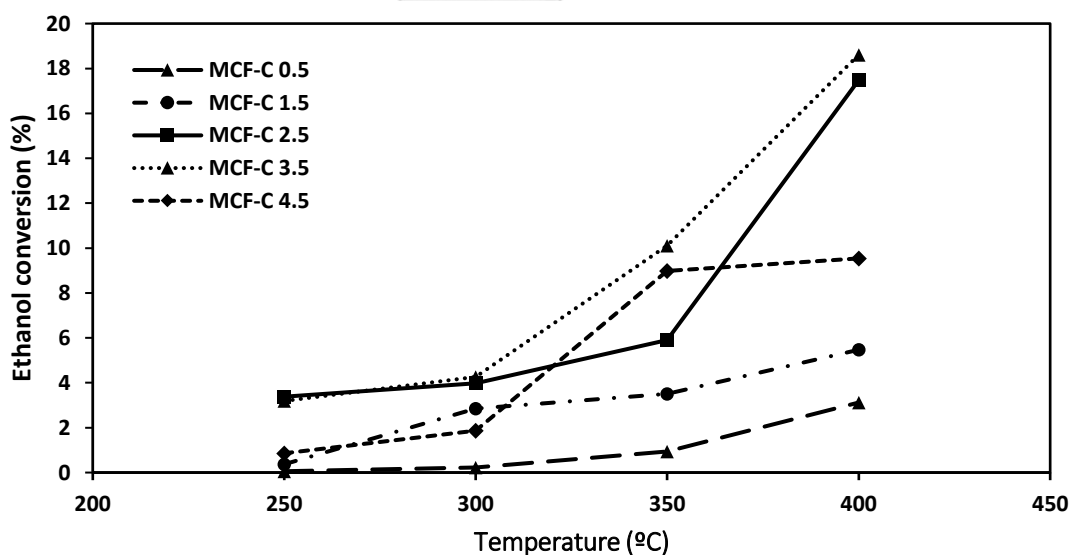


Figure 5. 28 Ethanol Conversion of all MCF-C catalysts on ethanol dehydrogenation.

Furthermore, MCF-C 3.5 could perform the highest yield of acetaldehyde at 400 °C with value of ca. 15.9 % as seen in **Figure 5.29**, but the selectivity of acetaldehyde of MCF-C 3.5 with value of ca. 85.6 % was not obviously higher than

other catalysts owing to the formation of other products when the reaction was operated under higher temperature. In contrast, the increase ratio of TMB/P123 to 4.5 did not exhibit higher catalytic activity as expected. The largest pore size of MCF-C 4.5 among others lowered the specific area, which probably affected to the surface of catalytic reaction. This suggested that the MCF-C 4.5 perhaps provided the excessive volume of the swelling agent, which was an explicit disadvantage for the active surface component [47]. Thus, the optimum of ratio of TMB/P123 as MCF-C 3.5 could be significantly improved with sequentially excessing the operating reaction temperature. In addition, the selectivity of byproducts for all catalysts on ethanol dehydrogenation as a function of reaction temperature is shown in **Table S1**. Byproducts as ethylene was explicitly observed in all catalysts, which clearly decreased acetaldehyde selectivity due to the formation of ethylene on acidic species of MCF-Cs surface [9]. On the contrary, it was remarkably observed on the MCF-C 3.5 catalyst that the byproducts, either ethyl acetate or acetic acid, were accidentally occurred among in the temperatures range of 350-400 °C. This phenomenon can be described via the complex pathway in the structure of MCF-C 3.5 which increased contact time of the ethanol and acetaldehyde to form ethyl acetate and acetic acid [11] as shown in **Scheme 4.4**. Principally, there are several possible factors which affect the catalytic activity in either physical (specific area, and pore structure etc.) or chemical properties (acidity, basicity, and functional group). Due to the difference in the added volume of TMB to the synthetic process, the structural and the active component on surface of synthesized mesoporous carbon catalysts (MCF-C) can be notably influential. The MCF-C 0.5 evidently performed the worst ethanol catalytic activity due to the nonporous character of the catalyst structure which resulted in the worst reactant diffusion. This low addition of the swelling agent impeded the formation of the pore structure, which lowered the catalytic performance.

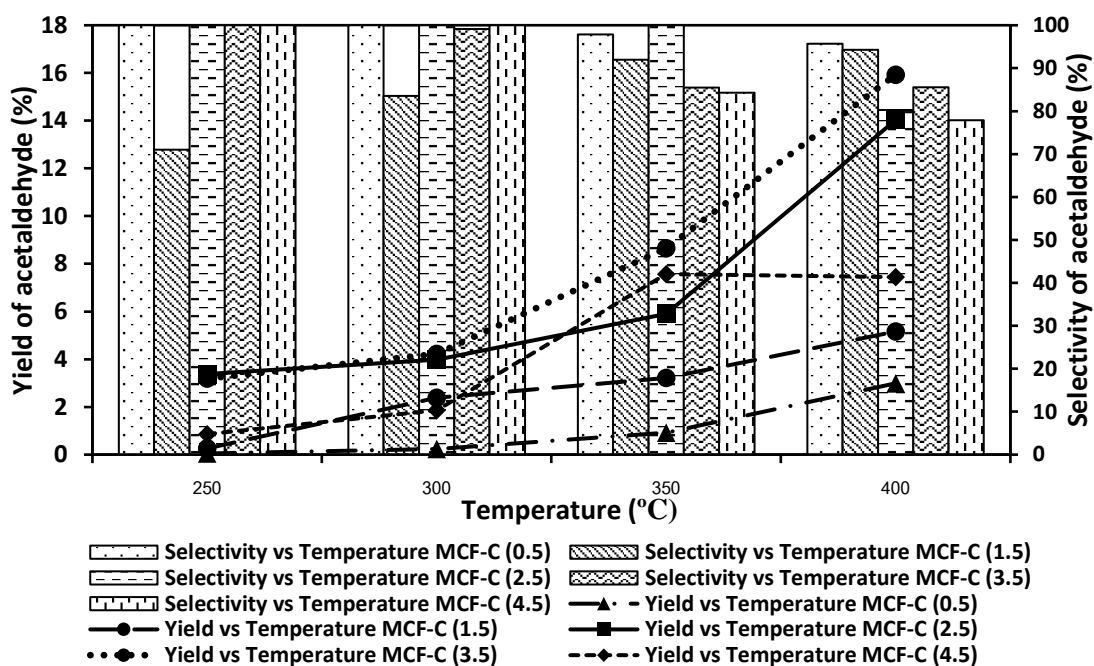
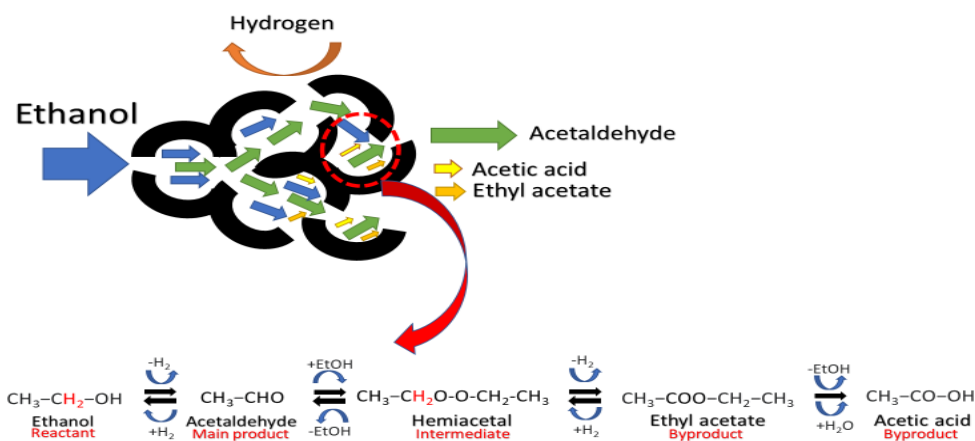


Figure 5. 29 Yield and selectivity of acetaldehyde vs temperature of all MCF-C catalysts on ethanol dehydrogenation.



Scheme 4.4. The pathway of ethanol dehydrogenation.

The physical property from BET result verifies that MCF-C 0.5 has the relatively small pore size and specific surface area, thereby decreasing the contacting possibility on the catalyst surface between the reactant molecule and active sites. In addition, the adsorption and activation ability of MCF-C 0.5 to ethanol was further affected MCF-

C 0.5 owing to its structural character. With subsequent increases in the amount of swelling, the synthesized MCF-C as MCF-C 1.5, 2.5, 3.5 and 4.5 had enlarged specific surface area and obviously improved pore structure. Therefore, the higher ratios of TMB/P123 significantly facilitated the migration and diffusion of reactant and product molecules in the pore structure. These behaviors contributed to higher catalytic activity. In other words, ethanol molecules could practically penetrate into the enlarged pore structure, which remarkably improved the utilization rate of the inner surface of catalysts to increase the adsorption and activation possibility of the investigated catalyst to reactant molecule such as ethanol. Similarly, the enlarged pore size and high specific surface area increasingly facilitated to desorb the target product i.e. acetaldehyde molecules, which directly promote the ethanol dehydrogenation to acetaldehyde.

Meanwhile, the rate of reaction and surface area were emphasized for distinguishing on the effect of physical properties to catalytic activity from changing the ratio of TMB/P123 as represented in **Figure 5.30**. The evidence suggested that the increase of TMB/P123 ratio from 0.5 to 4.5 could provide higher surface area, which obviously affected the rate of reaction, especially at the TMB/P123 ratio of 3.5. However, the rate of reaction was decreased when the ratio of TMB/P123 was increased from 3.5 to 4.5 with the lower surface area. Thus, the physical properties such as surface area played an important role for higher rate of reaction owing to higher active surface to catalyze the dehydrogenation of ethanol to acetaldehyde by altering the ratio of TMB/P123.

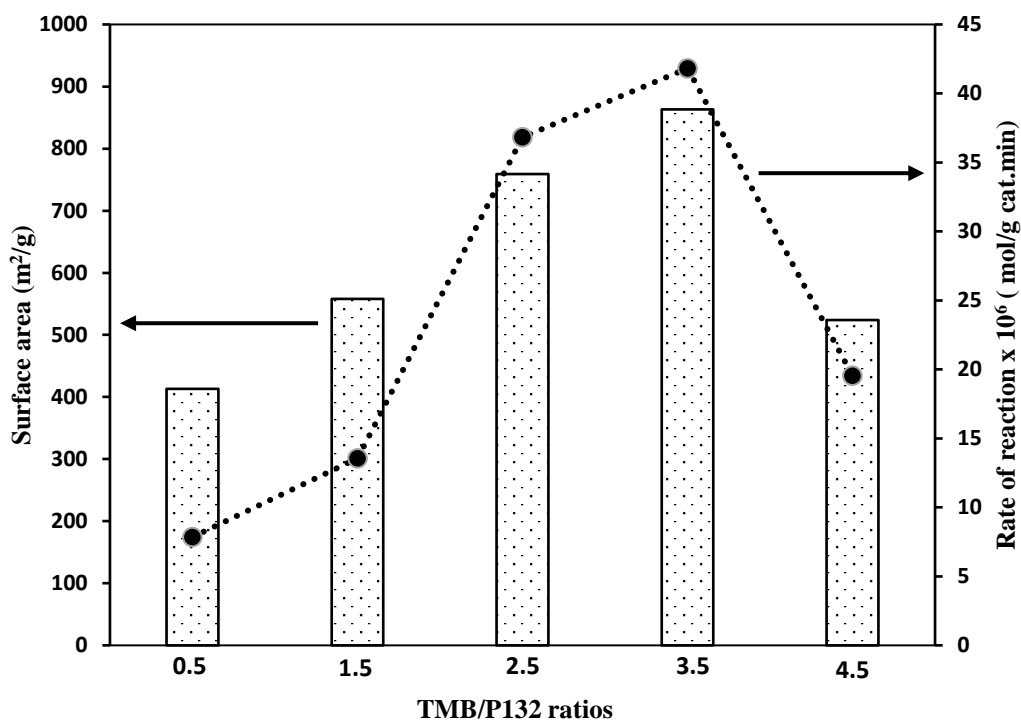


Figure 5.30 The relationship between the rate of reaction and surface area.

Changing the ratio of TMB/P123 could affect the catalytic activity which did not only depend on the physical property (the surface area or pore size), but also on the chemical properties (basicity or acidity). To clarify this point, **Table 5.17** illustrates the different specific activity based on basicity or acidity at the different ratios of TMB/P123. The results shows that the increased ratio of TMB/P123 significantly affected the specific activity of the basicity and acidity (the highest value), especially at ratio of TMB/P123 3.5. On the contrary, at TMB/P123 ratio of 4.5, MCF-C 4.5 exhibited lower specific activity due to the decreased amount of basic or acid sites. Therefore, there was the relationship between chemical properties as basicity or acidity and specific activity via changing the ratio of TMB/P123.

Table 5. 17 The specific activity based on basicity and acidity for all the MCF-C catalysts.

MCF-Cs (TMB/P123 ratio)	Specific activity based on basicity (mol/mol CO ₂ .min)	Specific activity based on acidity (mol/mol NH ₃ .min)
0.5	0.010	0.015
1.5	0.016	0.025
2.5	0.041	0.059
3.5	0.046	0.065
4.5	0.023	0.032

*Specific activity = rate of reaction

5.3.2.2 Time-on-stream behavior testing

To analyze the catalytic performance as percentage change of ethanol conversion and yield of acetaldehyde within the long period under constant temperature of all catalysts with the different ratios of TMB/P123. The stability test was employed under the operating system at temperature of 400 °C for 12 h as seen in **Figure 5.31**. The results show that MCF-C 3.5 evidently exhibited the lowest percentage change in the ethanol conversion and yield of acetaldehyde with value of ca.12.7 % and 14.8 %, while the highest percentage change in the ethanol conversion and yield of acetaldehyde was MCF-C 0.5 with the value of 58.4 % and 52.3 %. This evidence suggested that MCF-C 3.5 significantly provided the highest stability of catalyst in ethanol dehydrogenation reaction among other catalysts.

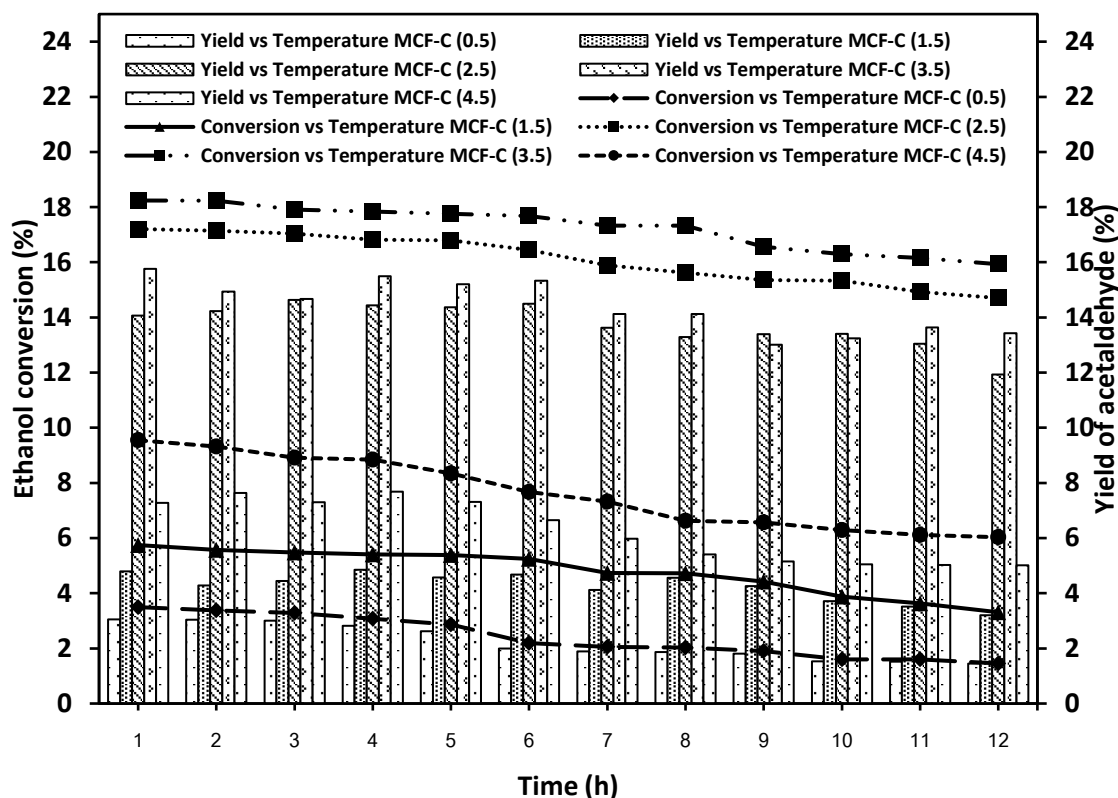


Figure 5.31 Stability test of all MCF-C catalysts for 12 h on ethanol dehydrogenation.

This phenomenon indicated that ethanol could still notably convert to the acetaldehyde in the larger pore size of catalyst with insignificant effect of the occurrence of the coke. It could be observed that the slightly change of ethanol conversion under the long period of operating condition. In other words, the large pore size of MCF-C 3.5 could promote the mass transfer inside of the porous catalyst, which directly affected the catalytic activity. However, the highest pore size of MCF-C 4.5 did not provide the stability of catalysts in ethanol dehydrogenation as expected. Thus, it could be notified that the optimization of TMB/P123 ratio was essential for the higher catalytic activity, which did not only depend on the appropriate morphology, but also relied on the chemical properties in both acidity and basicity.

5.3.2.2.1 Spent catalysts

After the reaction testing at temperature of 400 °C for 12 h for all tested catalysts, the spent catalysts of each ratio of TMB/P123 were characterized using SEM-

EDX technique to investigate either the change in textural of the catalysts or the existing of the elemental compositions for detecting the occurrence of the coke. **Figure 5.32** presents the external morphology both the fresh and spent catalyst. This evidence suggested that the surface particle of MCF-C 0.5 obviously changed the rod-like shape to agglomerate to other shape, which possibly affected the loss in the catalytic activity due to the pore blockage of catalysts. In addition, the coke was remarkably observed on the surface of catalysts in all the ratios of TMB/P123, but it was only slightly observed on catalyst surface between the fresh and spent catalyst of MCF-C 3.5. This was outstanding in the evacuating the coke formation as confirmed by EDX technique from **Table 5.18**. It was found that MCF-C 3.5 could maintain the tradition composition with the decrease of the least carbon change of ca. 2.54 %, meanwhile the increase of oxygen was the least change from 7.92 to 10.23 %. This indicated that MCF-C could facilitate the migration of the product or byproducts out of the catalysts to avoid the coke formation. Meanwhile, it was noticeably different from MCF-C 0.5 with the highest increase of oxygen composition from the fresh and spent catalyst owing to the encapsulation of the product or byproducts, which was possibly converted to the coke formation inside the catalyst leading to inhibition of the inter mass transfer [39].

Table 5. 18 The amount of each element near surface of fresh and spent catalyst granule obtained from EDX.

Catalyst	Amount of element on surface (wt%)					
	C		O		Si	
	Fresh	Spent	Fresh	Spent	Fresh	Spent
MCF- C 0.5	85.2	61	11.6	35.9	3.2	3.1
MCF- C 1.5	88.5	75.5	10.3	23.4	1.2	1.1
MCF- C 2.5	90.9	86.7	8.2	12.5	0.9	0.8
MCF- C 3.5	91.3	88.9	7.9	10.3	0.8	0.8
MCF- C 4.5	90.7	85.2	8.4	13.9	0.9	0.9

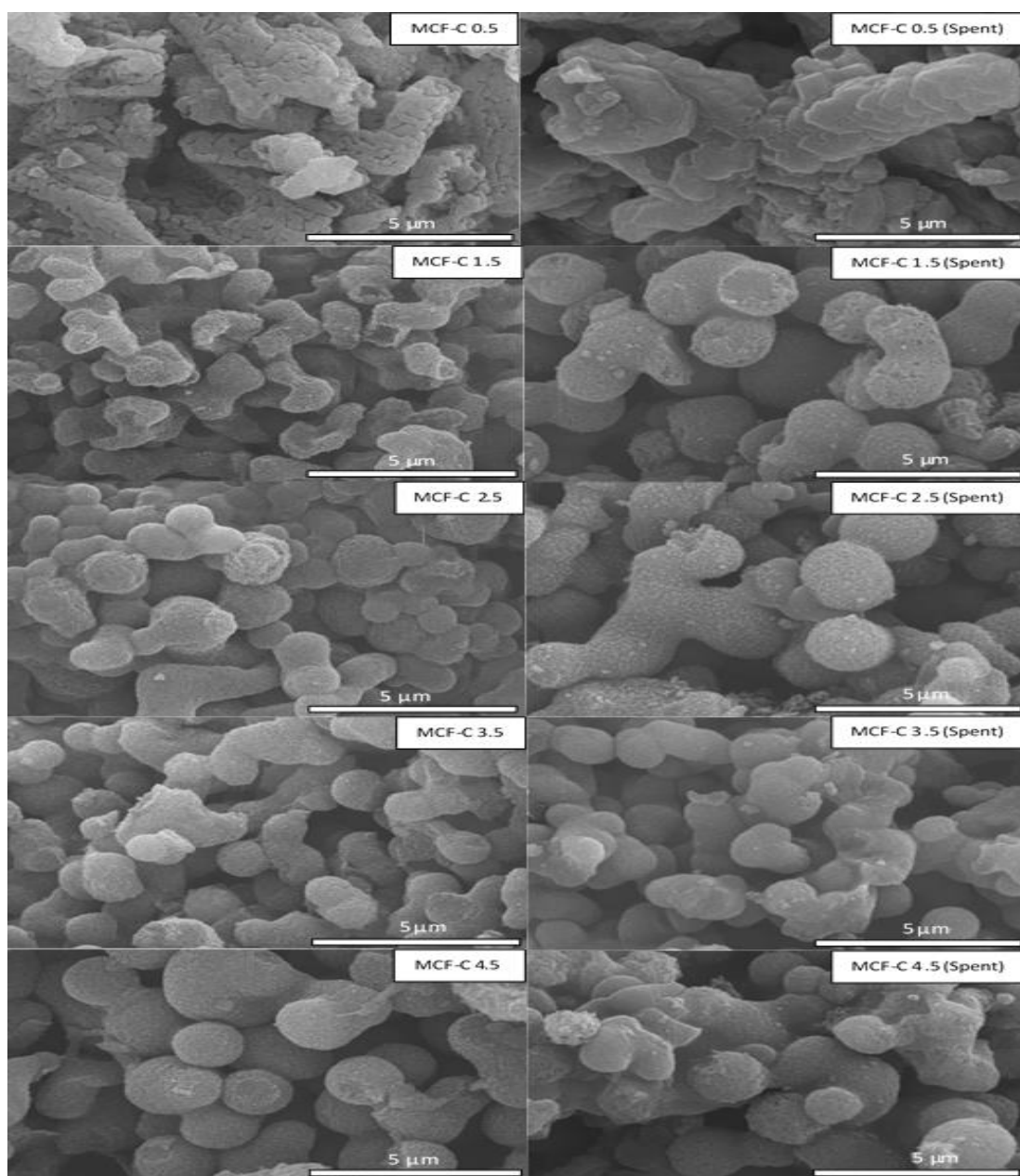


Figure 5. 32 Low magnification SEM image of spent and fresh catalysts of all MCF-C catalysts.

Chapter 6

General conclusion

6.1 General summary

This research aims to investigate the synthesis of MCF-C as a catalyst for dehydrogenation of ethanol. The study was classified into 3 parts. In the first part, the mesocellular foam silica (MCF-Si) was converted to mesocellular foam carbon using the surfactant residue as a carbon source, followed by testing MCF-C in the dehydrogenation of ethanol to acetaldehyde. The results suggested that the surfactant residue in MCF-Si could be converted to carbon in of the MCF-C, which was solidly confirmed by SEM-EDX. In addition, the obtained MCF-C could maintain meso-structure evidenced by BET. MCF-C was tested in the ethanol dehydrogenation. It was found that MCF-C potentially exhibited a better catalyze for ethanol dehydrogenation reaction than MCF-Si with higher ethanol conversion. For the second part, MCF-C was examined for catalyst deactivation due to the coke formation, which directly affected to the catalytic activity after the long period. The results showed that at the low operating temperature at 300 °C exhibited the highest ethanol conversion was obtained, which was accorded to the higher coke formation. Thus, the higher operating temperature of ethanol dehydrogenation using MCF-C as catalyst significantly affected the coke formation. In The final part, the effect of pore size of MCF-C was examined to optimize the selectivity and yield of acetaldehyde. MCF-C were synthesized at the various TMB/P123 ratios and were tested in ethanol dehydrogenation. The result revealed that the higher ratio of TMB/P123 significantly changed the physical properties of MCF-C such as pore size and surface area. Furthermore, the higher ratio of TMB/P123 notably provided the higher catalytic activity owing to the higher mass transfer of the reactants/products from enlarge por size and higher surface area.

6.2 Conclusion

Part 1: Synthesis, characteristics and application of mesocellular foam carbon (MCF-C) as catalyst for dehydrogenation of ethanol to acetaldehyde

This research investigated on the synthesis procedure of mesoporous carbon named mesocellular foam carbon (MCF-C), which was successfully synthesized using mesocellular foam silica (MCF-Si) as a template material using sulfuric acid for converting surfactant residue as a carbon source on the surface of silica. In addition, the hybrid composites catalyst material could be obtained during the synthesis, and silica was then, etched using NaOH. All the catalyst materials could maintain the structural characteristic of mesoporous material. On the other hand, some parts of the MCF-C were easily collapsed due to the etching process using NaOH, which directly affected the thin wall part of the material. Then, the different MCF materials were employed as catalysts in ethanol dehydrogenation to acetaldehyde. The MCF-C exhibited the highest ethanol conversion and yield of acetaldehyde at 400 °C. This was attributed to the high acidity and basicity. Moreover, MCF-C was also tested for its stability within 20 h of reaction which insignificant change of ethanol conversion, and selectivity of acetaldehyde were observed. Therefore, this catalyst material has the potential to apply in ethanol dehydrogenation.

Part 2: Study of deactivation in mesocellular foam carbon (MCF-C) catalyst used in gas-phase dehydrogenation of ethanol

In this research, the deactivation of mesocellular form carbon (MCF-C) catalyst during ethanol dehydrogenation to acetaldehyde was investigated under different operating temperatures. The lowest catalytic activity with MCF-C was found at the low temperature of 300 °C due to the highest coke formation, which directly affected deactivation of the catalyst. The presence of the coke in MCF-C not only decreased the pore volume and surface area, but also decreased the acidity of catalyst. In addition, the pore blockage also retarded the mass transfer of the reactant and product inside the pores. On the contrary, at the reaction temperature of 400 °C was softly deactivated due to less coke formation, which preserved the catalytic activity without a significant change in ethanol conversion. Thereby, the increasing of

reaction temperature in ethanol dehydrogenation to acetaldehyde using MCF-C as a catalyst significantly provided either lower deactivation of catalysts or higher catalytic activity.

Part 3: Effect of TMB/P123 ratios on physicochemical properties of mesocellular foam carbon (MCF-C) as catalyst for ethanol dehydrogenation

The different ratios of TMB/P123 were investigated in mesocellular foam carbon (MCF-C) on ethanol dehydrogenation to acetaldehyde. The high catalytic activity was significantly promoted due to the appropriate regulation of the catalyst structure and the precise preparation of chemical composition. The nitrogen isotherm revealed that the ratio of TMB/P123 of 3.5 as MCF-C 3.5 contained evidently great specific area and highly developed meso-structure of materials. In contrary, the volume of TMB as swelling agent was different leading to apparent difference in the structure of the prepared MCF-C, particularly in the pore size, specific surface area, and pore volume. Meanwhile, XRD patterns of all MCF-C were not much different indicating that the expanding of TMB volume did not directly affect the mesopore structure or even its crystallinity. The chemical properties such as acidity and basicity were observed in MCF-C 3.5 with the highest total acid and base sites of catalyst, which were beneficial to relative more reasonable active sites for enhancing the effective activation ability for ethanol dehydrogenation. Furthermore, MCF-C 3.5 evidently exhibited the highest catalytic activity in terms of ethanol conversion, yield of acetaldehyde, and even stability test for 12 h. This indicated that MCF-C 3.5 was outstanding in both the physical and chemical properties. Therefore, the MCF-C 3.5 was a promisingly potential catalyst for ethanol dehydrogenation to acetaldehyde.

6.3 Recommendations

- The ethanol conversion can be improved using additional metallic for improving the chemical properties of the catalyst either basicity or acidity.
- The types of coke formation should be classified using various techniques such as UV-Visible spectrophotometer or IR-Raman.
- IR-Pyridine should be applied to clarify Brønsted acid or base of surface reaction to understand the mechanism of ethanol dehydrogenation to acetaldehyde.



APPENDIX A

Table A1. 1 Ethanol conversion and selectivity of all MCF-C catalysts

MCF-C (TMB/P12 3 ratio)	Temp eratur e (°C)	Ethanol Conversion (%)	Selectivity (%)			
			Ethylene	Acetaldehy de	Ethyl acetate	Acetic acid
0.5	250	0.1	-	100	-	-
	300	0.2	-	100	-	-
	350	0.9	2.1	97.9	-	-
	400	3.1	4.3	95.7	-	-
1.5	250	0.4	28.9	71.1	-	-
	300	2.9	16.4	83.6	-	-
	350	3.5	8.2	91.8	-	-
	400	5.5	5.7	94.3	-	-
2.5	250	3.4	-	100	-	-
	300	3.9	-	100	-	-
	350	5.9	-	100	-	-
	400	17.5	9.7	80.3	-	10.0
3.5	250	3.2	-	100	-	-
	300	4.3	0.8	99.2	-	-
	350	10.1	3.6	85.3	7.1	4.0
	400	18.6	5.4	83.6	7.9	3.1
4.5	250	0.9	-	100	-	-
	300	1.9	-	100	-	-
	350	8.9	14.1	84.4	1.5	-
	400	9.5	19.8	77.9	2.3	-



จุฬาลงกรณ์มหาวิทยาลัย
CHULALONGKORN UNIVERSITY

APPENDIX

LIST OF PUBLICATIONS

B-1 Publications

1. Yootapong Klinthongchai, Seeroong Prichanont, Piyasan Prasertthdam, Bunjerd Jonsomjit, Synthesis, characteristics and application of mesocellular foam carbon (MCF-C) as catalyst for dehydrogenation of ethanol to acetaldehyde. *Journal of Environmental Chemical Engineering*, 2020. **8**(3).
2. Yootapong Klinthongchai, Seeroong Prichanont, Piyasan Prasertthdam, Bunjerd Jonsomjit, Effect of TMB/P123 ratios on physicochemical properties of mesocellular foam carbon (MCF-C) as catalyst for ethanol dehydrogenation. *Materials Today Chemistry*, 2021 (20).

B-2 Conference

1. Oral presentation: Yootapong Klinthongchai, Seeroong Prichanont, Piyasan Prasertthdam, and Bunjerd Jongsomjit, Kinetic study of ethanol dehydrogenation to acetaldehyde catalyzed by mesocellular foam carbon as solid catalyst, Fourth edition of International Conference on Catalysis and Chemical Engineering 2020 (CCE-2020), Los Angeles, California, United States, February 24-26, 2020.

References

1. Stawicka, K., et al., *Comparative study of acid-basic properties of MCF impregnated with niobium and cerium species*. Catalysis Today, 2019. **325**: p. 2-10.
2. Wayne W. Lukens, J., Peidong Yang, and Galen D. Stucky, *Synthesis of Mesocellular Silica Foams with Tunable Window and Cell Dimensions*. Chem. Mater., 2001. **13**: p. 28-34.
3. T. Sen , G.J.T.T., J.L. Casci , M.W. Anderson *Meso-cellular silica foams, macro-cellular silica foams and mesoporous solids: a study of emulsion-mediated synthesis*. Microporous and Mesoporous Materials, 2005. **78**: p. 255-263.
4. Piumetti, M., et al., *Novel vanadium-containing mesocellular foams (V-MCF) obtained by direct synthesis*. Microporous and Mesoporous Materials, 2011. **142**(1): p. 45-54.
5. Stawicka, K., et al., *Organosilanes affecting the structure and formation of mesoporous cellular foams*. Microporous and Mesoporous Materials, 2012. **155**: p. 143-152.
6. Ping, E.W., et al., *Oxidative Heck Coupling Using Pd(II) Supported on Organosilane-Functionalized Silica Mesocellular Foam*. Topics in Catalysis, 2010. **53**(15-18): p. 1048-1054.
7. Subagyo, D.J.N., et al., *CO₂ adsorption by amine modified siliceous mesostructured cellular foam (MCF) in humidified gas*. Microporous and Mesoporous Materials, 2014. **186**: p. 84-93.
8. Wolski, L., I. Sobczak, and M. Ziolk, *Development of multifunctional gold, copper, zinc, niobium containing MCF catalysts – Surface properties and activity in methanol oxidation*. Microporous and Mesoporous Materials, 2017. **243**: p. 339-350.
9. Ping, E.W., et al., *Highly dispersed palladium nanoparticles on ultra-porous silica mesocellular foam for the catalytic decarboxylation of stearic acid*. Microporous and Mesoporous Materials, 2010. **132**(1-2): p. 174-180.
10. Pompe, C.E., et al., *Stability of mesocellular foam supported copper catalysts for methanol synthesis*. Catalysis Today, 2019. **334**: p. 79-89.
11. Bilkova, I., et al., *The effect of zinc and copper in gold catalysts supported on MCF cellular foams on surface properties and catalytic activity in methanol oxidation*. Microporous and Mesoporous Materials, 2016. **232**: p. 97-108.
12. Wu, S., et al., *Ultra-sensitive biosensor based on mesocellular silica foam for organophosphorous pesticide detection*. Biosens Bioelectron, 2011. **26**(6): p. 2864-9.
13. Kim, J., et al., *Adsorption of biomolecules on mesostructured cellular foam silica: Effect of acid concentration and aging time in synthesis*. Microporous and Mesoporous Materials, 2012. **149**(1): p. 60-68.
14. Gao, F., et al., *CO₂ capture using mesocellular siliceous foam (MCF)-supported CaO*. Journal of the Energy Institute, 2019. **92**(5): p. 1591-1598.
15. Zhu, C., et al., *Synthesis of HKUST-1/MCF compositing materials for CO₂ adsorption*. Microporous and Mesoporous Materials, 2016. **226**: p. 476-481.
16. Azmi, A.A. and M.A.A. Aziz, *Mesoporous adsorbent for CO₂ capture application under mild condition: A review*. Journal of Environmental Chemical Engineering, 2019. **7**(2).

17. Srivastava, I., et al., *Preparation of mesoporous carbon composites and its highly enhanced removal capacity of toxic pollutants from air*. Journal of Environmental Chemical Engineering, 2019. **7**(4).
18. Liang, C., Z. Li, and S. Dai, *Mesoporous carbon materials: synthesis and modification*. Angew Chem Int Ed Engl, 2008. **47**(20): p. 3696-717.
19. Autthanit, C., P. Praserttham, and B. Jongsomjit, *Oxidative and non-oxidative dehydrogenation of ethanol to acetaldehyde over different VOx/SBA-15 catalysts*. Journal of Environmental Chemical Engineering, 2018. **6**(5): p. 6516-6529.
20. Liu, L., et al., *Ordered mesoporous carbon catalyst for dehydrogenation of propane to propylene*. Chem Commun (Camb), 2011. **47**(29): p. 8334-6.
21. Wang, Q.-N., L. Shi, and A.-H. Lu, *Highly Selective Copper Catalyst Supported on Mesoporous Carbon for the Dehydrogenation of Ethanol to Acetaldehyde*. ChemCatChem, 2015. **7**(18): p. 2846-2852.
22. Reilly, P.T.A. and W.B. Whitten, *The role of free radical condensates in the production of carbon nanotubes during the hydrocarbon CVD process*. Carbon, 2006. **44**(9): p. 1653-1660.
23. Valle-Vigón, P., M. Sevilla, and A.B. Fuertes, *Sulfonated mesoporous silica-carbon composites and their use as solid acid catalysts*. Applied Surface Science, 2012. **261**: p. 574-583.
24. Lazar, M.D., et al., *Crude Bioethanol Reforming Process*, in *Ethanol*. 2019. p. 257-288.
25. Manochio, C., et al., *Ethanol from biomass: A comparative overview*. Renewable and Sustainable Energy Reviews, 2017. **80**: p. 743-755.
26. Zacchi, G., *Production of ethanol from biomass*. Scientific & Industrial Research, 2005. **64**: p. 905-919.
27. Santacesaria, E., et al., *Ethanol dehydrogenation to ethyl acetate by using copper and copper chromite catalysts*. Chemical Engineering Journal, 2012. **179**: p. 209-220.
28. DeWilde, J.F., C.J. Czopinski, and A. Bhan, *Ethanol Dehydration and Dehydrogenation on γ -Al₂O₃: Mechanism of Acetaldehyde Formation*. ACS Catalysis, 2014. **4**(12): p. 4425-4433.
29. Tayrabekova, S., et al., *Catalytic dehydrogenation of ethanol into acetaldehyde and isobutanol using mono- and multicomponent copper catalysts*. Comptes Rendus Chimie, 2018. **21**(3-4): p. 194-209.
30. Han, S., et al., *Selective Oxidation of Acetaldehyde to Acetic Acid on Pd-Au Bimetallic Model Catalysts*. ACS Catalysis, 2019. **9**(5): p. 4360-4368.
31. Zea, L., et al., *Acetaldehyde as Key Compound for the Authenticity of Sherry Wines: A Study Covering 5 Decades*. Comprehensive Reviews in Food Science and Food Safety, 2015. **14**(6): p. 681-693.
32. Kiyoshi Otasuka, Y.U.a.M.H., *The partial oxidation of ethane to acetaldehyde*. Catalysis Today, 1992. **13**: p. 667-672.
33. A.Ponomarev, S.M.S.a.D., *Hydration of Acetylene*. Chemical Education, 2007. **84**.
34. Taiseki Kunugi, K.F.a.H.T., *Catalytic Oxidation of Ethylene to Acetaldehyde. Palladium Chloride-Active Charcoal Catalyst*. Ind. Eng. Chem., Prod. Res. Develop., 1974. **13**: p. 237-242.
35. Clarizia, L., et al., *Selective photo-oxidation of ethanol to acetaldehyde and acetic acid in water in presence of TiO₂ and cupric ions under UV-simulated solar radiation*. Chemical Engineering Journal, 2019. **361**: p. 1524-1534.
36. Ob-eye, J., P. Praserttham, and B. Jongsomjit, *Dehydrogenation of Ethanol to Acetaldehyde over Different Metals Supported on Carbon Catalysts*. Catalysts, 2019. **9**(1).

37. Patrick Schmidt-Winkel, W.W.L., Jr., Dongyuan Zhao, Peidong Yang, Bradley F. Chmelka, and Galen D. Stucky, *Mesocellular Siliceous Foams with Uniformly Sized Cells and Windows*. American chemical society, 1999. **121**: p. 254-255.
38. Hermida, L., A.Z. Abdullah, and A.R. Mohamed, *Synthesis and Characterization of Mesostructured Cellular Foam (MCF) Silica Loaded with Nickel Nanoparticles as a Novel Catalyst*. Materials Sciences and Applications, 2013. **04**(01): p. 52-62.
39. Hoffmann, F., et al., *Silica-based mesoporous organic-inorganic hybrid materials*. Angew Chem Int Ed Engl, 2006. **45**(20): p. 3216-51.
40. Zdravkov, B., et al., *Pore classification in the characterization of porous materials: A perspective*. Open Chemistry, 2007. **5**(2).
41. Chi, Y.-S., H.-P. Lin, and C.-Y. Mou, *CO oxidation over gold nanocatalyst confined in mesoporous silica*. Applied Catalysis A: General, 2005. **284**(1-2): p. 199-206.
42. W. Chouyyok, *The Immobilization Of Horseradish Peroxidase On Ag/Mesoporous Silica Nanocomposite*. 2008.
43. Oda, Y., et al., *Mesocellular Foam Carbons: Aggregates of Hollow Carbon Spheres with Open and Closed Wall Structures*. Chemistry of Materials, 2004. **16**(20): p. 3860-3866.
44. Watthanachai, C., C. Ngamcharussrivichai, and S. Pengprecha, *Synthesis and Characterization of Bimodal Mesoporous Silica Derived from Rice Husk Ash*. Engineering Journal, 2019. **23**(1): p. 25-34.
45. Marsh H, H.E., Rodriguez-Reinoso F, *Introduction to carbon technology*. 1997.
46. An, S., J. Joo, and J. Lee, *Ultra-low-cost route to mesocellular siliceous foam from steel slag and mesocellular carbon foam as catalyst support in fuel cell*. Microporous and Mesoporous Materials, 2012. **151**: p. 450-456.
47. Valle-Vigón, P., M. Sevilla, and A.B. Fuertes, *Mesostructured silica-carbon composites synthesized by employing surfactants as carbon source*. Microporous and Mesoporous Materials, 2010. **134**(1-3): p. 165-174.
48. Kim, J., J. Lee, and T. Hyeon, *Direct synthesis of uniform mesoporous carbons from the carbonization of as-synthesized silica/triblock copolymer nanocomposites*. Carbon, 2004. **42**(12-13): p. 2711-2719.
49. Sun, J. and Y. Wang, *Recent Advances in Catalytic Conversion of Ethanol to Chemicals*. ACS Catalysis, 2014. **4**(4): p. 1078-1090.
50. George W. Huber, S.I., and Avelino Corma, *Synthesis of Transportation Fuels from Biomass*. Chemistry, Catalysts, and Engineering Journal, 2006. **106**: p. 4044-4098.
51. Eckert, M., et al., *Acetaldehyde*, in *Ullmann's Encyclopedia of Industrial Chemistry*. 2006.
52. Shevchenko, D.A.P.a.S.M., *Hydration of Acetylene: A 125th Anniversary*. Journal of Chemical Education, 2007. **84**.
53. Kiyoshi Otsuka, Y.U.a.M.H., *THE PARTIAL OXIDATION OF ETHANE TO ACETALDEHYDE*. Catalysis Today, 1992. **13**: p. 667-672.
54. Kaoru Fujimoto, H.T., and Taisiki Kunugi, *Catalytic Oxidation of Ethylene to Acetaldehyde. Palladium Chloride-Active Charcoal Catalyst*. Ind. Eng. Chem., Prod. Res. Develop., 1974. **13**: p. 237-242.
55. Ob-eye, J. and B. Jongsomjit, *Dehydrogenation of Ethanol to Acetaldehyde over Co/C Catalysts*. Engineering Journal, 2019. **23**(3): p. 1-13.
56. Pinthong, P., P. Prasertdam, and B. Jongsomjit, *Effect of Calcination Temperature on Mg-Al Layered Double Hydroxides (LDH) as Promising Catalysts in Oxidative Dehydrogenation of Ethanol to Acetaldehyde*. J Oleo Sci, 2019. **68**(1): p. 95-102.

57. ARNOLD, R.E.D.A.M.R., *CATALYTIC DEHYDROGENATION OF PRIMARY AND SECONDARY ALCOHOLS WITH COPPER-CHROMIUM OXIDE*. 1945.
58. Jinwoo Lee, S.Y., Taeghwan Hyeon, Seung M. Oh, and Ki Bum Kim, *Synthesis of a new mesoporous carbon and its application to electrochemical double-layer capacitors*. The Royal Society of Chemistry, 1999: p. 2177-2178.
59. Ryong Ryoo, S.H.J., Michal Kruk, and Mietek Jaroniec, *Ordered Mesoporous Carbons*. *Advanced Materials*, 2001. **13**: p. 9.
60. Jaroniec, M.K.a.M., *Characterization of Ordered Mesoporous Carbons Synthesized Using MCM-48 Silicas as Templates*. American Chemical Society, 2000. **104**: p. 7960-7968.
61. Jinwoo Lee, K.S., and Taeghwan Hyeon, *Fabrication of Novel Mesocellular Carbon Foams with Uniform Ultralarge Mesopores*. American Chemical Society, 2001. **123**: p. 5146-5147.
62. Zhang, Y., et al., *Formation of an ink-bottle-like pore structure in SBA-15 by MOCVD*. *Chemical Communications*, 2008(41).
63. Pang, J., et al., *Hierarchical Mesoporous Carbon/Silica Nanocomposites from Phenyl-Bridged Organosilane*. *Advanced Materials*, 2005. **17**(6): p. 704-707.
64. Kwangjin Park, D.H., JeongKuk Shon, Seok Gwang Doo, and Seoksoo Lee, *Characterization of thin, uniform coating on P2-type Na₂/3Fe₁/2Mn₁/2O₂ cathode material for sodium-ion batteries*. The Royal Society of Chemistry, 2013. **00**: p. 1-3.
65. GRZEGORZ S. SZYMAŃSKI, G.R., and ARTUR P. TERZYK, *CATALYTIC CONVERSION OF ETHANOL ON CARBON CATALYSTS*. *Carbon*, 1994. **32**(2): p. 265-271.
66. Jasińska, J., B. Krzyżyńska, and M. Kozłowski, *Influence of activated carbon modifications on their catalytic activity in methanol and ethanol conversion reactions*. *Open Chemistry*, 2011. **9**(5).
67. Tveritinova, E.A., et al., *Catalytic conversion of aliphatic alcohols on carbon nanomaterials: The roles of structure and surface functional groups*. *Russian Journal of Physical Chemistry A*, 2017. **91**(3): p. 448-454.
68. Zhao, Z., et al., *Highly-Ordered Mesoporous Carbon Nitride with Ultrahigh Surface Area and Pore Volume as a Superior Dehydrogenation Catalyst*. *Chemistry of Materials*, 2014. **26**(10): p. 3151-3161.
69. Klinthongchai, Y., et al., *Synthesis, characteristics and application of mesocellular foam carbon (MCF-C) as catalyst for dehydrogenation of ethanol to acetaldehyde*. *Journal of Environmental Chemical Engineering*, 2020. **8**(3).
70. Vicente, J., et al., *Reaction pathway for ethanol steam reforming on a Ni/SiO₂ catalyst including coke formation*. *International Journal of Hydrogen Energy*, 2014. **39**(33): p. 18820-18834.
71. Bedia, J., et al., *Ethanol dehydration to ethylene on acid carbon catalysts*. *Applied Catalysis B: Environmental*, 2011. **103**(3-4): p. 302-310.
72. Wu, X. and L.R. Radovic, *Inhibition of catalytic oxidation of carbon/carbon composites by phosphorus*. *Carbon*, 2006. **44**(1): p. 141-151.
73. Carolina Montero, A.R., Beatriz Valle, Lide Oar-Arteta, Javier Bilbao, and a.A.G. Gayubo, *Origin and Nature of Coke in Ethanol Steam Reforming and Its Role in Deactivation of Ni/La₂O₃- α Al₂O₃ Catalyst*. *Ind. Eng. Chem. Res.*, 2019. **58**: p. 14736-14751.

74. Morales, M.V., et al., *Difference in the deactivation of Au catalysts during ethanol transformation when supported on ZnO and on TiO₂*. RSC Advances, 2018. **8**(14): p. 7473-7485.
75. Li, L., et al., *Controlled pore size of 3D mesoporous Cu-Ce based catalysts and influence of surface textures on the CO catalytic oxidation*. Microporous and Mesoporous Materials, 2016. **231**: p. 9-20.
76. Yuan, P., et al., *Effect of pore diameter and structure of mesoporous sieve supported catalysts on hydrodesulfurization performance*. Chemical Engineering Science, 2014. **111**: p. 381-389.
77. Pahalagedara, M.N., et al., *Ordered mesoporous mixed metal oxides: remarkable effect of pore size on catalytic activity*. Langmuir, 2014. **30**(27): p. 8228-37.
78. Thananukul, N., et al., *A comparative study on mesocellular foam silica with different template removal methods and their effects on enzyme immobilization*. Journal of Porous Materials, 2018. **26**(4): p. 1059-1068.



REFERENCES



จุฬาลงกรณ์มหาวิทยาลัย
CHULALONGKORN UNIVERSITY



จุฬาลงกรณ์มหาวิทยาลัย
CHULALONGKORN UNIVERSITY

VITA

NAME Yootapong Klinthongchai

DATE OF BIRTH 12 February 1992

PLACE OF BIRTH Nakhonratchasima

INSTITUTIONS ATTENDED B.Eng. (Chemical Engineering), King Mongkut's University of
technology Thonburi
M.Eng. (Chemical Engineering), Chulalongkorn
University, 2017
D.Eng. (Chemical Engineering), Chulalongkorn
University, 2021

HOME ADDRESS 145 Moo.8, Poklang, Meaung Nakhonratchasima,
Nakhonratchasima 30000

PUBLICATION

1. Y. Klinthongchai, S. Prichanont, P. Prasertthdam and
B. Jongsomjit, "Synthesis, characteristics and application of
mesocellular foam carbon (MCF-C) as catalyst for
dehydrogenation of ethanol to acetaldehyde", Journal of
Environmental Chemical Engineering (2020) 8, 103752
2. Y. Klinthongchai, S. Prichanont, P. Prasertthdam and
B. Jongsomjit, "Effect of TMB/P123 ratios on
physicochemical properties of mesocellular foam carbon
(MCF-C) as catalyst for ethanol dehydrogenation",
Materials Today Chemistry (2021)